Leibniz Universität Hannover

Annual Report 2022

IfES

Institute of Electric Power Systems
Division of High Voltage Engineering and Asset Management
Schering-Institute

Leibniz Universität Hannover
Institut für Elektrische Energiesysteme
Fachgebiet Hochspannungstechnik und Asset Management — Schering-Institut
Callinstraße 25 A
30167 Hannover
- GERMANY -
Tel: +49 511 762 2718
Fax: +49 511 762 2726
www.ifes.uni-hannover.de
schering@ifes.uni-hannover.de

Table of Content

1 Foreword

Dear Friends of the Schering-Institute,

as announced in the last newsletter, this year we are publishing again a detailed annual report, which we have prepared for the first time in both German and English language, as we have more and more contacts and projects with foreign industrial cooperation partners and universities.

After the pandemic situation improved significantly last year, so that in 2022 the students were back from home office to the university, much has changed again with Russia's unlawful war of aggression against Ukraine. In addition to the energy crisis, there were significant price increases and supply shortages of a wide variety of materials and components, which also affected the work at the Schering-Institute, as it continues to be particularly pronounced experimentally. Thus, we all continue to live in unusually turbulent times, and it is hard to estimate how the situation will develop further, so that there is nothing left to do but hope for the good sense of all concerned.

Of course, the energy crisis is currently giving our area a special, trendsetting significance, which means that the opportunities on the job market for our students are excellent. This will continue for some decades, because in addition to the current change in the energy system toward renewable energies - based primarily on sun and wind - the next energy turnaround is already in sight in a few decades, as a result of the progress in nuclear fusion, as recently reported from the United States. This will certainly have a positive influence on future high school graduates, so that more and more young people will be interested in studying energy technology, but this does not help much at the moment, because the universities cannot meet the actual demand for electrical engineers. As a consequence, this will lead to a delay of the major power engineering projects and thus also to a prolongation of the energy transition in its entirety. As already outlined in the last newsletter, a transformation towards e-mobility and a changed e-supply - in the medium to long term also towards an e-heating supply - simply requires many more e-engineers, and parallel efforts should be made to also inspire more female engineers for this industry.

The current shortage of students in electrical engineering is, of course, also noticeable at the Schering-Institute. However, in the last year we were able to recruit three new members: Mr. Balali, Mr. Moh'd and Mr. Wang, while Dr. Zhou successfully completed his PhD thesis. In addition, last year we welcomed Prof. Akbari Azirani from our partner university in Iran - K.N. Toosi University of Technology in Tehran - as well as Mr. Ariannik as a PhD student from York University in Toronto, Canada as visiting scientists, who performed parts of their research at the Schering-Institute.

Another positive aspect in 2022 was that we were able to participate in various conferences again, resulting in more than 20 national and international publications. We were also able to hold our TLM (Transformer Life Management) conference in

Bad Gögging (Bavaria) in September without any special requirements, thus more than 200 visitors and almost 30 professional exhibitors could participate. In the course of the TLM, which has now been held for more than 10 years, many small modifications have been made, so that TLM 2022 now includes intensive workshops on various topics in addition to the approximately 20 oral presentations and the technical exhibition mentioned above. Furthermore a poster session was now integrated, during which young researchers can present their work. The TLM 2023 will take place on September 18th and 19th in Schweinfurt (Germany) and will certainly again be used intensively by our PhD students to expand their own network and to discuss details of their research work with experienced visitors. This will also be supported by working in committees, so that since last year some of the more experienced PhD students now also participate in working groups of CIGRÉ, thus a continuous international exchange is established.

As you can see from these introductory words, an eventful but also work-intensive year was ending, so that we would like to conclude by expressing our sincere thanks for the good cooperation, funding and support to you, our cooperation and industry partners, the ZIM (Central Innovation Program for SMEs) of the BMWK (Federal Ministry of Economics and Climate Protection), the AiF (German Federation of Industrial Research Associations) "Otto von Guericke" e. V. - Projekt GmbH, the VDI/VDE Innovation + Technik GmbH, the German Research Foundation (DFG), the German Academic Exchange Service (DAAD) and the Alexander von Humboldt Foundation (AvH).

We are looking forward to continue these collaborations in the new year and in the meantime we wish you and your families a healthy, successful, and peaceful new year!

Hannover, January 2023

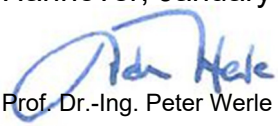

Prof. Dr.-Ing. Peter Werle

2 Personnel

Director of the Institute:	Prof. Dr.-Ing. Peter Werle
Senior Engineer:	M.Sc. Moritz Kuhnke
Secretary:	Hala Ahmi
Workshop:	Erich Semke (Lead)
	Ina Riekeberg
Retired Professors:	Prof. Dr.-Ing. Ernst Gockenbach
	Prof. Dr.-Ing. habil. Hossein Borsi
Ext. Lecturers:	Hon.-Prof. Dr.-Ing. Stephan Pöhler
	Hon.-Prof. Dr.-Ing. Monika Sturm
Guest Scientists:	Prof. Dr.-Ing. Asghar Akbari
PhD Students:	M.Sc. Behnam Balali
	M.Sc. Sebastian Braun
	M.Sc. Kristin Homeier
	M.Sc. Mahmoud Moh'd
	M.Sc. Büsra Özdemir
	M.Sc. Henning Schnittker
	M.Sc. Junaid Shaikh
	M.Sc. Aref Sharifi
	M.Sc. Laureen Stahl
	M.Sc. Javier Torres
	M.Sc. Yunfei Wang
Ext. PhD Students:	M.Sc. Oliver Derigs
	Dipl.-Ing. (FH) Henry Hirte
	M.Sc. Sebastian Schreiter
PhD-thesis in Preparation:	Dipl.-Ing. Mirnes Aganbegović
	M.Sc. Mohammad Akbari Azirani
	M.Sc. Mohammad Taghi Imani
	Dipl.-Ing. Tobias Kinkeldey
	M.Sc. Tobias Münster
	M.Sc. Sahand Seifi

3 Lectures

Prof. Dr.-Ing. P. Werle

High Voltage Technique I
(SS, Lecture 2 SWH, Tutorial 1 SWH, Excercise1 SWH)

Tasks and Future of High Voltage Engineering
Generation of high voltages (AC, DC and impulse voltages)
Cascade circuits
Measurement of high AC, DC and impulse voltages
Measurement of high currents at high potential
Electrical strength theory
Electrostatic field
Measurement and calculation of equivalent arrangements
Breakdown mechanisms
Breakdown of gases
Polarity effect
Breakdowns in insulating materials

High Voltage Technique II
(WS, Lecture 2 SWH, Tutorial 1 SWH, Excercise1 SWH)

Breakdown types in liquid insulating materials
Breakdown types in solid insulating materials
Influencing factors on the breakdown voltage
Lifetime characteristic, volume effect
Dielectric behavior of liquid and solid insulating materials
Dielectric measurements
Schering bridge
Partial discharge measurements
Determination of breakdown voltage according to standard

High Voltage Apparatus I
(WS, Lecture 2 SWH, Tutorial 1 SWH, Excercise1 SWH)

Switch-on and switch-off processes in networks
Consideration of occurring overloads
Functionality and design of high voltage switches
Arc characteristics
Circuit breakers, load breakers, disconnectors and earthing switches
SF6 systems, substitute gases
Current and voltage transformers, behavior during travelling waves
High voltage cables
Comparison of power transmission systems
Bushings and feedthroughs
Dimensioning and field calculation
High voltage power capacitors
Surge arresters
Protection concepts

High Voltage Apparatus II
(SS, Lecture 2 SWH, Tutorial 1 SWH, Excercise1 SWH)
Energy transition: Cause and effect
Transformers: Types, design, calculation, manufacture, testing, service.
Overhead power lines: Materials, construction, poles, design, oscillations
High voltage direct current (HVDC) transmission systems
Superconducting equipment
Conventional generation systems
Energy storage and nuclear fusion
Lightning protection and EMC

Condition Assessment and Asset Management
(WS, Lecture 2 SWH, Tutorial 1 SWH, Excercise1 SWH
Asset Management Basics
Standards, ISO, IEC, VDE, IEEE
DIN ISO 55000, 55001, 55002
DIN EN ISO 12100, DIN ISO 31000, DIN EN 60812, DIN EN 60300, DIN EN 61025
IEC 60422, IEC 60599
Energy Industry Act
Tasks of the asset manager
Fleet management
Maintenance strategies
Risk-importance diagrams
Condition analysis methods
Oil analysis, DFR, FRA, PD, insulation measurements, thermovision
Sensor techniques
Monitoring systems
Data correlation techniques
Condition improvement strategies
Economic efficiency calculations

M.Sc. M. Kuhnke

Electrotechnical Basic Laboratory I (EE)
(SS, practical laboratory course, 2 SWH)
Current and voltage measurements
DC networks
Characteristics of electrical components
Simple AC circuits

Electrotechnical Basic Laboratory II (EE)
(WS, practical laboratory course, 3 SWH)
Field measurements
Oscillating circuits
Power measurement for AC
Three-phase alternating current
Technical writing

Electrotechnical Basic Laboratory III (EE)
(SS, practical laboratory course, 2 SWH)
Switching operations
Semiconductor circuits and operational amplifiers
Spectral analysis and synthesis of periodic signals
Field effect transistor and CMOS basic circuits

Electrotechnical Basic Laboratory for Mechanical Engineers
(WS, SS, practical laboratory course, 2 SWH)
Current and voltage measurements
Direct current networks
Characteristics of electrical components
Oscillating circuits

Physics Laboratory for Engineering and Business Administration
(WS, practical laboratory course, 1 SWH)
Field measurements
Oscillating circuits
Power with alternating current
Three-phase alternating current

Electrotechnical Basic Laboratory f. Sustainable Engineering
(SS, practical laboratory course, 1 SWS)
Characteristics of electrical components
Oscillating circuits

Prof. Dr.-Ing. P. Werle / Prof. Dr.-Ing. habil. L. Hofmann

Laboratory Power Supply and High Voltage Engineering
(SS, WS, practical laboratory course, 4 SWS)
Measurement of high alternating voltages
Electric breakdown in gases
Measurement of electric fields
Determination of the breakdown voltage of mineral oil
Star point grounding & equalization procedures (at IEE)
Short circuit current calculation with PC (at IEE)
Wind turbine (at IEE)
Tilt oscillations (at IEE)

Hon.-Prof. Dr.-Ing. S. Pöhler / Prof. Dr.-Ing. P. Werle

Componenents of High Voltage Transmissions Systems and their Insulating Materials
(SS, Lecture 3 SWH, Excercise1 SWH)
Energy industry introduction
High Voltage Switching Technology
High voltage transmission technology
Long-distance transmission of electrical energy
Causes and effects of instabilities in the transmission system
Flexible AC Transmission Systems (FACTS)
High-voltage direct current transmission
Transmission systems for on- and offshore applications
Physical fundamentals of insulating materials
Electrical and dielectric behavior of insulating material systems
Manufacture, characteristics, applications, advantages and disadvantages of various insulating materials
Technically relevant gaseous, liquid and solid insulating materials
Mixed dielectrics

Hon.-Prof. Dr.-Ing. M. Sturm

Systems for Future Energy Optimization and Marketing
(SS, Lecture 2 SWH)
Market requirements
Energy industry environment
Structures, processes, models, objectives
Decentralized/regenerative systems
Optimized energy use
Cross-utility optimization
Interaction between utility and industry
Smart grid
Communication/distributed intelligence
Electromobility
Smart Metering

4 New Employees and Guest Scientists

M.Sc. Mahmoud Moh’d

In 2010, I started my bachelor's degree in electrical engineering at Al-Balqa Applied University in Jordan. After that, I did my internship in Amman East Station (AES) - Combined Cycle Power Plant in the maintenance department. In 2014, I took a job in Qatar as a site engineer in the field of cable laying and substations. In 2015, I moved to Jordan to work as a design-and-application engineer in the solar photovoltaic field at Philadelphia-Solar. In this job, I was responsible for the design, installation as well as costing of the projects. Among other things, I installed a photovoltaic system with a capacity of 50 megawatts here together with work colleagues.

In 2019, I started my master's degree in power engineering at Leibniz Universität Hannover (LUH). I was able to successfully complete my studies in 2022 with a master's thesis at the Schering Institute with the topic "Application of classification models to support the evaluation of power transformers". Since then, I have been working at the Schering Institute as a research assistant. Currently, I am working on free-breathing power transformers. During operation, transformers are exposed to various stresses, such as thermal, electrical, chemical and mechanical stresses. A major problem is the ingestion of moisture and oxygen from outside, which can lead to chemical reactions and accelerate degradation mechanisms throughout the insulation system of oil-paper-insulated transformers. In particular, for free-breathing transformers that have contact with ambient air through the expansion tank, moisture and oxygen are introduced when the transformer is inhaled. In this context, I am developing a method to extend the life of these power transformers.

M.Sc. Behnam Balali

In 2014, I started my bachelor's degree in electrical engineering at Science and Culture University, Tehran, Iran. After receiving my B.Sc. degree in 2018, I started my master's studies in electrical engineering, power electronics and electrical machines at K. N. Toosi University of Technology, Tehran, Iran. The title of my master's thesis was " Modeling Faults of Synchronous Power Generators Based on Their Frequency Response Analysis and insulation Status Detection Feasibility". In this thesis, firstly, a high frequency equivalent circuit of the power synchronous generator was presented. Then, using simulation the 3D model of a salient pole synchronous power generator in Ansys Maxwell, all the parameters of the windings and core of a real power synchronous generator were extracted. Finally, some insulation defects were modeled simultaneously with the effect of the rotor position on the frequency response of the stator windings, and diagnosis was done using frequency response analysis (FRA).

Furthermore, during my master's degree, I gained valuable experience as an electronics laboratory supervisor and as a lecturer for this course at the University of Science and Culture. After completing my master's degree in 2021, I continued my research on condition monitoring of high voltage generators in the high voltage laboratory of K. N. Toosi University of Technology.

Since May 2022, I have been a member of the Schering Institute research team to pursue my PhD program. My current research topic is "Development and investigation of an online monitoring system for Hermetically Sealed Power Transformers ". Medium voltage hermetic transformers are commonly used in wind turbines to boost the output voltage of the turbine generator from a few hundred volts to the medium voltage level of the collector system. One of the most common forms is hermetically sealed oil-filled transformers. To prevent exposure of the insulating liquid to ambient air and moisture, the transformer is sealed with a gas cushion, usually of nitrogen or dry air. In severe fault conditions, a significant amount of fault gases can be expected to be generated, and in hermetically sealed power transformers, these gases gradually escape from the insulating liquid and diffuse into the gas cushion. Dissolved gas analysis (DGA) is one of the most effective diagnostic methods for power transformers. Therefore, a cost-effective alternative online monitoring system is to be developed at the Schering Institute.

M.Sc. Yunfei Wang

I have been working as a research associate at the Schering Institute since February 2022. In 2015 I completed my bachelor's degree in Thermal Energy and Power Engineering in China and then worked for one year in the operation and maintenance department of turbine generator systems in a thermal power plant in China. After that, I decided to do the master's degree in Germany and came to the Leibniz University Hannover in 2017 to study Energy Technology with a specialization in Electric Power Engineering. I completed the master's degree in 2021 with a master's thesis at the Schering Institute on the topic "Investigation of the diffusion behavior of different acid configurations in insulating paper in a closed transformer system".

I am currently working on cooling and insulating media for hybrid-electric propulsion systems of aircraft. Due to demands to mitigate greenhouse gas emissions, approaches to further improve energy efficiency and energy conservation are increasingly becoming a focus of research in the aerospace sector. Hybrid-electric as well as all-electric propulsion technologies offer the possibility of partially or completely displacing fossil fuels from regional aviation. They continue to offer the opportunity to go beyond traditional fixed-wing aircraft and develop transportation concepts that are integrated into sustainable urban living. Against this background, high demands are placed not only on the technologies used in all-electric and hybrid-electric flight, and also on the associated cooling and insulating media. Efficient systems with high power densities also require high power dissipation densities in the electric motor, power electronics, and battery. The electrical components of the system could generate large amounts of heat that must be dissipated to ensure the system safety and reliability. Under the control of the thermal management system, the waste heat from electrical components is transferred via a cooling medium. Therefore, the implementation of hybrid-electric flight is not feasible without a suitable cooling and insulating medium. Currently, there are two different options pursued in parallel. On the one hand, the electric propulsion system is cooled by a dielectric insulating fluid and on the other hand by air. Both approaches have advantages and disadvantages.

In cooperation with industrial partners, cooling fluids for hybrid-electric propulsion systems are being investigated for their aging behaviors and lifetime characteristics. This involves the thermal and dielectric properties of the cooling fluids.

Prof. Dr.-Ing. Asghar Akbari Azirani

Visiting Professor at the Schering-Institute

As part of the long-standing academic collaboration between the Electrical Engineering Department of K.N. Toosi University of Technology, where I work, and the Schering Institute, this report presents two recent research projects conducted under my supervision with the use of the well-equipped laboratories and facilities of this Institute. In 2021 and 2022, I have worked as a visiting professor at the Schering Institute.

Measuring partial discharge under fast repetitive impulses of static converters

The conventional setup for partial discharge measurement is explained in the IEC 60270 standard. Under a pure sinusoidal high voltage waveform, where a capacitor known as the PD coupler provides a low impedance closed loop for partial discharge current pulses originate from the test object. The simplest idea for the measurement of a PD current pulse could be placement of an impedance just in series with the coupling capacitor for picking up the pulses.

However, in terms of test objects fed by static converters, at the instant of high voltage change caused by power electronic the so-called PD coupler of conventional setup has a capacitive inrush current impulse. The rise time of such impulses could be few nanoseconds; hence, one can expect that their frequency components are extended up to several hundred MHz. As a result, the conventional measuring impedance, which is designed to separate the power frequency current from the PD, cannot distinguish the two mentioned pulses. Moreover, under square shape high voltage it is important to measure the PD pulses generated just at the instant of voltage change. Fig. 1-1 depicts the capacitive inrush current of a 1.5 nF coupler in the conventional PD measuring circuit. The applied voltage in this experiment is only 100 volts peak-to-peak, where the voltage amplitude for the actual PD measurement is usually in the range of several kV.

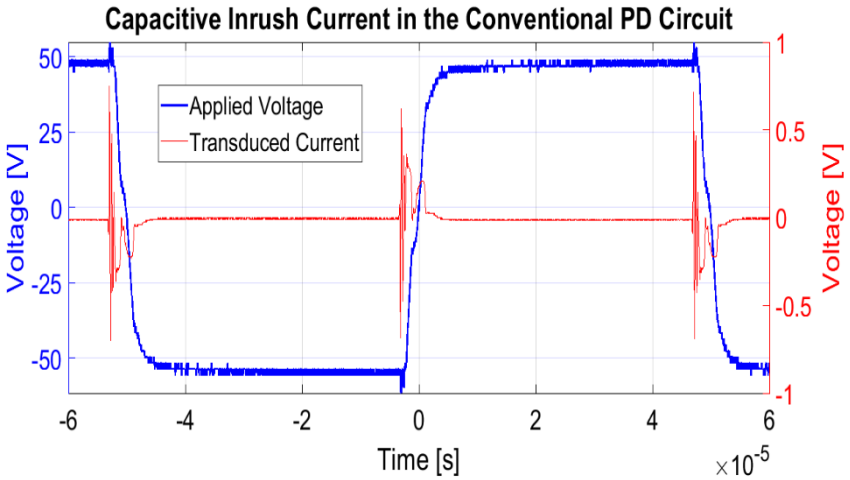

Fig. 1-1: The nature of dissociation current in a 1.5 nF coupling capacitor fed by a 100 V peak-to-peak square wave voltage.

In this research, a full bridge two quadrant topology

was implemented for fast switching realization. The setup in this contribution employs high voltage IGBTs as depicted in Fig. 1-2, where the full bridge converter feeds samples through the front and tail resistors in order to control the rise and the fall times respectively.

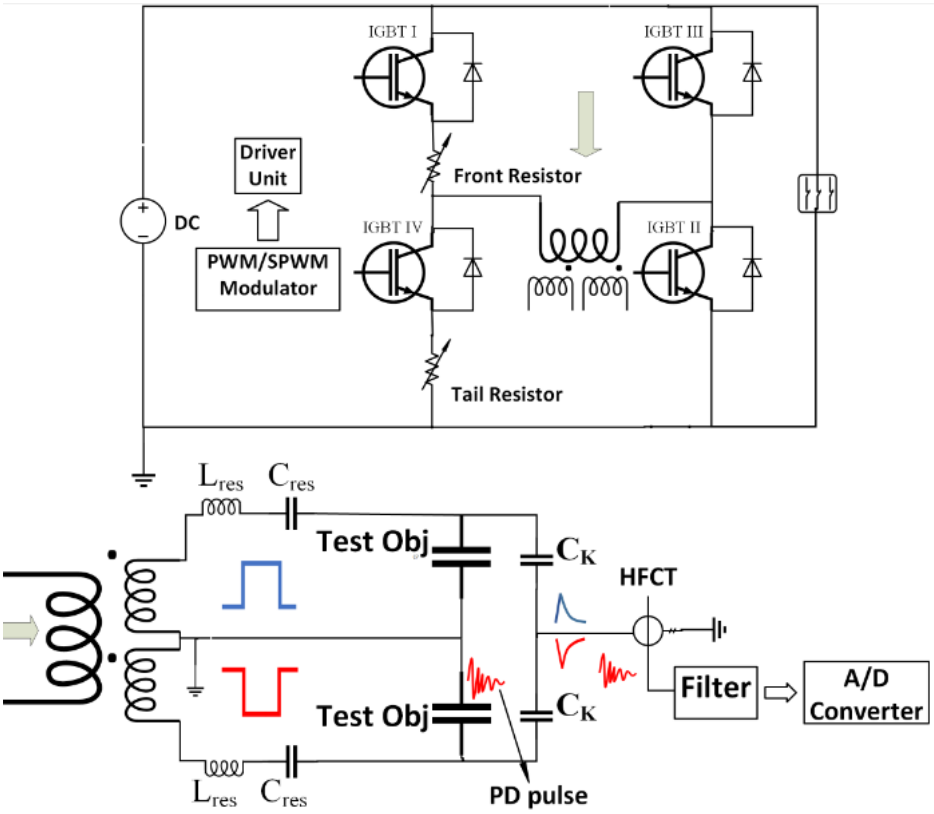

Fig. 1-2: The introduced circuit for the partial discharge measurement. specially designed converter (up) and PD measuring setup(down)

This circuit is capable of producing both bipolar and unipolar PWM/SPWM voltage waveform. A set of external inductances and capacitances shown by L_{res} and C_{res} could be added to adjust the desire resonant frequencies. The PD current was also detected by HFCT directly connected to the measuring equipment.

Fig. 1-3 left shows a portion of the recorded signals at almost 1.5 kV peak-to-peak 36 kHz without the PD source mainly due to residual inrush current both during fall and rise time. Also, Fig. 1-3 right depicts the corresponding signals with the PD source, where the PDs are obvious in switching transitions both during rise and fall times of applied high Voltage.

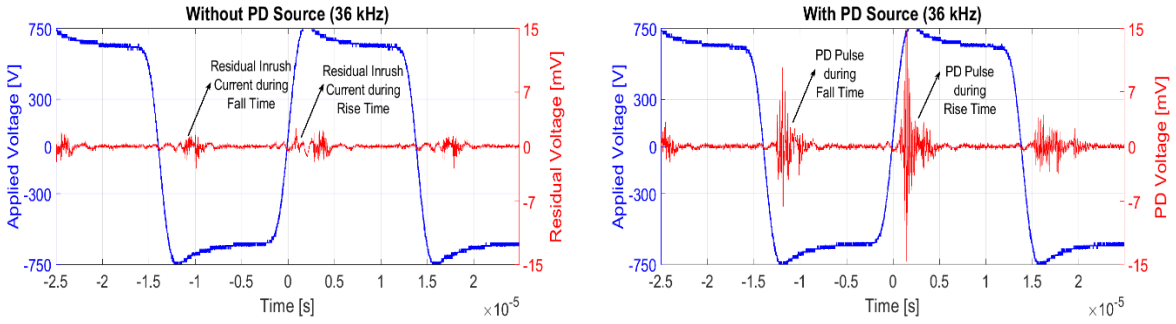

Fig. 1-3: The recorded signals. Left: mainly due to residual inrush current without the PD source, right: when a PD source was paralleled with one of the test samples.

For detailed description please refer to the paper published under the title of '*A novel wideband partial discharge measuring circuit under fast repetitive impulses of static converters*' in Elsevier **Measurement** Journal, paper 108895.

UHF EM wave propagation of negative and positive Corona Discharge in the tank of power transformer

In recent years PD measurement using non-conventional methods like acoustic and Ultra High Frequency (UHF) techniques have been employed as online monitoring and localization tools for power transformers. A challenge to use the UHF PD Measuring method is that it cannot be calibrated, then severity of the captured signals cannot be correlated with the measured PD.

To investigate the possibility of calibration when UHF PD measuring is used, all parameters that affect the measurement output including: detection frequency range, PD type, antenna radiation pattern, antenna polarization, the distance between PD source and the probe as well as the influence of the transformer active part must be considered. Although some researches on propagation of EM waves inside the transformer tank has been established, but the PD source has been simulated easily using a monopole antenna which cannot consider the whole aspect of a real PD source as a complicated transmitter of UHF EM waves. To overcome these shortcomings, an accurate simulation of the PD sources regarding to propagation of the EM waves is essential, which is partly performed in this research.

In this research a drift-diffusion based model has been developed to simulate corona discharge in the air under the both negative and positive high voltage. Essential electron impact reactions namely ionization of nitrogen and oxygen, attachment of electrons to oxygen molecules, and photoionization due to impact of photons on oxygen and wall of configuration, are involved. This is an efficient model to examine propagation of the EM waves on the one hand, and provides a comparison between the characteristics of two forms of corona discharge on the other hand.

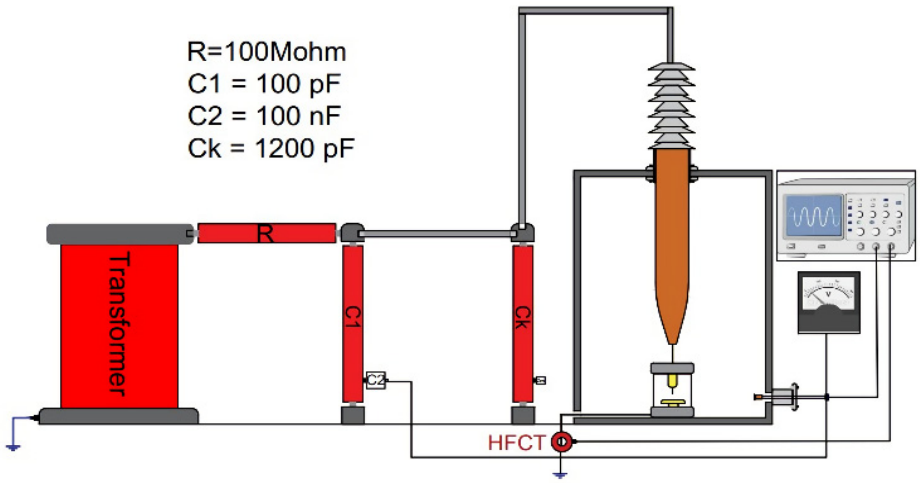

Fig. 2-1: Experimental setup to capture corona discharge signals

In order to investigate the validation of the proposed discharge model, an experimental setup as shown in Figure 2-1 was prepared in HV laboratory. The Measuring of PD activity is carried out in two different ways. Lower frequency components up to 200 MHz is measured using a high frequency current transformer (HFCT), and higher frequency components measuring is accomplished by a monopole antenna inserted inside the transformer tank through the DN80 valve. The reason of using the HFCT instead of the measuring impedance is the higher bandwidth of HFCT that is suitable in the examination of corona discharge behavior. On the other hand, the use of an antenna is essential, because higher frequency components of PD could not be acquired by electrical method. In addition, higher frequency components energy propagates via electromagnetic waves.

The described model aims to solve the differential equations for electron number density, electron energy, photoionization, heavy species, and electric potential. To achieve correct and unique answer, it is necessary to apply the appropriate boundary condition. For the sake of brevity, I have not included formulas, partial differential equations, used relations and simulation boundary conditions.

To compare between the simulated and the measured signals via HFCT, at the lower frequencies, a low pass filter with a cutoff frequency of 200 MHz is applied on the simulated signal. Figure 2-2 left shows the simulated and measured signals at the frequencies less than 200 MHz. The results are promising in terms of amplitude and rise time of the signals, but decay of the simulated signal is less than the measured one. This could be the effect of the measuring path of the experiment setup that extends time duration of the discharge signal.

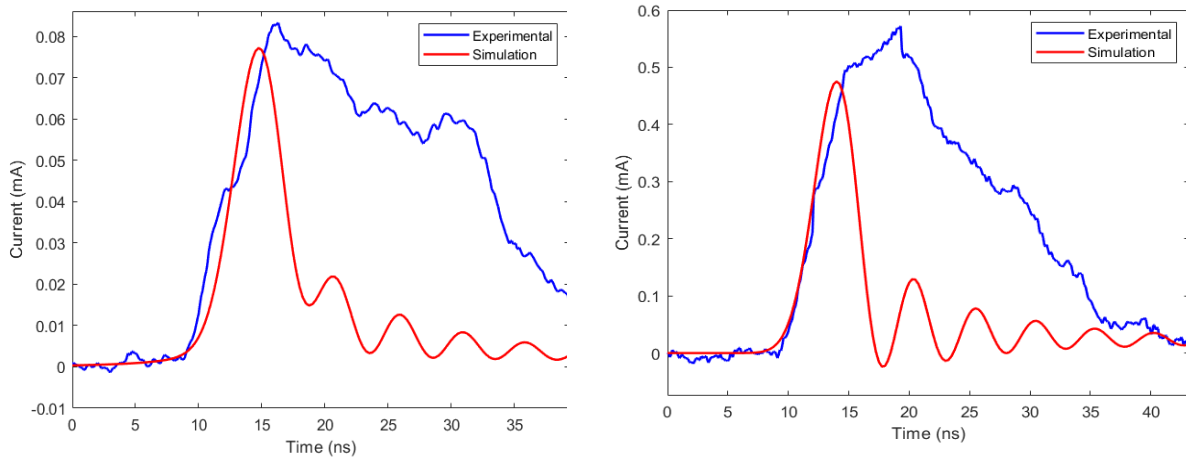

Fig. 2-2: Simulated and experimental negative (left) and positive (right) corona discharge signals under 200 MHz frequency range.

Similar to the negative corona discharge, verification is accomplished for the positive corona discharge at the lower frequencies as well. Figure 2-2 right shows the experimentally measured and the simulated positive corona discharge which a low pass filter with a cutoff frequency of 200 MHz has been applied on that. Results showed that the simulation current signal is in a good agreement with the experiment in terms of rise time and the amplitude of the signals, but the fall time of the simulated current signal is less than the measured one similar to the negative corona discharge.

In general, the relative agreement of the measurement and simulation results validate the simulation method of this complicated process.

As conclusion, the differences between positive and negative corona discharges were examined in this research. Results showed that these two types of corona discharges exhibit different behavior at low and high frequencies which was verified by experimental results.

The effect of the voltage level on the shape of the discharge current was also investigated. It was shown that increasing the voltage level cause decreasing the rise time of the positive and negative corona discharges in different manners. For negative corona discharge time from initiation of discharge to electron avalanche decreases, while for positive corona discharge this effect occurs near the peak of the discharge current.

For detailed description please refer to the paper published under the title of '*Simulation of Negative and Positive Corona Discharges in Air for Investigation of Electromagnetic Waves Propagation*' in **IEEE Transactions on Plasma Science**, volume 50, 2022, issue 9.

M.Sc. Mohamadreza Ariannik

My name is Mohamadreza Ariannik, a 4th year Ph.D. candidate at York University in Toronto, Canada. I am grateful to have the opportunity to complete my internship at Schering Institute in Hanover, Germany in 2022. The well-equipped laboratory at the institute allowed me to complete my experiments by the end of a four-month internship.

Research project: Power transformers are designed to operate below certain loading thresholds. The operating limits on hot-spot temperature (HST) of transformers are stipulated in standards such as *IEC 60076-7* and *IEEE C57.91*. The limitations on the HST are imposed to ensure the safe operation of power transformers and prolong their lifetime. Accelerated ageing of the insulation system, fire point of the insulating oil, and formation of gaseous bubbles justify imposing restrictions on the loading and, therefore, HST of the transformers.

Certain conditions cause an increase in the HST beyond the standard limits. My research evaluates the effects of geomagnetic disturbances and geomagnetically induced currents in power systems and transformers. Powerful solar phenomena such as coronal mass ejections cause the eruption of plasma from the sun's surface. Interaction of the plasma with the earth's magnetic field causes geomagnetic disturbances. As a result, quasi-dc currents known as geomagnetically induced currents (GICs) flow along long conductors in the power system. The increase in the HST of transformers due to GICs cause accelerated ageing of the oil-paper insulation and formation of gaseous bubbles. My research focuses on the latter phenomenon.

I developed a test setup at the Schering Institute to investigate bubble formation on the surface of paper insulation immersed in insulating oil. A schematic of the test setup is shown in Fig. 1. A Jumo iTRON microprocessor controls the temperature rise rate on

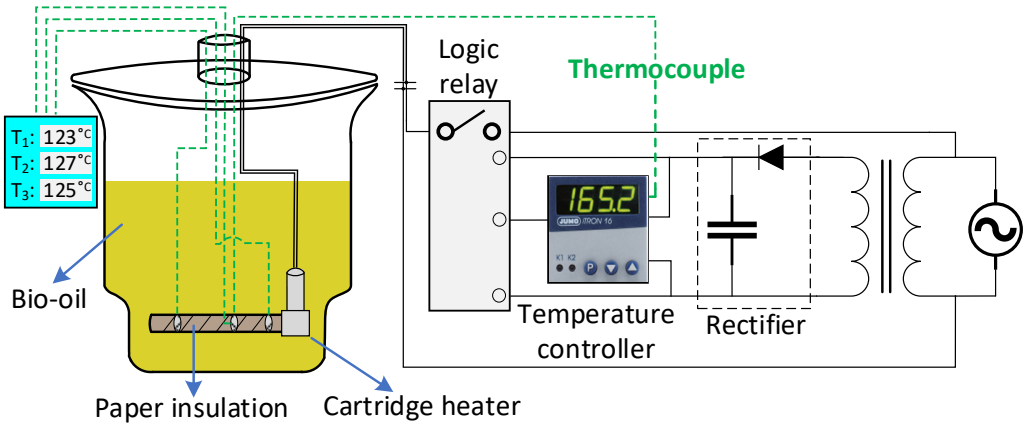

Figure 1: Schematic of the test setup

the heater's surface. Two types of paper insulation, including Kraft and thermally upgraded papers, are used in the experiments. The cartridge heater is inserted in a vessel filled with Midel 7131 synthetic ester oil. Several strips of the paper insulations are heated and then remain in contact with ambient air to absorb moisture at different levels. The moisture content of the paper samples is verified by monitoring the increase in weight using a high-resolution scale.

The power transformer loading guides are developed for mineral-oil-immersed transformers. They do not account for biodegradable ester oils, which are more desirable and preferred over conventional mineral insulating oils. Compared to mineral oils, biodegradability, higher thermal conductivity, and higher flash point are among the advantages of natural and synthetic ester oils. Furthermore, a few experimental results are available for alternative paper insulations. In this regard, my experiments at the Schering Institute are performed on synthetic ester oil, Kraft paper, and TUP. Furthermore, the experiments are repeated at two different temperature rise rates, 3 °C/min and 20 °C/min, to account for normal and emergency loadings during geomagnetic disturbances.

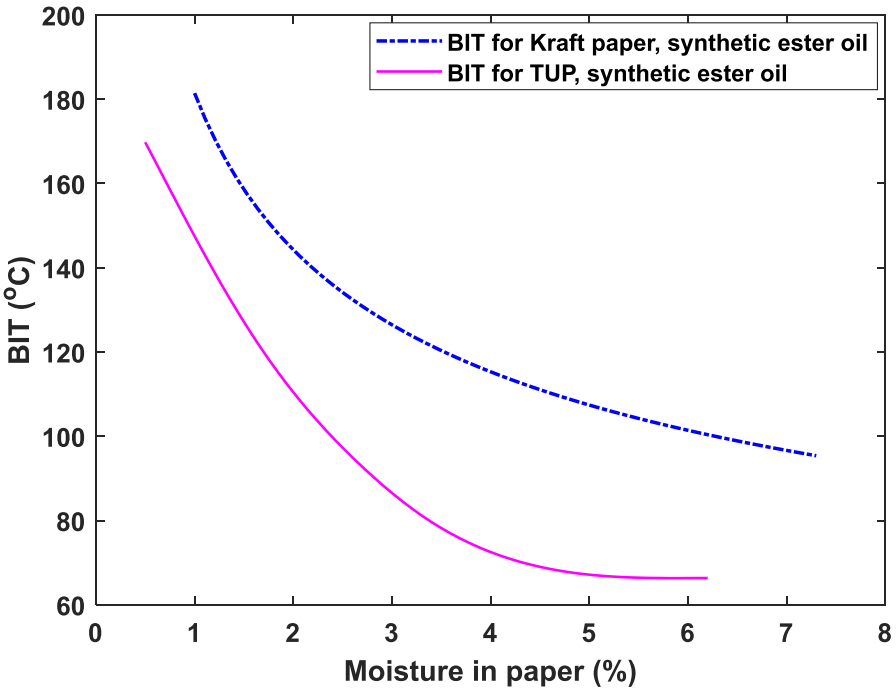

Figure 2: BIT for Kraft paper and TUP

Bubbling inception temperature (BIT) is considered a criterion in the transformer loading guides to protect the insulation strength of the transformers. Video recordings of the experiments are scrutinized to detect the BITs for both Kraft paper and TUP. A curve is fitted to the results of the experiments conducted at 3 °C/min temperature rise rate, as depicted in Fig. 2.

The results for the Kraft paper reveal that using synthetic ester oil instead of mineral oil has negligible influence on BIT concerning the experimental results reported in the literature. Note that the loading standards consider a 140 °C limit at 2 % moisture content in the paper insulation. Nevertheless, based on the BIT curve, proposing a single value for BIT endangers older units with higher moisture content. On the other hand, the results indicate that at the same moisture level, bubbles emerge on TUP's surface at a considerably lower temperature than on Kraft paper. However, it was observed that the accumulation of bubbles on the paper's surface and the rate of bubble generation differ between these two papers. Fig. 3 shows an extensive bubble accumulation on the surface of the Kraft paper. Even though BIT is lower for TUP, significantly fewer bubbles emerge on its surface than on Kraft paper. Therefore, a more inclusive comparison is required to evaluate bubbling phenomena on TUP and develop operating limits for power transformers.

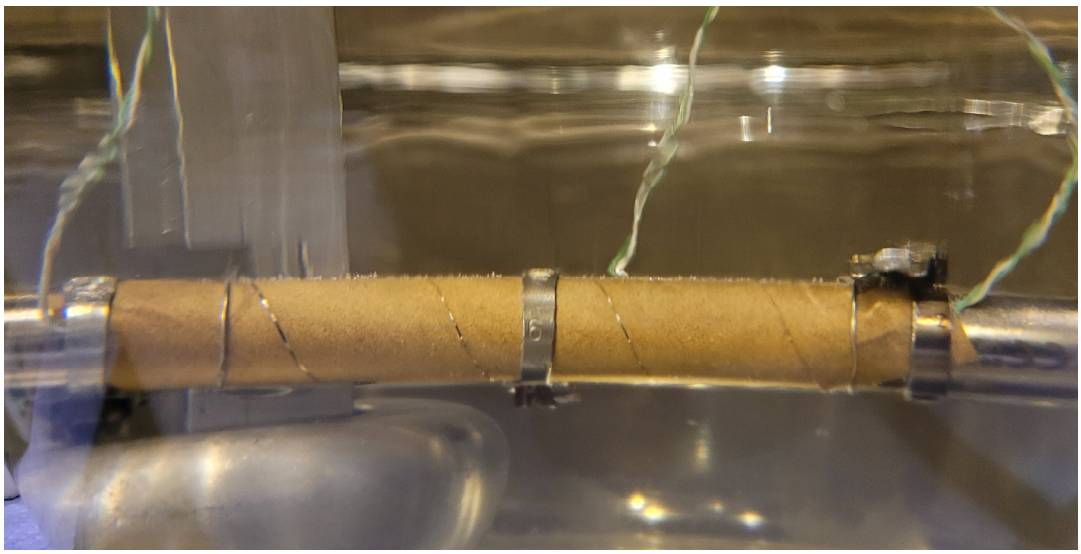

Figure 3: Accumulation of bubbles on Kraft paper

The Rate of hot-spot temperature rise during a severe geomagnetic disturbance is significantly higher. In this regard, the experiments are repeated at a 20 °C/min rate, and it was observed that BIT could be as low as 30 °C. As expected, the differences between Kraft paper and TUP are not limited to BIT. A stream of continuous bubbles is released from Kraft paper, whereas a few occasional bubbles emerge on TUP. Considering both Kraft paper and TUP suffer from a low BIT at high temperature rise rates, other parameters are required to be introduced to evaluate and compare their insulation strength.

Interpreting the experimental results and analyzing the detrimental effects of bubble accumulation and generation rate constitute an ongoing phase of the research collaboration. The results of this joint research project between York University and Schering Institute at Leibniz University Hanover are soon to be published.

5 Doctorates

Study of oil/pressboard progressive creeping discharge under divergent electric field

M.Sc. Xin Zhou **Promotion day: 16.03.2022**

Motivation and Research Outline

The oil/pressboard progressive creeping discharge is a particularly dangerous phenomenon, as it can fail the major insulation system even under normal operating conditions. However, the progressive creeping discharges have thus far still not been fully understood, making it still a difficult task to effectively detect the ongoing incidents. This problem is largely due to the highly intricate nature of the progressive creeping discharge. On the one hand, it involves multiple materials, exhibits varying discharge patterns, and features different accompanying phenomena. On the other hand, it can generate distinct faults and fails the insulation system in utterly different manners.

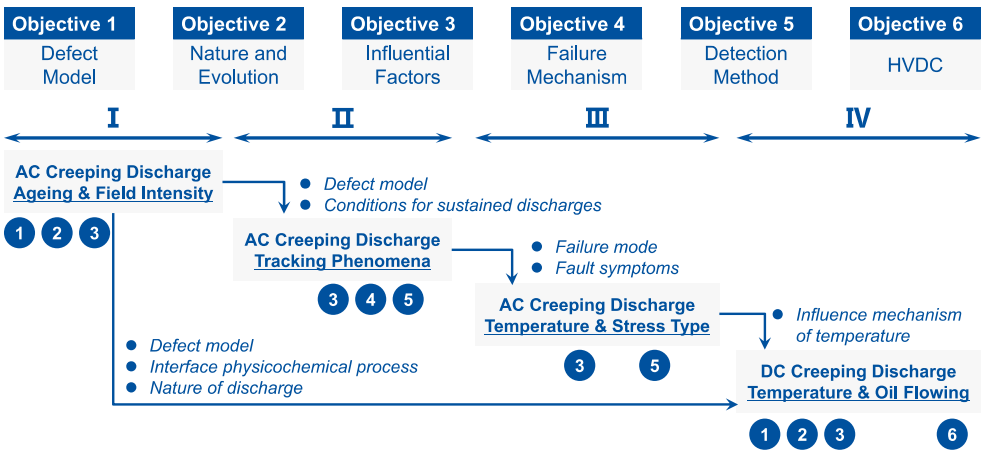

Figure 1: Research outline

The present work aims to provide a better understanding of progressive creeping discharges. The primary objectives are:

(1) to formulate a valid defect model of creeping discharge as well as to identify its discharge sources, discharge pattern, and discharge signals;
(2) to draw a clear line between damage-free creeping discharges and failure-inducing creeping discharges;
(3) to give clear illustrations and convincing explanations to the typical accompanying phenomena, such as white marks, tracking, and bubbling;
(4) to investigate the effects of critical influential factors on the inception and development of creeping discharges under AC voltage;
(5) to propose a tentative methodology to detect dangerous creeping discharges in power transformers;
(6) to examine the progressive creeping discharges under the DC field based on the relevant knowledge obtained under AC voltage.

To fulfill the task, this work carries out four consecutive and independent investigations (I, II, III, and IV), and Figure 1 illustrates the research outline of the entire work.

Investigation I

The first investigation focuses on the fundamental phenomena of the progressive creeping discharge as well as the influences of pressboard ageing and voltage amplitude under divergent AC voltages. The major purposes are to better understand the fundamental characteristics of creeping discharge, to examine its long-term trend, and to revisit the influences of ageing and voltage with deeper insights.

We used a special electrode configuration to generate sustained creeping discharges. A ramp-stress test is used to determine the interface partial discharge inception voltage (PDIV) and the flashover voltage versus pressboard ageing. Constant-stress tests are carried out to investigate the partial discharge (PD) behaviors, the pressboard surface temperature, and the oil-dissolved gases. Besides, we also explored the oil/pressboard interface morphology, studied the interface field distribution, and systematically interpreted the competing effects of ageing by analyzing the pressboard water absorption capability, fiber integrity, and absolute water contents.

It is found that the progressive creeping discharge is a multi-sourced discharge that comprises primarily oil corona discharge and surface discharge. The pressboard ageing affects only the interface PDIV. The progressive discharges exhibit in general a constant PD pattern but a diminishing intensity, and nevertheless can be sustained for the severely-aged pressboards under strong voltages. The major reason for a sustained creeping discharge is the intensified negative discharges, which are possibly due to the field emission in the triple-junction area. The general diminishing trend of progressive creeping discharge is probably caused by the interface moisture emigration governed by the competing effects of pressboard aging. Hydrogen is the key faulty gas of progressive creeping discharge and its concentration grows with voltage and ageing, and no pressboard overheat is found during the discharge process.

Investigation II

The second investigation presents both an experimental study and a theoretical discussion on the relevant faults resulting from progressive creeping discharge. The primary objectives are to demonstrate the fault progression, investigate their characteristic phenomena, and explore the failure mechanisms.

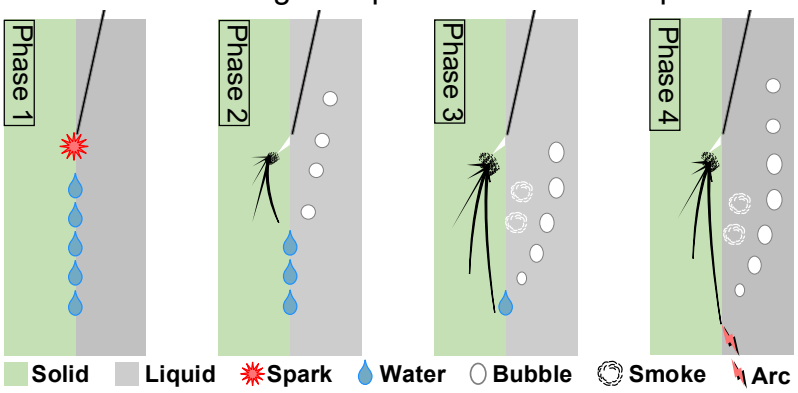

Figure 2: The failure mode of internal treeing due to creeping discharge

Pressboard ageing, voltage amplitude, and pressboard type are configured to generate the faults under divergent creeping stresses. The fault progression is recorded by a high-resolution camera, partial discharge (PD) device, and optic-fiber thermometer. The damaged pressboards are scrutinized by microscopy and image-processing techniques, and gas chromatography is used to analyze the gas compositions.

The results show that the progressive creeping discharges could generate either internal treeing or surface tracking to the pressboard. The fault type is dependent on the pressboard density, the voltage amplitude, and the pressboard ageing. The progression of internal treeing shows distinct stages of different interface phenomena, such as spark discharge, white marks, and bubbling effect, as well as varying discharge patterns. In contrast, the progression of surface tracking is a simple but hardly noticeable process due to the PD disappearance. The internal carbonization channels are the fundamental causes of interface phenomena and a theoretical model is proposed to expound the development of the internal carbonization channels, which considers the charge emission, the pressboard pyrolysis, and the percolation theory. The failure mode of internal treeing is schematically illustrated using a four-phase model (see Figure 2). The development of surface tracking is governed by ageing-induced moisture behaviors and field distortion due to carbonization. A detailed comparison is made between internal treeing and surface tracking in terms of the occurrence condition, initiation mechanism, growth driver, and growth characteristics.

Investigation III

The third investigation studies the effects of temperature and stress type under divergent AC voltage. The primary objectives are to investigate the effects of temperature and stress type on creeping discharge and its related failure modes, to examine the discharge behaviors during fault progression, to explore the mechanisms of influential factors, and to propose a novel method for detecting developing faults.

A ramp-stress test determines the short-time interface electric strengths, and long-term tests are carried out at different temperatures using constant and step stresses, respectively. Afterwards, a novel methodology is proposed to detect the developing fault using synchronous partial discharge (PD) and online dielectric measurements.

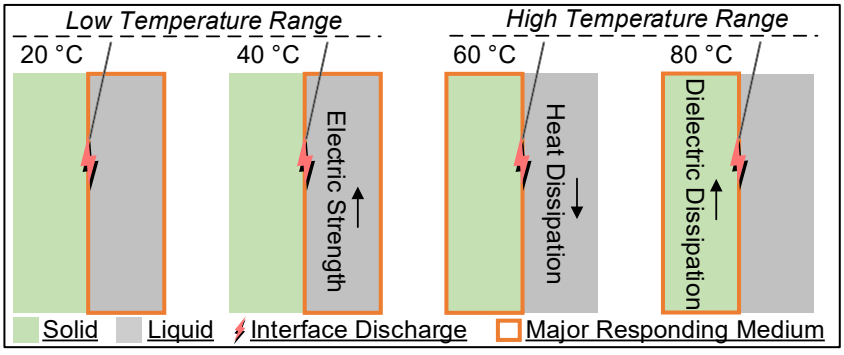

Figure 3: Illustration of temperature's influence on creeping discharges

It is found that the interface short-time electric strengths correlate positively with the temperature. In long-term tests, the creeping discharges can generate three failure modes to oil/pressboard insulation: interface flashover, surface

tracking, and internal treeing. Different failure modes vary significantly in the discharge characteristics and the severities of damage to the pressboard. The temperature exerts complex influences on the creeping discharges. It influences the material physical properties, acts synergistically with the field in exacerbating the pressboard dielectric dissipation, and changes the interface field and loss distributions. The failure mode of creeping discharge is subject to these factors and their sophisticated interplays. The principal influential factor would vary as the temperature rises, thereby resulting in different failure modes (see Figure 3). The influence of stress type is related to the cumulative effect of stressing and the voltage rising steepness. The proposed methodology of synchronous PD and online dielectric measurements proves a potent tool for detecting internal treeing. The PD measurement can identify the discharge type, whereas the online dielectric measurement is highly indicative of the pressboard damage and show superior detection sensitivity.

Investigation IV

The fourth investigation studies the influences of temperatures and forced oil flows on oil/pressboard progressive creeping discharges under DC voltage. The primary purpose is to examine the fundamentals of oil/pressboard creeping discharge under DC voltage.

It is found that the temperature rises increase the oil and pressboard DC conductivities exponentially, widen the permittivity mismatch, and narrow the conductivity mismatch. Under static oil, DC creeping discharges exhibit two kinds of PDs (PD 1 and PD 2), which show distinctions in the inception voltage, magnitude, intervals, and intensity. PD 1 is probably the oil discharge, and PD 2 is the pressboard cavity discharge, which is enabled by an extra local field due to field ionization. The temperature rise has competing effects on PD 1, including the decline of oil relative saturation and the augmentation of oil field intensity. By comparison, the temperature rise exerts a straightforward effect on PD 2, increasing its magnitude while decreasing its intensity.

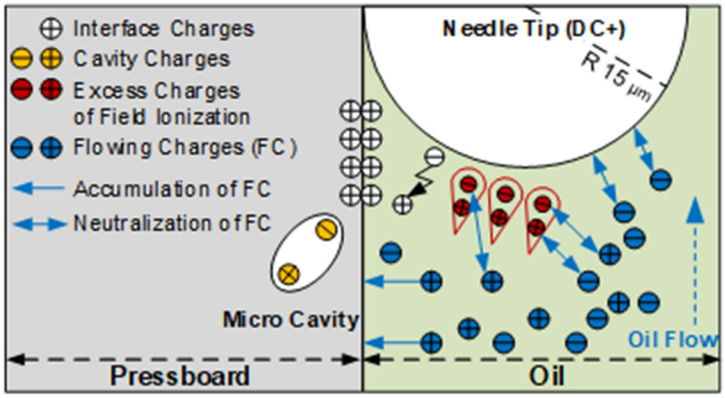

Figure 4: Electrical and physical processes at triple-junction area with oil flows

The forced oil flow shortens the interface withstand time and generates erratic PD pulse trains. The pulse train results possibly from the massive neutralization of excessive space charges from streaming electrification (see Figure 4). The oil speeds and the competing effects of temperature determine the quantities of the space charges, thus influencing the pulse trains.

Summary
The present work extends the fundamental knowledge of the oil/pressboard progressive creeping discharges under AC and DC fields, systematically revisits the multi-faceted influences of critical factors, provides a clear demonstration and reasonable elucidation of relevant faults and failures, and offers a framework for monitoring and diagnosing the dangerous creeping discharge in power transformers. The research results are expected to serve as a base for future scientific studies and a piece of valuable information for practical applications.

6 Research

Development of non-contact measuring systems for the measurement of pulsed high voltages

M.Sc. Moritz Kuhnke

Impulse voltages are required in high-voltage tests to simulate the stresses caused by external and internal overvoltages and for basic investigations of breakdown processes. The testing of high-voltage equipment for resistance to atmospheric and/or switching-induced impulse voltages is carried out with full or chopped impulse voltages whose peak values and time parameters must be recorded with high accuracy. For the metrological determination of these values, commercial measuring instruments are available to the users, which operate with measurement uncertainties in the range of 1 % for full and also chopped impulse voltages. Due to the worldwide expansion of energy transport capacities, which in many places can only be covered by ultra-high voltage (UHV) lines, high-voltage pulse generators with increasingly higher voltages are required for testing, as well as the associated measuring systems.

Usually, high-voltage impulse measurement is performed with a resistive or damped capacitive voltage divider. The dividers used for impulse measurement have a similar geometrical height (insulation coordination) as the pulse generator. However, for static reasons, they also require large bases and support structures that take up a lot of space in the high-voltage test field. They are also high-cost devices due to the use of precision components. The dividers add a capacitive load to the test circuit, which reduces the efficiency of the pulse generators. Linearity studies in the measurement of lightning and switching impulse voltages show some problematic aspects. Investigations have shown, for example, that the use of unshielded voltage dividers can lead to undesired distortions of the measurement results due to the nonlinear field distribution, corona discharges or the proximity effect.

The German national metrology lab (*PTB*) and the *Schering Institute* have started to investigate measurement systems which work contactless and use wireless data transmission with comparatively little effort, thus operating completely galvanically isolated. These systems (Fig. 1) are light and compact and can easily be used anywhere with the aid of a battery pack. They offer the possibility to measure even high voltages completely contactless and can be remote controlled via WLAN. The precision of such field probes is not yet comparable with ohmic or damped capacitive dividers.

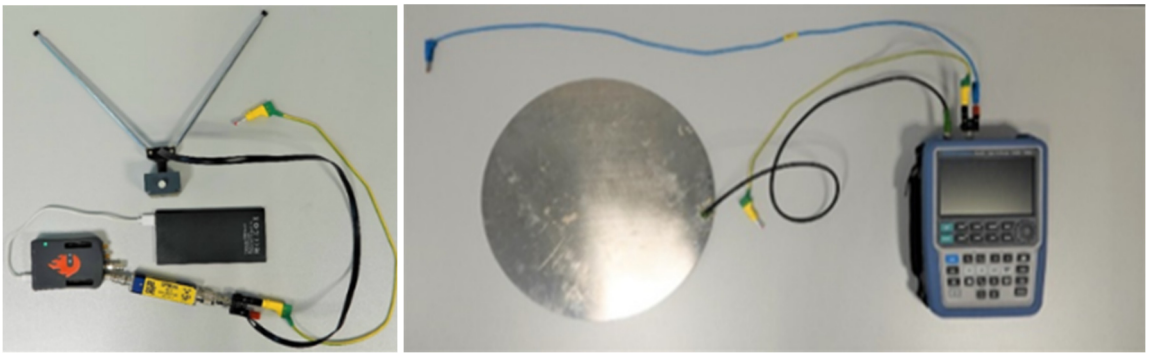

Figure 1: Field probes and measuring instruments "*Stemlabs Red Pitaya*" (left) and "*Rohde und Schwarz RTH1002*" (right).

The reference measuring system of the *PTB* and the *Schering Institute* of the *LUH* was used as a reference for checking the field probes. In the case of *PTB*, this is an in-house development based on a National Instruments system, while the Schering Institute of *LUH* used a *HiRES* system from the manufacturer *High-Volt*.

The measurement setup in the high-voltage hall of *PTB* was carried out with a standard configuration of the reference measurement system. A pulse voltage generator (Marx generator) generates pulses which are recorded with the aid of the reference measuring system (Zängl divider). The reference divider is a damped capacitive voltage divider up to 1000 kV peak voltage. The probes were set up at a distance of approx. 6 meters (*Rohde und Schwarz RTH 1002*) and approx. 10 meters (*Stemlabs Red Pitaya*). Voltages of up to approx. 800 kV were generated with the pulse voltage generator. These pulses were recorded simultaneously from all the systems described. Figure 2 shows some important results of the measurements against the reference divider.

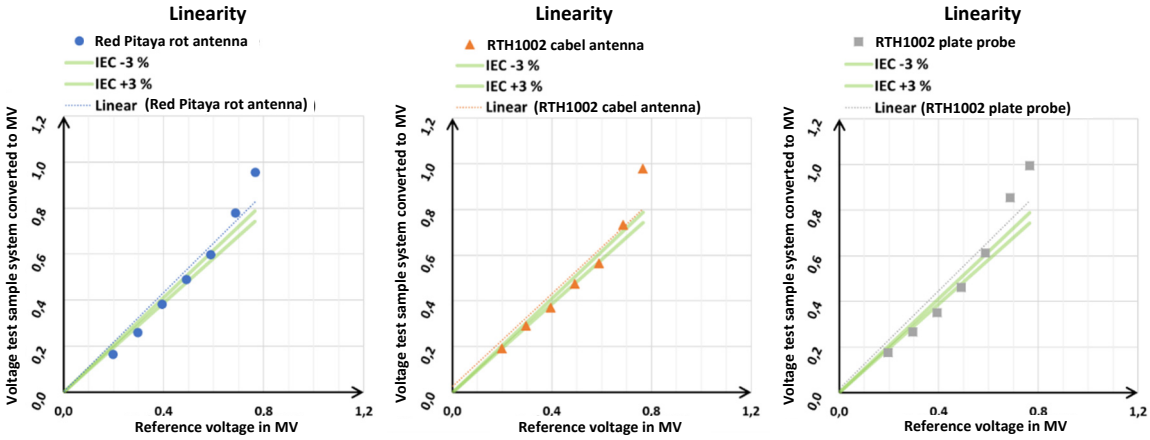

Figure 2: First series of measurements on the voltage linearity of the field probes up to 800 kV

Due to the good first results and the promising application possibilities, these investigations are to be further investigated together with *PTB* within the framework of a *DFG* project. The corresponding application was submitted this year.

An Investigation of an Online Monitoring System for Hermetically Sealed Transformers

M.Sc. Behnam Balali

Power transformers are key elements of the power grid. Their condition-based maintenance has in today's industrial world proven to be financially beneficial for the operators since any failure of the equipment is associated with enormous costs. For optimized maintenance, the trend is moving toward the use of online monitoring systems. Medium voltage step-up power transformers are widely used in wind power generators to boost the turbine generator output voltage from a few hundred volts to the collector system's medium voltage levels. Since these transformers are usually installed inside the tower or nacelle of the wind turbine or in a small utility close to the tower, size is an important factor. The manufacturers design these types of transformers as compactly as possible. One of the most common forms is hermetically sealed oil filled transformers. Since the temperature of these transformers changes frequently under wind conditions, special measures are taken into account considering the expansion of the insulating liquid. The sealed tank can be equipped with fins that expand due to higher temperatures. Moreover, in order to prevent the insulating liquid to be exposed to ambient air and humidity, thus preserving its electrical properties, the transformer is sealed utilizing a gas cushion, usually out of nitrogen or dry air.

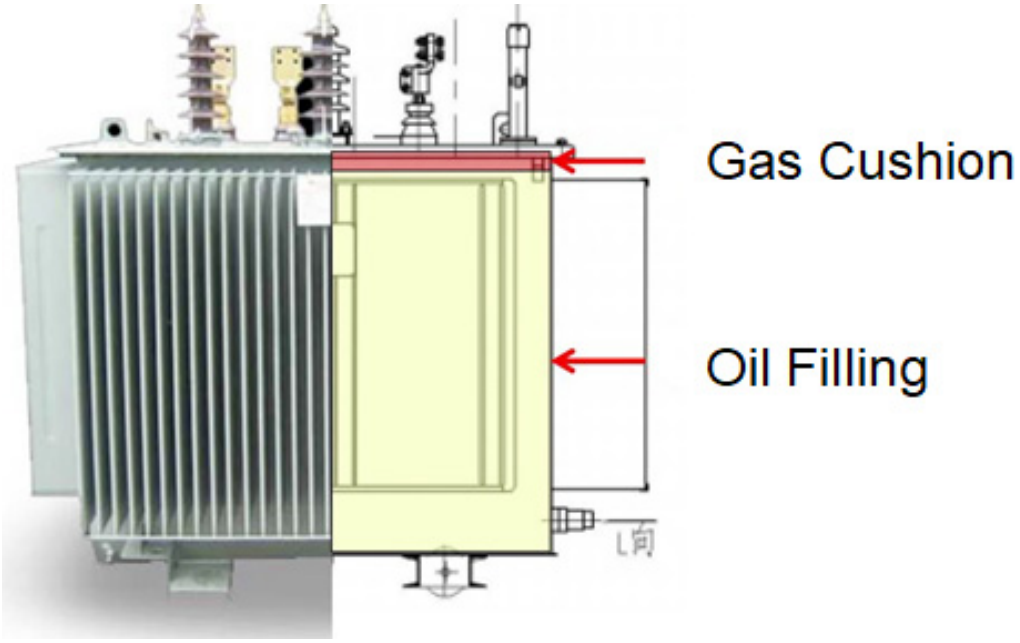

Figure 1: Structure of a hermetically sealed transformer

In case of severe faults, the generation of a considerable amount of fault gases is expected, which will, in the case of hermetically sealed power transformers, gradually escape from the insulating liquid and diffuse into the gas cushion. Hydrogen is one of

the byproducts generated in the process of most common faults in power transformers. Dissolved gas analysis (DGA) is one of the most effective diagnostic methods in power transformers. An oil sample is taken from the transformer and analyzed by extracting the gas from the liquid and separating it into its constituent gas elements. Modern techniques enable the identification of potential faults long before they occur. There are online DGA monitoring systems available on the market, but since the monitoring cost exceeds the budget envisaged by the manufacturers and operators, they usually are not applicable for small hermetically sealed power transformers.

As a cost-effective and compact alternative to gas chromatography, a semiconductor-based online monitoring system of undissolved fault gases is developed at the Schering-Institute. This monitoring system is based on a set of integrated sensors, tracking the concentration of fault gases in the gas cushion continuously, through which faults in the insulating system can be detected early. Furthermore, physical parameters such as temperature, pressure, and humidity are also recorded permanently. A pipe is suitable for the installation of the monitoring system since all undissolved fault gases accumulate under the lid of the transformer, move up the pipe, and gradually reach the fault gas sensors. Furthermore, due to the length of the pipe, there is some distance between the surface of the insulating liquid and the monitoring system, which offers additional protection for the fault gas sensors.

Figure 2: Overview of the hermetic transformer with the installed online monitoring system

Development and Construction of a Pulse Voltage Generator for the Excitation of Space Charges in Polymeric Insulating Materials

M.Sc. Sebastian Braun, B.Sc. Christian Kohlsaat

Until now, there is no standardized procedure with which the service life of solid insulating materials can be determined as a function of the electric field strength under DC voltage stress. This is mainly due to the formation of space charges in the insulating medium, which influence the reliability and service life. The Pulsed-Electro-Acoustic (PEA) method can be used to determine the space charge distribution. This is a non-destructive method based on Coloumb's law. If a force acts on the space charges, triggered by an electrical voltage pulse, an acoustic wave proportional to the space charge distribution is generated in the insulating material. This can be measured with a piezoelectric foil. This paper presents the design of a pulse voltage generator for the excitation of space charges in polymeric insulating materials. The voltage shape of the pulse influences the quality of the waveform of the acoustic wave. Errors or inaccuracies in the voltage pulse would, therefore, affect the entire measurement. From the classes of pulse voltage generators, the line pulse generator was chosen because it is an inexpensive and simple method to generate voltage pulses with the desired requirements. Other methods, such as the Marx generator with peak and tailcut switches and a semiconductor circuit, were not implemented because they either take up too much space and are therefore, not suitable for a compact PEA system, or require a complex correction of the signal because they have the property of a strong reverberation that disturbs the acoustic signal. The circuit diagram of the line pulse generator is shown in Figure 1.

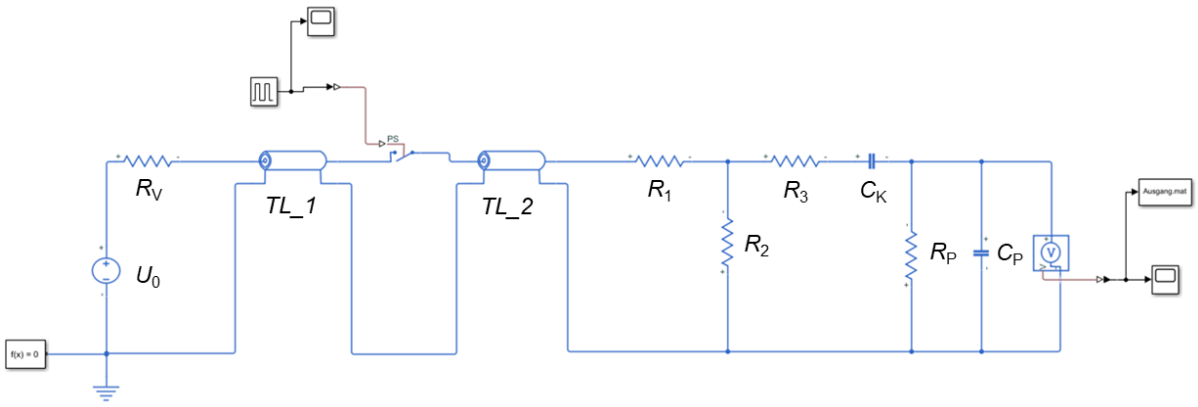

Figure 1: Circuit diagram of the pulse voltage generator

This consists of a DC voltage source U_0, a series resistor R_V, a coupling capacitor C_K, a load or the test object consisting of R_p and C_P, two coaxial cables *TL_1* and *TL_2*

and an impedance matching consisting of R_1, R_2 and R_3. The pulse generation of a line pulse generator is based on the travelling wave effect. After the first coaxial cable *TL_1* has been charged to voltage U_0, two transient travelling waves with an amplitude of 0.5 U_0 are generated when the relay is closed, since both coaxial cables have the same wave impedance. One wave travels with positive amplitude in the direction of the test object. The other part of the wave travels with negative amplitude towards the voltage source and is completely reflected in front of it at the series resistor due to the high impedance difference. The pulse width is determined by the length of the first cable (*TL_1*) and the propagation speed in the cable. To ensure that the voltage waves are not reflected after passing through the second coaxial cable *TL_2*, the terminating impedance was matched to the wave impedance of the coaxial cables using a T-element. For this purpose, simulations were used to determine resistor combinations that represent the most accurate possible compliance with the wave impedance of 50 Ω. In addition to the desired rectangular shape of the pulse, the pulse width was set to a maximum of 20 ns and the amplitude to 500 V as additional design goals. The values of the individual components determined according to these criteria as well as the sizes of the DUT can be taken from Table 1 and the simulated voltage pulse is shown in Figure 2.

Table 1: Component and test item sizes of the pulse generator

Component	R_V	R_1	R_2	R_3	C_K	R_P	C_P
Size	1 MΩ	10 Ω	68 Ω	47 Ω	700 pF	1 GΩ	33,4 pF

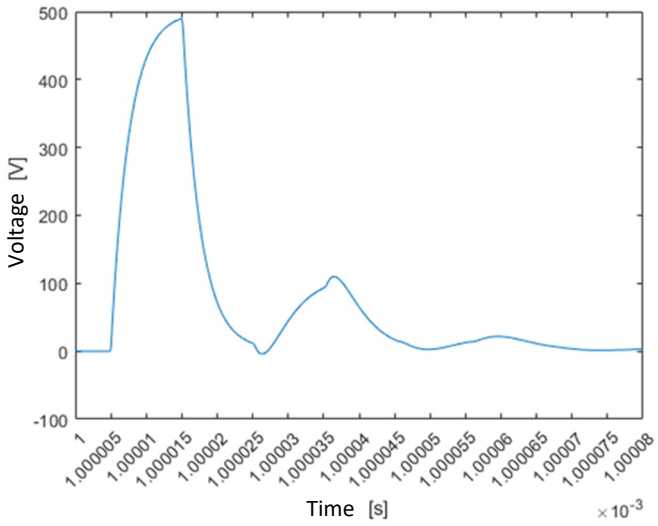

Figure 2: Simulated voltage pulse with low post oscillations

After completing the simulation of the pulse voltage generator, circuit boards were designed to create a good quality and, as well as, to get a compact generator circuit design. A circuit board was created for the fuse protection of the voltage source, one for the switching relay, including the generation of the 100 Hz switching signal, and a circuit board for the impedance matching. Dividing the circuit groups into individual

boards is advantageous, since it prevents internal interactions between the respective circuit groups. Furthermore, a conductor path wave impedance of 50 Ω was taken into account in the board design for the main boards and the conductor paths were kept as short as possible in order to minimize interferences. In addition, SMD resistors were chosen as the type of component for impedance matching in order to reduce further interference, in particular due to the formation of conductor loops and the associated inductive voltage coupling. Interferences were also attenuated with the help of relatively large copper surfaces with earth contacts. For further shielding against external interference, the assembled boards were installed in grounded metal housings. Furthermore, all boards were designed modularly so that an extension of voltage pulses with the same characteristics can be easily implemented. The developed pulse voltage generator is to be used in a PEA measuring system in the future.

Concept for Long-Term Space Charge Measurement of Polymeric Insulating Materials Under High DC Voltage Stress

M.Sc. Sebastian Braun

As a result of the worldwide energy transition and the associated changes in the energy system, new high-voltage transmission systems are being installed which, in contrast to the previously used alternating voltage technology, will be based on direct voltage transmission. Solid polymer insulating materials are increasingly being used in high-voltage direct current transmission systems (HVDC). In projects such as Suedlink or SuedOstLink, lines with a length of up to 700 km are to be realised with extra-high voltage cables whose insulation system consists of cross-linked polyethylene (XLPE). The question here is whether the reliability and durability of the HVDC components is at least as good as that of the AC systems. Long-term experience with polymeric insulating materials in HVDC systems is limited compared to that of AC systems. The service life of a high-voltage component is largely determined by the insulation system used, whereby methods have been developed for AC voltage with which the service life of solid polymer insulating materials can be determined as a function of the electric field strength. Such a method is currently not available for DC voltage, which makes the lifetime estimation of the insulation system almost impossible. One reason for this is the formation of space charges in the insulation system under DC voltage, which significantly influence the service life of the insulation. In order to be able to estimate the service life of polymeric insulating materials under DC stress in a similar way as under AC stress, it is necessary to measure the formation of space charges in the insulating material volume during the entire ageing process and thus to be able to investigate the influence of these on the service life exponent at different field strengths, temperatures and ageing periods. For this purpose, a concept and a set-up for the ageing of polymeric insulating materials are presented in this article. The measurement set-up enables the simultaneous ageing of five test specimens with field strengths of up to 100 kV/mm and temperatures in the range of 20 to 80 °C. Furthermore, the measuring device enables a continuous measurement of the space charge distribution in the insulating material volume over the entire duration of the ageing by means of the Pulsed-Electro-Acoustic method (PEA). Figure 1 shows the schematic

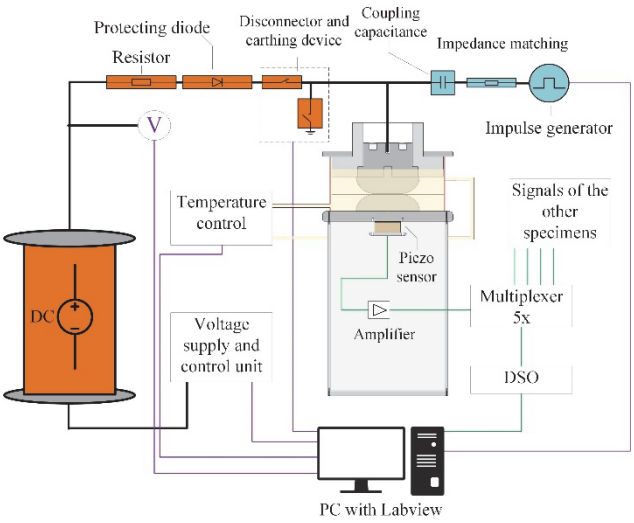

Figure 1: Overall measurement set-up for ageing polymer insulating materials and simultaneous space charge measurement

structure of the entire measuring system. The test specimens (5 in total) are aged in parallel via a DC voltage source and a simultaneous space charge measurement of all test specimens is carried out. The DC voltage source shown on the left in Figure 1 ages the test specimens with a DC voltage of up to 200 kV, depending on their thickness. The acoustic detection unit, including piezoelectric foil, is mounted under the earth electrode in a shielded housing. The space charges are excited by a square-wave voltage pulse in the nanosecond range from a line pulse generator. This is connected to the respective test object via a coupling capacitor. The measurement data acquisition, temperature control, as well as, the control of the automatic separation and earthing of a punctured test specimen is carried out by a LabVIEW program on the measuring PC. The planned structure of the electrodes is shown in Figure 2. The insulating material to be tested is located between two electrodes, which have a Rogowski contour and are made of aluminum. The high-voltage electrode is plugged into a stamp electrode above it. The stamp electrode serves as a receptacle for the electrode stamp made of polytetrafluoroethylene (PTFE) lying on it. Furthermore, on the upper side of the stamp electrode there are holes or receptacles for the connection of the high voltage, as well as, for two compressed air cylinders, which serve to control the contact pressure. The concept presented here is intended to investigate the ageing behavior of a series of polymeric insulating materials. The aim is to investigate the space charge behavior over long periods of time during ageing, since changes in the space charge density distribution can still occur after several weeks, which have an influence on the ageing mechanisms in the insulating material volume. Specifically, five test specimens with a thickness of 1 mm are to be aged electrothermally for up to 3000 h with voltages of up to 100 kV. For a better statistical evaluation, the measurements will then be repeated with identical boundary conditions with five further test specimens. The ageing is to be carried out at a total of seven different voltage levels, from which a type of endurance life law is then to be determined. In addition, the described measurements will be carried out at different temperatures. Further investigations, such as the exact determination of the influence of the residual ripple of the voltage source on the space charge behavior, as well as, the variation of the thickness of the test specimens to investigate the volume effect, are planned. The investigations are taking place within a project funded by the German Research Foundation (DFG) and in cooperation with the Zittau/Görlitz University of Applied Sciences.

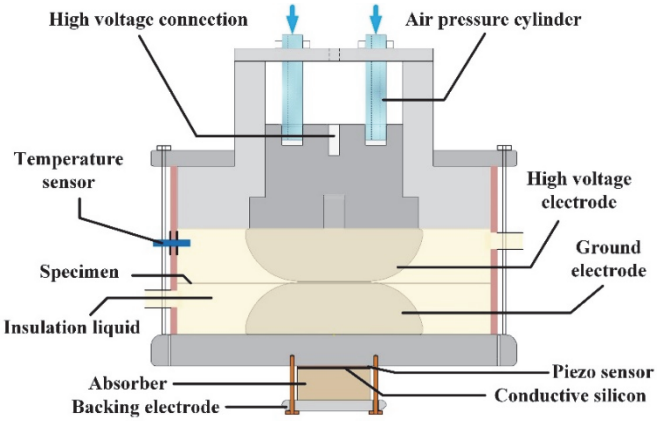

Figure 2: Upper part of the measuring set-up with electrodes, housing and compressed air cylinder for controlling the contact pressure

Test rig for space charge measurement with LIPP method and simultaneous aging of polymeric insulating materials under high DC voltage

Dipl.-Ing. (FH) Henry Hirte

In parallel to the upcoming investigations on aging and long-term space charge measurement at the Schering Institute, a similar test set up is being worked on at the University of Applied Sciences in Zittau/Görlitz. This is also used for the simultaneously electrothermal aging of five polymeric insulating materials specimens, but with the difference, that the LIPP (laser-induced-pressure-pusle) method is used here. In addition to the comparability and mutual validation of the space charge measurement methods, the aim is to determine the voltage endurance characteristics of polymeric insulating materials at high DC voltages. The joint work in the panel of the IEC technical committee 112 allows to actively shape the standards in the field of voltage endurance testing at DC with the results of this project.
The research work of the last decades has already been able to investigate many dependencies in space charge formation. For example, the formation and movement of space charges in polymeric insulating materials depends not only on the electric field strength but also on temperature, contact-pressure, material production and electrode material, among other factors. Also, some models have been developed that attempt to physically explain the relationship between space charge formation and aging. Even though it has been proven that space charges have a significant effect on the aging of an insulating material under DC voltage, there is still no existing research work on this subject that aims to adapt the current test method for determining voltage endurance tests at high DC voltage.
It is therefore planned to investigate a group of selected, widely used insulating materials consisting of silicone, HDPE and cast resin in order to develop a valid method for the determination of the voltage endurance coefficient under DC. The test duration is divided in seven stages with 3000h at the last stage. For a series of tests, 10 samples will be used and the series of tests will be performed once at room temperature and once at 80°C in order to investigate the temperature effect on space charge formation. The corresponding test set up can be seen in Figure 1.

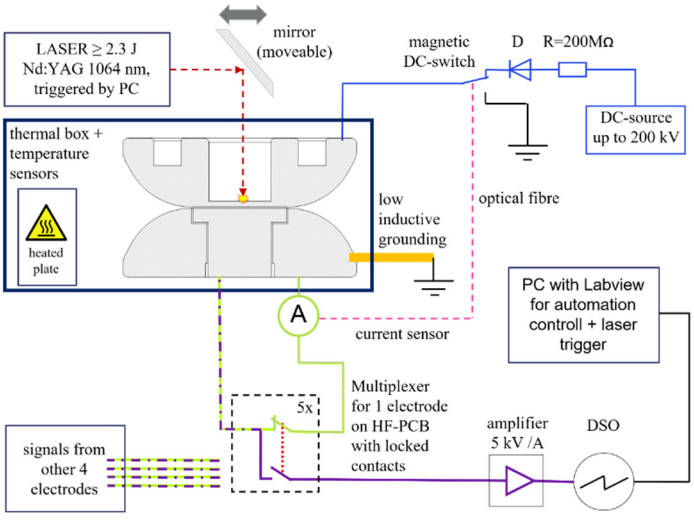

Fig. 1: test set up for space charge measurement with LIPP-method and aging under DC

In addition to the temperature, the contact pressure of the electrodes on the test specimen can also be regulated via compressed air, as indicated by the cylinders in Figure 2. The electrode arrangement is adapted to the application of the LIPP method. For

this purpose, the high-voltage electrodes were reduced to 4 mm in the center to provide the target area for the laser. A 200 µm pocket is incorporated at the interface to the test specimen, which is filled with a conductive acoustic coupling material. This is needed to conduct the pressure wave from the metal into the test specimen.

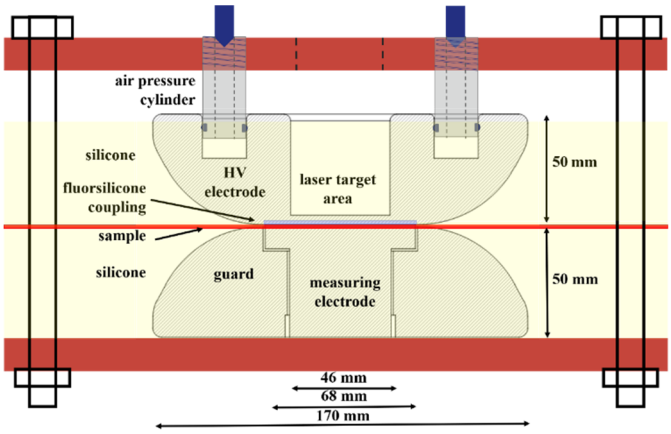

Fig. 2: Electrode arrangement in mounting

The disconnection of the voltage is realized by a self-developed DC switch, which disconnects the contact simultaneously via compressed air and by using an electromagnet, as can be seen in figure 3. The failure of a DUT is detected by a limit relay and optically transmitted to the magnet control which is placed at high voltage potential. An electrical permanent magnet is then switched on, whereupon the magnetic force decreases and the contact drops down onto a grounded metal sheet. To increase reliability, a blast of compressed air is generated at the same time, which releases the contact from the magnet.

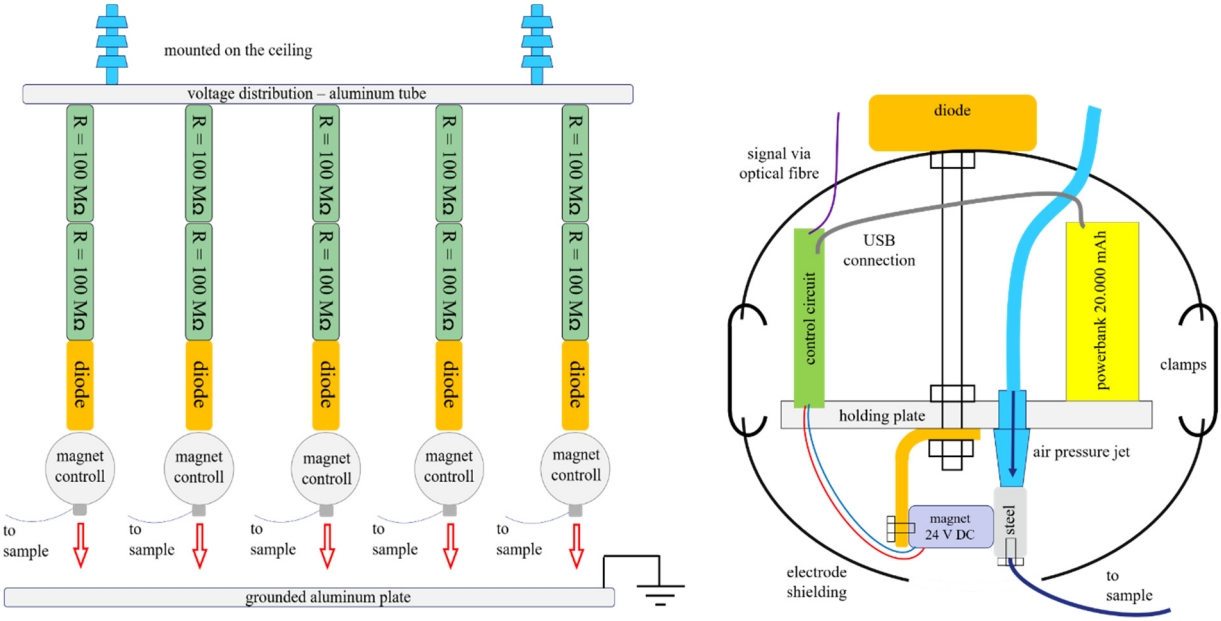

Fig. 3: DC-switch with magnetic control unit and compressed air backup

Formation of higher-value Hydrocarbons in Insulation Liquids stressed by Transformer Faults
Part 1: Paper/Oil aging

M.Sc. Kristin Homeier

Dissolved gas analysis (DGA) is a well-established and promising method to evaluate the condition of the insulation system of a power transformer, to detect transformer faults at an early stage and to allow countermeasures to be initiated in time. Due to various loads during transformer operation, different aging mechanisms take place in the insulation system, which usually consists of a combination of solid insulating material (e.g. cellulose) and insulation liquid. The insulation materials usually possess a chemical structure consisting of various hydrocarbon compounds, which are broken up producing different aging products. The aging products can appear in gaseous (fault gases), liquid (acid, alcohols, furans, water) and solid form (sludge, X-wax) and can act as catalysts for further aging reactions. In particular, the fault gases dissolved in oil provide a suitable basis for transformer diagnosis.

There are a large number of DGA interpretation methods on the market, but most of them are based on experience with mineral oil. The increasing use of alternative insulation liquids, which differ in their chemical structure and especially in their electrical, dielectric and physicochemical behavior, complicates the reliability of the DGA interpretation. In addition, the solubility of low-value hydrocarbons in the insulation liquid, such as methane and hydrogen, is low, so that volatilization of the gases can occur during oil sampling and transport, thus reducing the measurement accuracy of DGA. In extreme cases, this can lead to misinterpretation and thus incorrect decisions.

Thus, a DGA measuring device was developed together with the project partner Elektrochemie Halle GmbH, which allows the detection of higher-value C_4 and C_5 hydrocarbons as well as further C_3 hydrocarbons, in addition to the conventional fault gases. A correlation between gas solubility and the amount of carbon atoms seems to exits: the greater the number of higher-value hydrocarbons, the higher the gas solubility of the insulation liquid. Thus, the additional consideration of the higher-value hydrocarbons may be a suitable method to reduce the sampling and transport error significantly, so that the reliability of the DGA interpretation could be increased.

In order to investigate the formation of higher-value hydrocarbons, various transformer fault models were developed and built in the laboratory. Depending on the transformer fault, various aging mechanisms occur in the insulation liquids, so that different fault gas types with various concentrations and ratios are generated as a result of aging.

In this first part of the presentation of the research results, the formation of the higher-value fault gases in addition to the conventional fault gases during paper and oil aging is shown. In order to perform paper aging (PA), the insulation paper, impregnated with

the oil, was cut into strips and then stored together with the oil in a 10:1 oil to paper weight ratio in a closed Erlenmeyer flask at 120 °C in a heating chamber. Samples were taken after different duration times. To investigate the oil aging (OA), the same volume of oil was filled into an Erlenmeyer flask and kept in a sealed environment under the same conditions. The generated fault gases are depicted in Fig. 1 on the example of the alternative insulation liquids, synthetic ester and GtL oil.

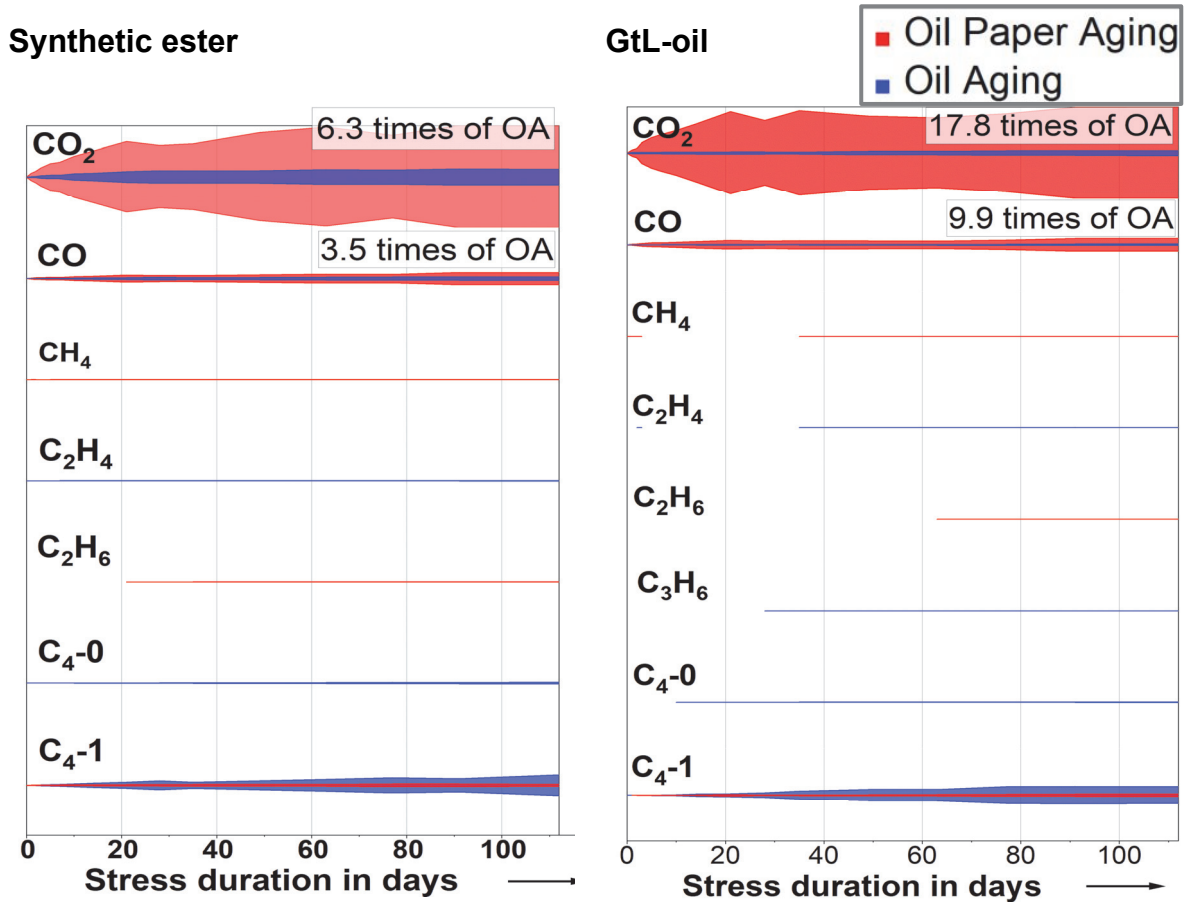

Fig 1: Comparison of generated fault gases in paper aging (PA) (red) and oil aging (OA) (blue) in the synthetic ester fluid (left) and GtL oil (right)

In the case of the alternative insulating fluids, a significantly higher concentration of CO_2 and CO was produced during paper oil aging than during pure oil aging. In addition, methane and ethane are also formed during paper oil aging, while oil aging primarily generates ethene and, in the case of GtL oil, propene as well.

In general, higher-value hydrocarbons were generated in addition to the conventional fault gases. The C_4 hydrocarbons C_4-0 and C_4-1 are the main characteristic gases. Especially, the C_4-0 was only formed during pure oil aging and can therefore serve as a distinguishing factor between the two defect types.

These initial measurement results highlight that the consideration of higher-value hydrocarbons in a DGA interpretation algorithm is a promising approach to classify a fault more accurately and increase the reliability of the DGA interpretation.

Formation of higher-value Hydrocarbons in Insulation Liquids stressed by Transformer Faults
Part 2: Thermal faults

M.Sc. Kristin Homeier

Depending on the transformer fault, different reactions and secondary reactions occur in the insulating fluids, so that different fault gases are generated as aging products. The formation of higher-value hydrocarbons as a result of thermal faults is presented in this second part.

A local thermal hot-spot fault in a transformer is reproduced using a resistance wire winding made out of constantan, which is stressed by a transformer with different currents. The constantan wire is wound around a ceramic rod. In order to increase the local hot-spot temperature and thus the fault gas amount, a copper tube with PTFE spacers was also placed over the wrapped ceramic rod, as shown in Fig. 1. This transformer fault model is fixed in a test vessel filled with the respective insulation liquid. To ensure a local thermal Hot-Spot fault, the surrounding insulation liquid is actively cooled by a cooling liquid in the double jacket of this test vessel using a circulating thermostat. Different insulation liquids were subjected to different currents and thus hot-spot temperatures as well as stress durations. Afterwards, the oils were analyzed by DGA in the new special DGA measuring device developed with the project partner Elektrochemie Halle GmbH for the additional detection of higher-value hydrocarbons.

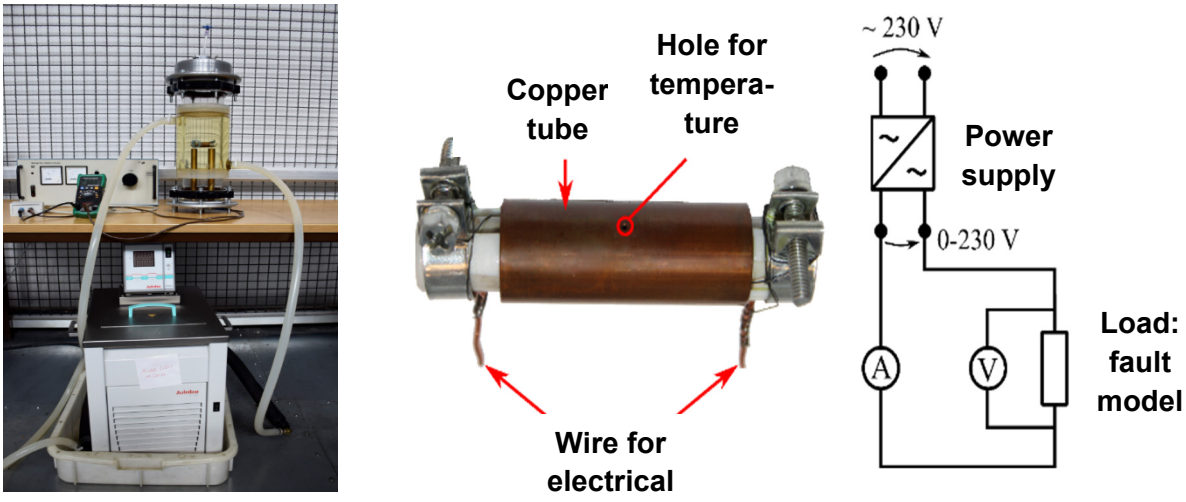

Fig. 1: Test setup for reproduction of a local thermal hot-spot transformer fault complete test setup (left); resistor model (right)

Fig. 2 shows the generated higher-value fault gases in different insulation liquids under stress with a thermal T1 fault for 1 h stress duration. First, the four selected and calibrated C_4 and C_5 hydrocarbons (HC), i- and n-butane and i- and n-pentane, are presented.

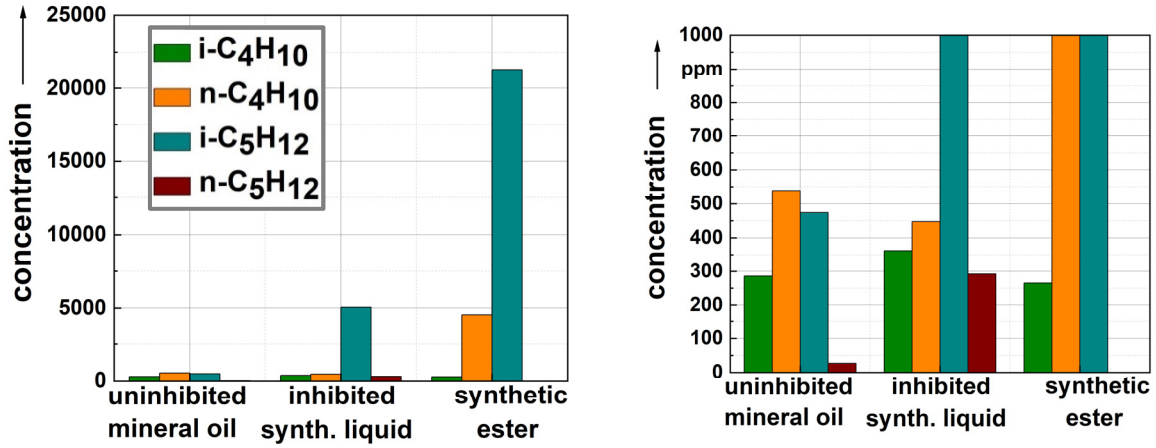

Fig 2: Selected generated C_4 and C_5 hydrocarbons (HC) in different insulation liquids: total concentration range (left); scaled-down section (right).

In all the insulation liquids, higher-value hydrocarbons are generated in high concentrations after only an hour stress duration, even in the case of T1 fault. It is noticeable that the synthetic ester liquid shows the highest concentrations, especially of n-butane and i-pentane, while in the uninhibited mineral oil the lowest concentrations are formed generally.

In addition to the selected calibrated fault gases, further previously unknown fault gases are also detected, as shown in Fig. 3 on the left. Furthermore, the relation between fault gas concentration and temperature is demonstrated on the right in Fig. 3 using the example of the synthetic ester liquid.

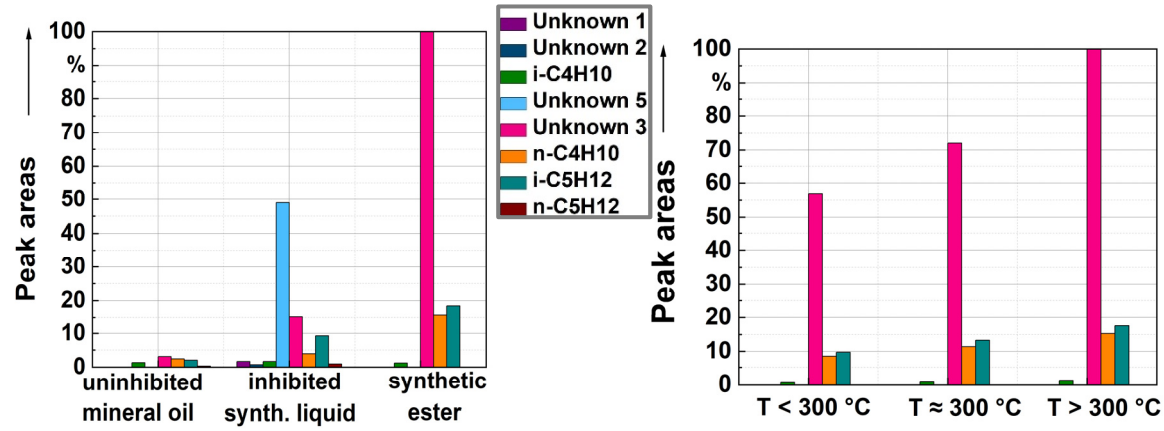

Fig. 3: Normalized peak areas of C_4 and C_5 HCs in different insulation liquids (left) Normalized peak areas of C_4 and C_5 HCs at different temperatures (right) in synthetic ester

Among the unknown fault gases formed (Unknown, since these could not yet be structurally assigned), Unknown 3 especially is prominent in high peak areas in the synthetic ester liquid. This fault gas is also detected in the other insulation liquids. In contrast,

the unknown fault gas Unknown 5 is noticeable in the inhibited synthetic insulation liquids and has the highest peak areas.

Furthermore, the example of the synthetic ester liquid highlights the relationship between temperature and fault gas amount in Unknown 3 and also in n-butane and i-pentane: the higher the temperature, the higher the fault gas concentration.

These DGA measurement results also provide a promising opportunity in improving DGA interpretation by including various higher-value hydrocarbons. However, it is clear that an insulation-liquid-specific DGA interpretation is useful.

Formation of higher-value Hydrocarbons in Insulation Liquids stressed by Transformer Faults
Part 3: Electrical faults

M.Sc. Kristin Homeier

Electrical faults are usually identified as the critical transformer faults. It is divided into electrical faults in the form of discharges with different energies as well as partial discharges. Therefore, in this third contribution, an overview of the influence of discharges in the form of impulse voltages with different energies and numbers of impulses regarding the formation of higher-value hydrocarbons is shown.

Various insulation liquids were subjected to lightning impulse voltage in the laboratory using a test setup illustrated in Fig. 1 with a needle-ball electrode arrangement with 25 mm electrode distance in accordance with the *IEC 60897* test standard.

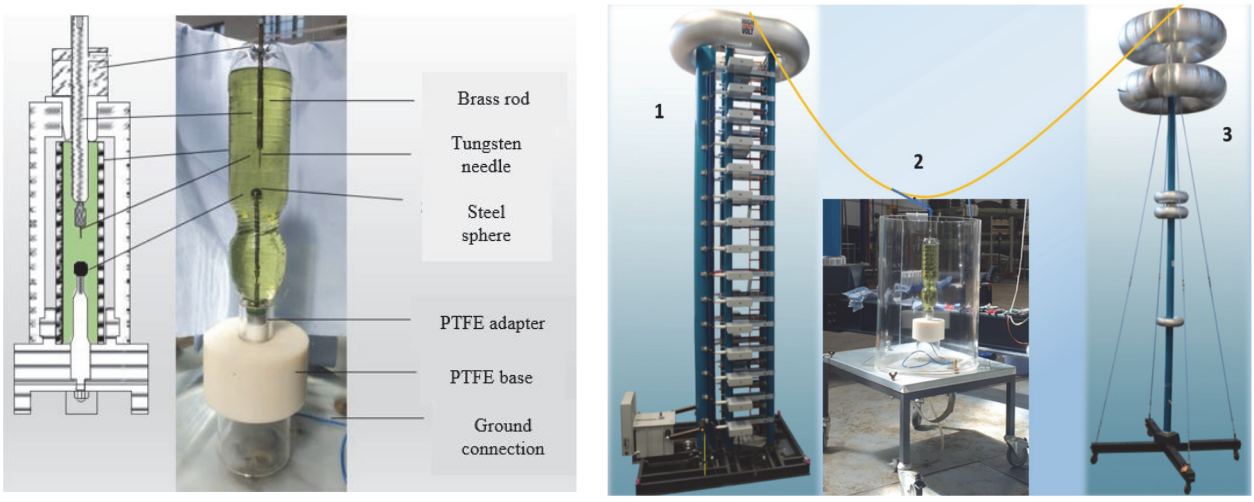

Fig. 1: Test setup for electrical fault model: test vessel (left), whole test setup (right)

To improve the comparability, the negative and positive breakdown impulse voltages of all insulating fluids were initially determined, as shown in Fig. 2. Significant differences between the insulation liquids can be observed, especially in the case of negative polarity. While the uninhibited mineral oil and the synthetic insulation liquid possess a negative breakdown impulse voltage of approx. 300 kV to 400 kV, ester fluids only show a negative breakdown impulse voltage of approx. 130 kV. In contrast, in the case of positive polarity, all the insulation liquids have approximately similar breakdown lightning impulse voltages of about 100 kV. The differences can be explained by the different streamer mechanisms occurring in the various insulation liquids due to their chemical structure as well as the polarity effect. Furthermore, a moderate reduction of the breakdown lightning impulse voltage with a decreasing water content is obvious.

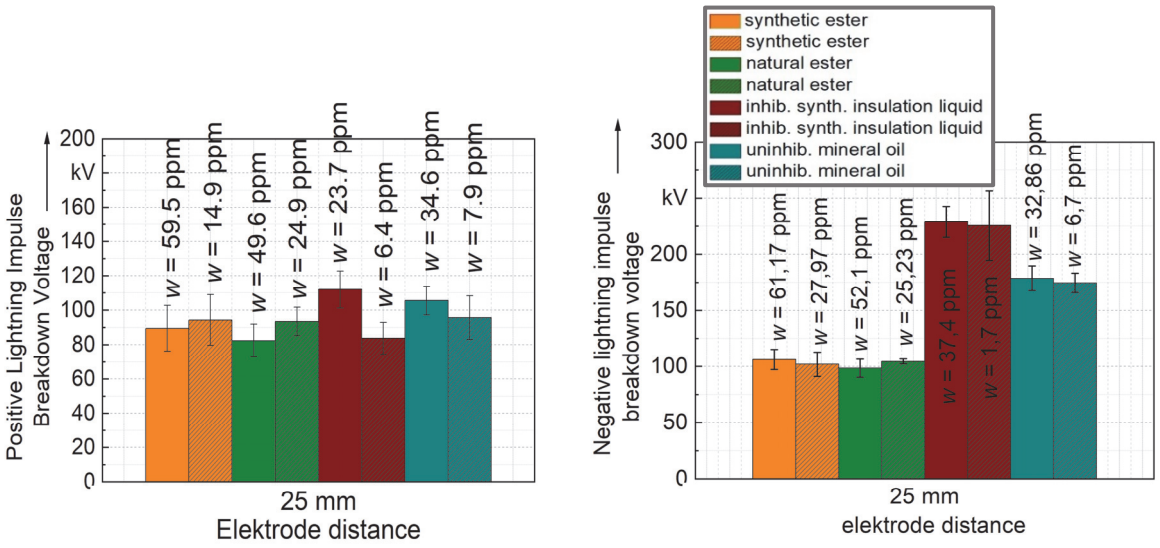

Fig. 2: Breakdown voltages of various insulation liquids at lightning impulse voltages of different polarities: positive lightning impulse voltage (left), negative lightning impulse voltage (right)

The negative breakdown voltages determined for the respective insulation liquids are defined in the following as 100 % breakdown impulse voltage for the investigation of the formation of fault gases. The insulation liquids were subjected to 5 impulses at 25 mm electrode distance at different negative lightning impulse voltages and afterwards a DGA was performed. As an example, Fig. 3 shows the generated C_3 and C_4 hydrocarbons in uninhibited mineral oil.

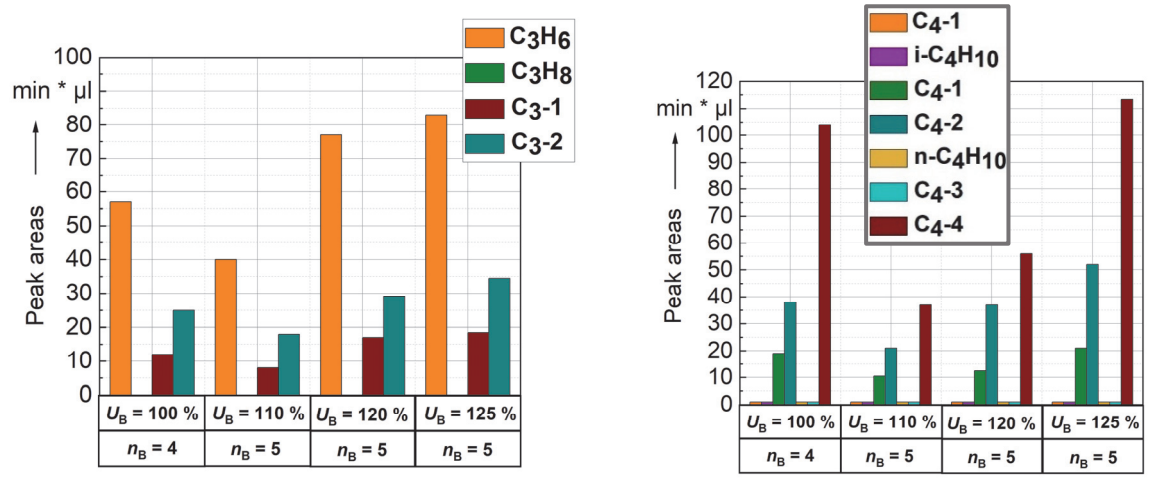

Fig. 3: Peak areas of C_3-hydrocarbons in uninhibited mineral oil (left)
Peak areas of C_4- hydrocarbons in uninhibited mineral oil (right)

In the uninhibited mineral oil, in addition to propene, the unknown C_3-1 and C_3-2 are also generated as C_3 hydrocarbons. With the exception of the 100 % voltage, where an incomplete impulse occurred, an increase in the peak areas with the impulse voltage energy can generally be registered. A similar trend can be observed for the C_4

hydrocarbons formed: with an increase in voltage, the concentrations increase. There, especially the unknown C_4-1, C_4-2, and C_4-4 appear as characteristic fault gases for an electrical fault.

The influence of the number of impulses on the gassing behavior was also investigated, shown in Fig. 4 using the example of uninhibited mineral oil and natural ester at 120 % lightning impulse voltage.

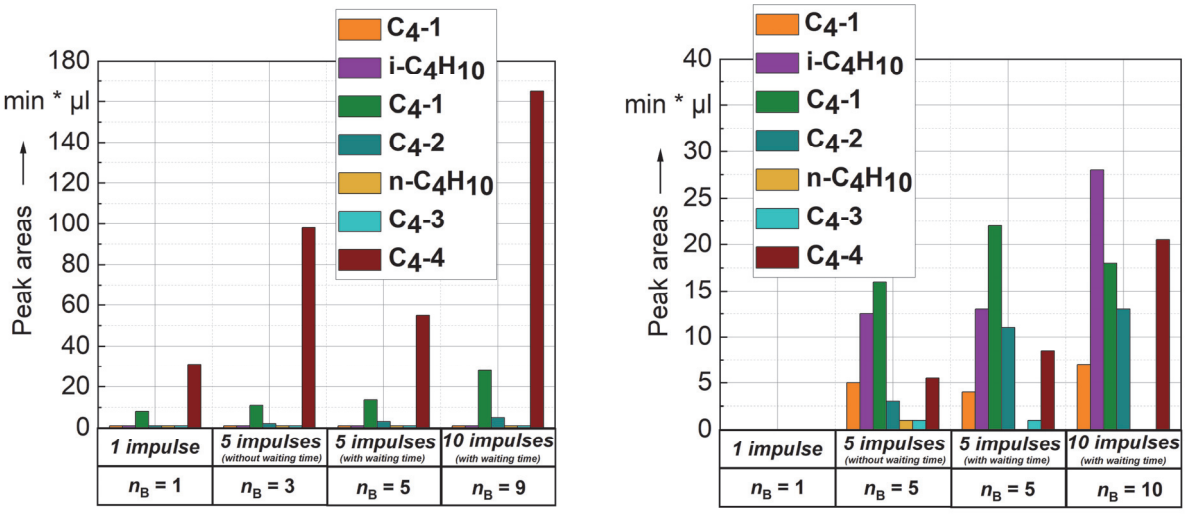

Fig. 4: Peak areas of C_4- hydrocarbons in uninhibited mineral oil (left)
Peak areas of C_4- hydrocarbons in natural ester (right)

A tendential relation between number of impulse and concentration can be observed: the more discharges, the higher the concentration. If the waiting time between the impulses were reduced to a minimum, the uninhibited mineral oil showed an increase of the C_4-4 concentration, whereas for the natural ester a reduction of all C_4 hydrocarbons were more evident. The peak areas are significantly higher with the mineral oil compared to the natural ester. However, the significantly lower 100 % voltage of natural ester must be taken into account here.

In general, it can be noticed that in all transformer fault types, higher-value hydrocarbons are generated in addition to the conventional fault gases. Depending on the type of transformer fault and insulation liquid, different characteristic fault gases are formed. Thus, these DGA results show a promising opportunity for the improvement of the DGA interpretation by including different higher-value hydrocarbons in consideration. However, these results on the electrical fault again demonstrate that an insulation-liquid-specific DGA interpretation is useful.

Development of a regenerative device to reduce moisture intake by free breathing power transformers

M.Sc. Mahmoud Moh'd

During operation, transformers are subjected to various stresses. The TEAM stresses are thermal, electrical, mechanical stress and environmental influences. The environmental influences are mainly moisture and oxygen from the environment, which can lead to chemical reactions and accelerate the reaction mechanisms in the entire insulation system of the transformer. Especially in free-breathing transformers, which have contact with the ambient air through the expansion tank, moisture is introduced when the transformer is inhaled. To prevent this, there are a variety of dehumidifiers on the market. However, these reduce humidity and are usually non-regenerative and thus require high maintenance. For this reason, a new type of dehumidifier is to be developed which, reduces the moisture. In addition, it is desirable for the final product developed also to be regenerable.

Suitable materials or material mixtures for moisture reduction are to be found. The aim is to achieve a residual moisture content of < 3 % RH. For this purpose, suitable materials are tested with respect to various influences on the reduction, such as volume or weight ratios, different temperatures and starting moisture contents, and the influence of air flow. Finally, a setup is to be built to test or optimize the regeneration of the dry material. The investigation was carried out step by step. Firstly, suitable materials for air dehumidification were to be tested. For this purpose, desiccant materials of various particle sizes such as silica gel, zeolite, bentonite and mixtures of these materials were tested. The desiccants, as well as, the mixtures were first tested statically in a glass vessel of 1 l capacity. Then the influence of the volume was controlled with a 3 l vessel. Subsequently, the influence of the starting moisture content on the moisture absorption of the desiccant was checked. Finally, the first regeneration experiment was carried out with a setup consisting of a brass pipe, a heating element - or foil, and temperature sensors (*see Figure 1*), programmed with an Arduino-Uno.

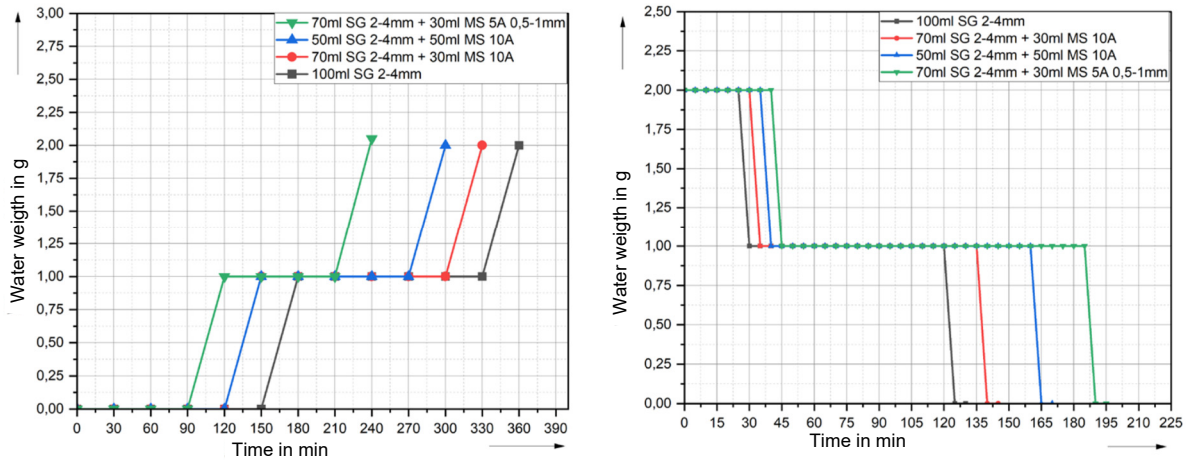

Figure 1: **Left -** An example of humidifying the mixtures of silica gel (blue) and molecular sieve up to 2 g water weight, which represents 12.5 % of the water absorption capacity (20 % of the sample weight). The total sample weighs 80 g. **Right -** Regeneration tests of the mixtures of silica gel - blue and molecular sieve using a regeneration set-up at a temperature of 125 °C.

The final setup for the regeneration of the desiccant has yet to be developed (*see Figure 2*). The proposed setup is currently in the production stage.

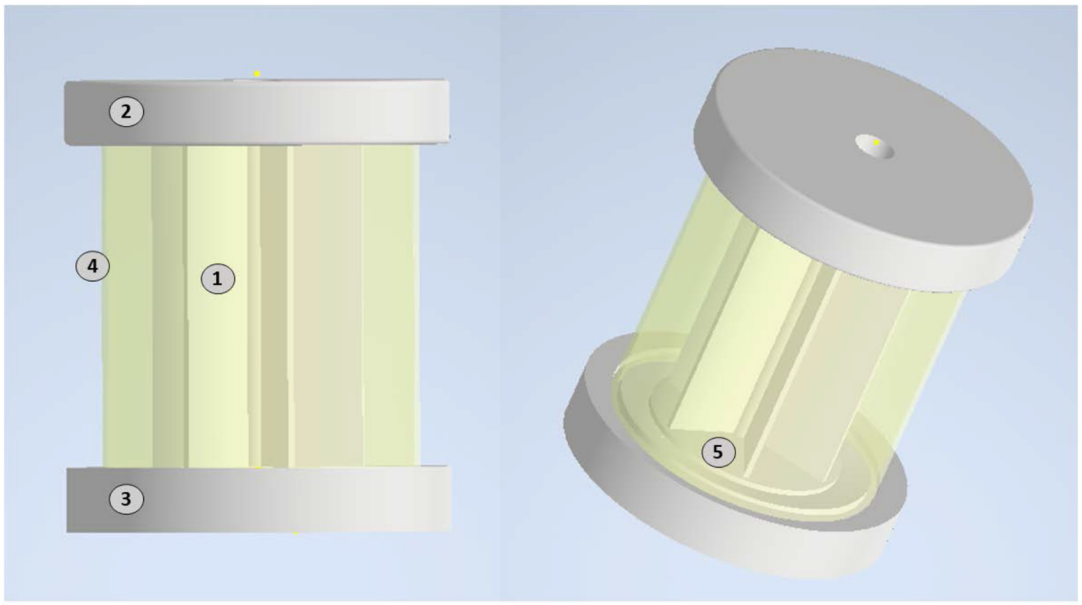

Figure 2: Proposed setup for desiccant regeneration with a built-in heating element in the center of the core. 1 - core with a built-in heating element, 2 - upper flange., 3 - lower flange with cone for water drain, 4 - glass, 5 - lower plate.

To summarize, the aim of this project is to develop a regenerative dehumidifier. The main focus was on testing suitable materials or mixtures for dehumidification. For the drying tests, the materials silica gel, molecular sieve as well as bentonite, each with different particle sizes and types, were used. Various factors were taken into account when selecting the drying materials, such as regeneration temperature, regeneration time, water absorption capacity and life cycle. The investigations were carried out step

by step and under different conditions. The desired mixtures were further investigated under the influence of the starting air humidity, volume ratio, as well as, the air flow. Finally, a setup consisting of a brass tube, heating foil as well as temperature sensors was prepared to evaluate the regeneration capability of the mixtures. Finally, a setup for desiccant regeneration was developed and is currently being fabricated. The setup consists of several parts with a heating element installed in the center to generate heat for the regeneration of the desiccants and to distribute it as uniformly as possible to the desiccants based on the strips.

A new method for health index determination using power transformers as an example

M.Sc. Mahmoud Moh'd, M.Sc. Henning Schnittker

A widely used method for evaluation the condition of power transformers is the determination of health index. The different methods for evaluating the health index of power transformers from the CIGRÉ technical brochure TB-761 are associated with advantages and disadvantages. The main disadvantage with some methods is the masking of the defects i.e. the rating does not indicate the correct condition of the transformer, since a defect is masked or hidden by other measured values. Therefore, an accurate and comprehensive method has been developed to overcome these drawbacks and to determine the condition of power transformers in the form of a health index value.

According to the CIGRÉ technical brochure TB-761, different health indices are available, which are distinguished according to the objective of the evaluation. These methods are either numerical methods or symbolic methods. The newly developed procedure consists of five steps:

1. Determination of the evaluation matrix with a division of the categories (levels) and corresponding colors. One possibility is shown in Table 1, where each level or color in the evaluation matrix represents a certain evaluation. The number of levels in the evaluation matrix can be defined arbitrarily and it only influences the accuracy of the overall evaluation.
2. Evaluation of the individual measurements using the evaluation matrix. In particular, the number of measurements that are relevant for the evaluation of the asset, as this is used to determine the weights in step 3.
3. The basic idea of this procedure is that the weight G_i of a level i in the evaluation matrix multiplied by the number of measurements N must be smaller than the weight of the next level (see formula 1).

$$N \cdot G_i < G_{i+1} \tag{1}$$

In this formula, N represents the number of considered types of defects or measurements to determine the health index (HI), G_i represents the weight of level i, and G_{i+1} represents the weight of the subsequent level. The formula is always applied between a level and the subsequent level.

4. Summation of the weights of each measurement to determine the overall condition of the asset (see formula 2).

$$\sum_{1}^{N} G \tag{2}$$

Subsequently, scaling on a desired scale such as 1-10 is possible. Scaling facilitates the overview and enables comparability between resources. Retrospectively, the number of individual evaluations can be directly inferred from the index number (as with method count per category).

5. Creation of a label: this step is optional, but defines the action statement and therefore reflects the goal of the HI (replacement index, repair index, etc.).

In the following, the principle of calculation is applied exemplarily for typical measurements on power transformers:

Step 1, the evaluation matrix is created. In this case, the division into 5 levels or colors was chosen (see Table 1).

Step 2, the measurements are evaluated. In this example, 4 measurements are considered. These measurements are winding resistance measurement (R), feedthrough measurement ($tan\,\delta$ and C), standard oil test (SOT) and gas-in-oil analysis (DGA). In this case, 15 transformers were randomly considered as an example to illustrate the procedure. The individual ratings can be seen in Table 2.

Step 3, a weight is assigned to each evaluation level or color. This weight depends on the number of measurements (see formula 1). For the four measurements considered, applying the formula for the first level leads to 4 ·0 = 0 i.e. the weight of the next level (good) can be 1. Since 1 is greater than 0, the condition in formula 1 is satisfied. For the second level, this results in 4 ·1 = 4, so the next level (medium) must receive at least 5 as its weight.

Step 4, the weights of all measurements are summed to determine the overall condition of the transformer. For example, 4 measurements with the rating very bad result in 4 ·125 = 600. In this way, the condition index in Table 2 is obtained.

Table 1: Weight per level in the assessment matrix

Levels in the considered evaluation matrix	Very good	Good	Medium	Poor	Very poor
Weight	0	1	5	25	125

Step 5, a label is introduced. The label has a scale of 0-5 and defines the states very good to very bad (see Table 3). Since there are states before a fault, as well as, after a fault, this corresponds more to a composite index.

Table 2: Exemplary evaluation of the measurements with different transformers

Trafo #	R	tan δ	DGA	SOT	Condition index	Norming	Lable
1					600	10,00	5
2					251	4,18	4
3					255	4,25	4
4					300	5,00	4
5					175	2,92	4
6					128	2,13	4
7					132	2,20	4
8					176	2,93	4
9					180	3,00	4
10					56	0,93	3
11					36	0,60	3
12					32	0,53	3
13					16	0,27	2
14					11	0,18	2
15					0	0,00	0

Table 3: Rating scale of the model, including the condition, normalization and label from 0 (very good) to 5 (very bad)

	Scale					
Condition	Very good	Good	Medium	Sufficient	Poor	Very poor
Norming	< 0,02	0,02 - 0,07	0,08 - 0,33	0,42 - 1,67	2,08 – 4,166	6,25 - 10
Lable	0	1	2	3	4	5

The limits (normalization) given in Table 3 represent the rating of each transformer. The label was added in this case for at least one appearance of a measurement.

A new health index method for evaluating equipment was presented using transformers as examples. The method determines an index number that represents a detailed statement of the condition of the equipment. Many disadvantages of the methods presented in TB-761 of CIGRÉ can thus be avoided. This makes the condition determination more flexible and develops an individually adequate solution for a more accurate evaluation of power transformers. This method can also be easily extended to a higher number of diagnostic measurements.

Investigation of the Diffusion Behaviour of Different Acid Configurations in Insulating Paper in a Closed Transformer System

M.Sc. Büsra Özdemir

As an important part of the energy supply chain, transformers must operate safely and reliably. The limit of service life depends largely on the transformer's insulation system. The most common insulation system is oil-paper insulation, whose organic content can deteriorate over time. When mineral oil ages in the oil-paper insulation system, both low-molecular and high-molecular organic acids can be formed, whereas only low-molecular organic acids form when insulating paper ages. The content of low-molecular acids in insulating paper is about 100 times higher than that of low-molecular acids in oil. Various studies have shown that low-molecular acids in particular, which have a strong tendency to dissociate in synergy with water, can accelerate the ageing of cellulose. Therefore, the investigation of the diffusion behaviour of acids in oil-paper insulations is of great importance. This basic research can provide a basis to better understand the chemical behaviour of acids in an oil-paper insulation system. For this purpose, the IR spectra of insulating oil and insulating paper are recorded under different ageing conditions and the changes in the absorption values of the C=O double bond of the samples are compared. A correlation between the acidity of the insulating paper and the spectral information is established to capture the diffusion mechanism at different temperatures on a molecular level. In this investigation, levulinic acid (LS), acetic acid (ES) and formic acid (AS) were used. To investigate the diffusion behaviour of these acids, three experimental series were prepared, each with one type of acid. Each experimental series was stored at different temperatures, namely at room temperature (RT), 70 °C and 100 ºC. The measurement points were set to 6, 24, 72, 120, 168, 240, 384, 744 and 1224 h. A sample bottle contained 30 ml of gas-to-liquids oil (C) and five paper strips pre-treated with acid. The acid number and IR spectra of paper and oil samples were recorded to investigate diffusion. Each paper strip of the AS test series was treated with 10 µl acid, while the papers for the ES and LS test series were treated with 20 µl acid. Due to the low molar mass of formic acid, the dosage was halved. To determine a reference standard for the diffusion state of the acid, the total amount of acid added to the 5 papers per sample was calculated. This amount of acid was converted to the corresponding acid number using the acid-base reaction relationship.

Discussion

The initial acid number of the fresh oil after drying and degassing is very low at 0.02 mg KOH/g oil. The initial acid number of the fresh oil after drying and degassing is very low at 0.02 mg KOH/g oil. Fig. 1 (top) shows the curve of the acid number of the oil samples.

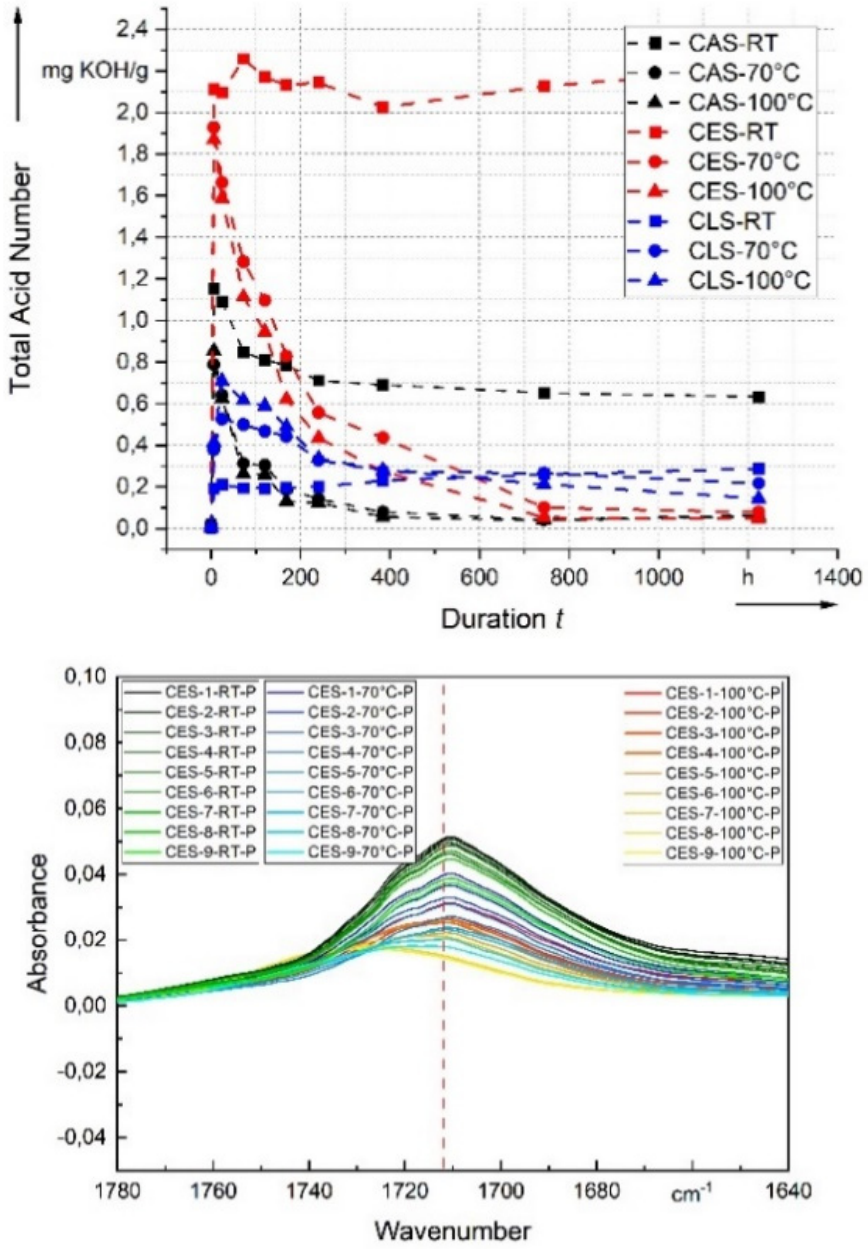

Figure 1: Acid number of the samples (top) and IR spectra of the paper samples treated with acetic acid (bottom)

Due to the concentration gradient, part of the acid diffuses out of the paper strip into the oil. Basically, it can be seen that the acid level of the samples reaches a maximum value within the first 24 h at all temperatures. It can be assumed that the diffusion process between paper and oil is completed. The approximate percentage of acid that passes into the oil can be calculated from the reference standard. About 37.47 % of the AS, 12.54 % of the LS and 51.74 % of the ES diffuse into the insulating oil within 24 h. After 24 h it can be seen that the acid numbers decrease differently depending on the temperature. At RT, the acid numbers of all oil samples remain almost constant, which means that the acid concentration of paper and oil is in relative equilibrium at

this point. At 70 °C and 100 °C the acid numbers of all oil samples start to decrease continuously. The same can be observed in the IR spectra of the paper samples (Fig.1 bottom). Since the results of the acids are similar, only the results of the acetic acid samples are shown in Fig. 1. First, a clearly pronounced acid peak at 1712 cm^{-1} can be seen in the paper spectrum after 6 -24 hours. However, the acid level decreases continuously regardless of the temperature, whereas the decrease is the strongest at 70 °C and 100 °C. Based on these observations, it could be assumed that the acid from the paper continues to pass into the oil. However, the acid number of the insulating oil does not increase according to Fig.1 (top). On the contrary, it continues to decrease. The same could also be proven spectroscopically. Basically, it could also be observed that the water content decreased continuously just like the acid number and reached a relatively stable level in the course of the diffusion time. It is suspected that the low-molecular-weight acids could undergo further reactions at high temperatures, possibly with water.

Conclusion

The investigations show that acids diffuse between the paper and the insulating oil. Overall, the acid peaks at RT were significantly higher than at 70 °C and 100 °C and decreased continuously. Considering the decreasing acid number and water content, it can be suspected that the acids and water might be involved in an unknown chemical reaction. The results show that the added acids do not exclusively diffuse into the paper, as is usually assumed. The oil and paper parameters investigated also show that levulinic acid is significantly more inert and overall more chemically stable than formic and acetic acid due to its molecular weight. The study provides a basis for further investigations to map the reaction processes of the acids in paper-oil insulations more precisely.

Investigation on the effect of water in association with acids on paper-oil insulations

M.Sc. Büsra Özdemir

Power transformers are exposed to high thermal, electrical and sometimes also mechanical loads. As a result, the organic insulation system ages over the years of operation.

It usually consists of cellulose and an insulating fluid, most commonly mineral oil. The ageing leads to a degradation of the dielectric and mechanical properties of the cellulose and insulating oil, whereby the service life of the transformer depends mainly on the insulation system. Two important ageing mechanisms are pyrolysis and acid-catalysed hydrolysis. At high temperatures, the pyrolysis is dominant and a random break-up of the cellulose chain and the glucose rings takes place. Besides, water and various acids are formed. These two ageing products can react with each other and acid dissociation can occur. This leads to an acid-catalysed hydrolysis, whereby the glycosidic bond of the cellulose is cleaved. In this process, a single glucose monomer can be released. This can react through further acid-catalysed processes to furans, which can ultimately decompose further to low-molecular-weight acids (NMS) and accelerate ageing. It can be stated that the chemical ageing of the insulation system is quite complex, as the different ageing mechanisms influence each other. In order to gain a better understanding of the chemical relationships, the influence of a water-acid combination on a paper-oil insulation was therefore investigated.

To investigate the effects of the water-acid combination on a paper-oil insulation, a total of 12 sample series were prepared. Basically, each sample consisted of 220 g *Shell Diala S4 ZX-I* (C) and 22 g insulation paper. The samples differed in 3 ageing parameters. In order to observe the influence of temperature, two main groups were created, which were aged at 70 °C and 130 °C. The samples were then investigated for their ageing properties. Two types of acid were used for each temperature. These were levulinic acid (CLS), which is a low-molecular-weight acid (NMS), and stearic acid (CSS), which is a high-molecular-weight acid (HMS). The acid concentration was set to 0.6 mg KOH/g oil. Lastly, each acid type was configured with three different moisture levels per temperature, so that there were dry (T) samples with about 0 wt% moisture, wet (F) samples with about 2 wt% moisture and very wet (SF) samples with about 8 wt% moisture. Finally, each sample was hermetically sealed. Samples were taken at defined time points. Each sample was analysed for water content, acid value, DP value and carbonyl groups using an IR-spectrometer. Similarly, all F and SF samples were analysed for furans by HPLC.

Discussion

The water content in the oil shows a clear dependence on the original moisture configuration and the temperature. Basically, three curves can be seen in Fig. 1 (left). The water content in the oil shows a clear dependence on the original moisture configuration and the temperature. Basically, three patterns can be seen in Fig. 1 (left). Between 0-50 ppm the T-samples show up. A continuous increase in moisture can be observed over the entire ageing period at 130 °C. The reason for this is probably pyrolysis, as for 70 °C the water content is quite constant at 10 ppm. All F and SF samples at 70 °C contain between 150-200 ppm of moisture. Due to the concentration gradient, the water diffuses from the paper into the oil according to *Fick*'s law. Therefore, an increased water content can be observed. However, this remains relatively constant over the entire ageing period. The water content of the F and SF samples at 130 °C shows a different pattern. First, a strong increase of the water content to approx. 430 ppm can be seen, which falls exponentially. At 1680 h, the F and SF samples have fallen to about 50 ppm, which corresponds to the level of the T samples at 130 °C. Due to the relatively strong water consumption, a very strong hydrolysis or other water-consuming processes can be concluded. The influence of the acid type generally does not seem to have any influence on the water content.

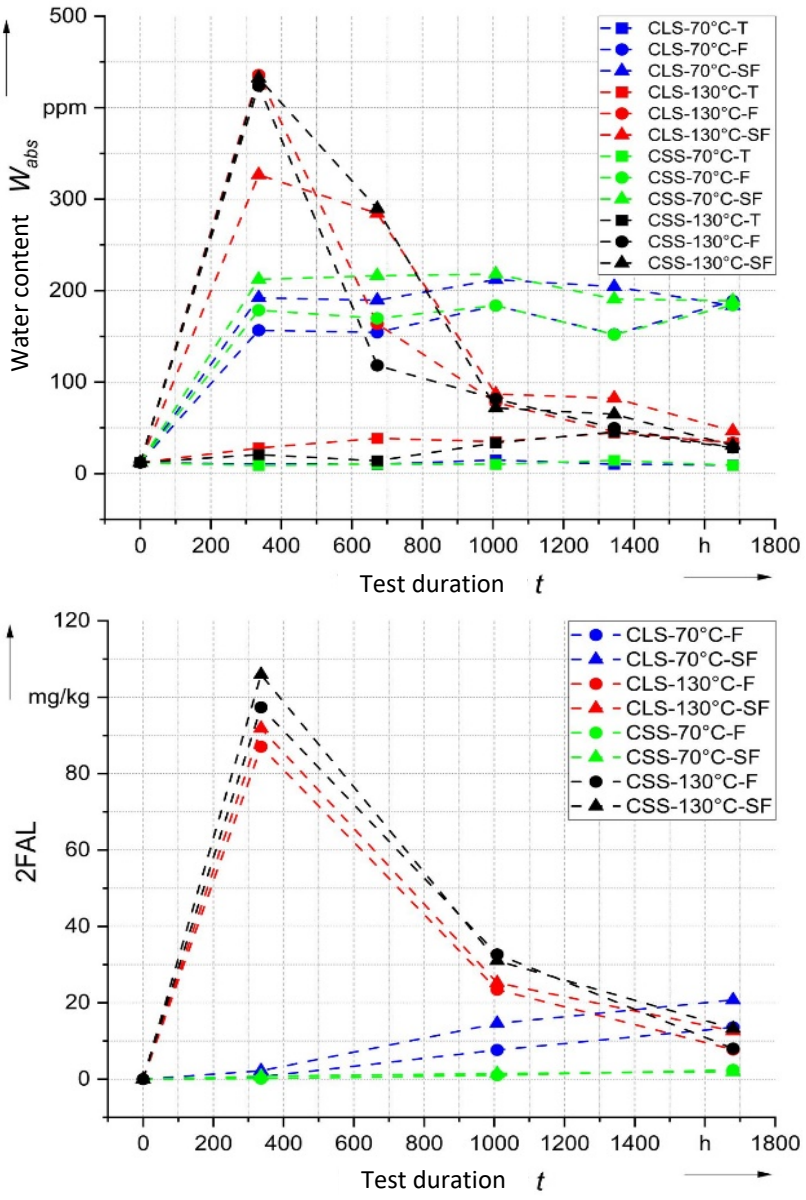

Fig. 1: Water content and 2FAL

A possible cause for the strong decrease of the water content might be, apart from the hydrolytic cleavage of the glucose chain, the hydrolytic decomposition of the furan 2FAL in NMS. Figure 1 also shows the progression of the 2FAL concentration, which falls exponentially at about 336 h for 130 °C, in other words at about the same time as the water content. This happens independently of the acid type. Contrary to this, at 70 °C a significant dependence on the acid type appears. For CLS, a stronger furan formation occurs than for CSS. Also, there is no decomposition of the 2FAL.

As NMS accumulate particularly in the paper due to their relatively strong polarity, a significantly increased absorbance is to be assumed at 1712 cm^{-1}. According to Figure 1, this should be independent of the acid type, since the water content and 2FAL concentration at 130 °C also fall independently of the acid type. On the other hand, a comparatively low absorbance should be seen for 70 °C, since no 2FAL decay can be observed. This could also be verified in the IR-spectrum. The absorbances of the F and SF samples at 130 °C showed only marginal differences between CLS and CSS. The IR-spectrum of the T-samples at 130 °C shows a clear difference. In this case, the absorbances of the CLS samples were about twice as high as those of the CSS samples. The CLS and CSS samples at 70 °C, on the other hand, showed the weakest absorbances, which also exhibited an unsystematic pattern. In general, the CLS samples showed a higher absorbance for 70 °C, which was, however, to be ex-

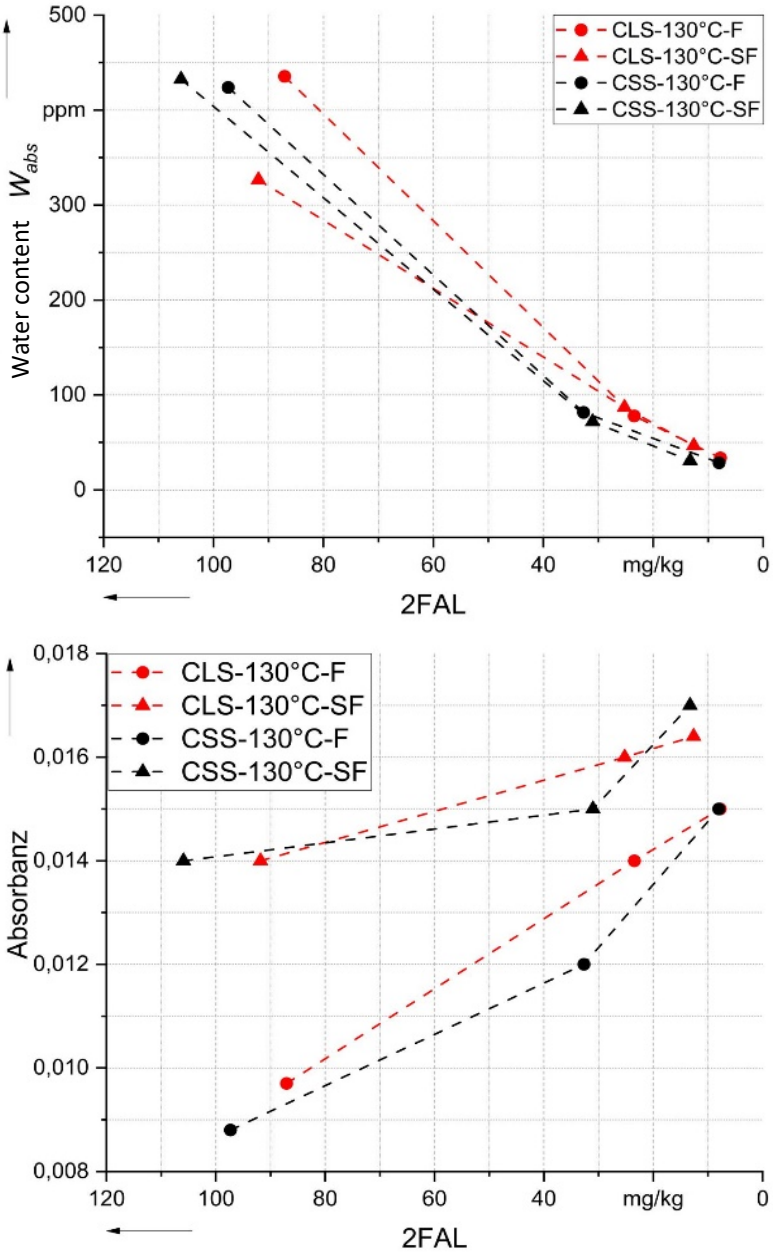

Fig. 2: Water content and absorbance over 2FAL concentration

pected due to the low-molecular properties of CLS. According to the results, high temperatures in combination with water and a generally acidic environment lead to a strong formation of 2FAL and carbonyl groups, as well as a strong reduction of the DP-value. The acid type seems to play a greater role in drier environments and lower temperatures.

The correlation between the decay of 2FAL with the reduction of the water content and the increase of the absorbance at 1712 cm^{-1} is particularly evident in Figure 2. There, linear correlations can be clearly seen. With the decay of 2FAL the water content is decreasing and at the same time the absorbance of the carbonyl groups is increasing. The carbonyl groups do not necessarily have to be carboxylic acids, as many organic molecules have a C=O double bond (e.g. esters, ketones, aldehydes etc). However, since 2FAL is used in the chemical industry by acid-catalysed hydrolysis to obtain levulinic acid, which reinforces the assumption that the carbonyl groups belong carboxylic acids.

Conclusion

The investigations revealed that the formation of carbonyl groups in the cellulose shows a strong correlation to the decay of the 2FAL. This was shown by the fact that the absorbance increased by 1712 cm^{-1}, with a decrease in the 2FAL concentration. This assumption is further confirmed by the fact that at 70 °C the 2FAL concentration increased continuously, which means that no decay took place, and at the same time no change was observed in the IR spectrum. Since the decay occurred with a strong consumption of water, it can be assumed that the carbonyl groups are carboxylic acids. However, this cannot be definitively determined, as only the absorbance of the C=O double bonds could be measured with the spectrometer.

Since NMS have a damaging effect on cellulose, further studies on the identification and composition of the carbonyl groups are useful to better understand and predict ageing processes.

Bayesian Risk-based Maintenance

M.Sc. Henning Schnittker

Risk-based maintenance can be advantageous for utilities, especially for Asset Management approaches. A risk can be calculated out of a probability and a consequence.

$$risk = probability \cdot consequences$$

A central difficulty is to quantify the probability of a risk individually and flexibly in dependence of available data, the needs of the utility and cost-benefit consideration of the assessment itself. Bayesian inference enables assessing the probability of a risk individually and flexibly, because of the fundamental view to see probability as an expression for a degree of knowledge. Updating a probability using Bayes' theorem is the fundamental idea of the developed approach.

The procedure is exemplified in the following on a fictional asset. The annual failure rate of this asset be $\lambda = 1\,\%$. Further, it is assumed that a measurement *A* detects a failure of the asset by a chance of 80 % (e.g. a contact resistance measurement may not detect failures of the insulation system). Moreover, the measurement *A* may wrongly sign (or indicate) a failure when there is actually no failure by a chance of 3 % (e.g. an incorrect execution of the measurement). Then the hypothesis "failure of the asset" can be proposed and be connected to the evidence "*measurement A*" with the following probabilities:

- The a priori probability that the hypothesis "failure of the asset" is true is described by $p(H) = 1\,\%$ as the annual failure rate of the asset.
- The probability that the hypothesis "failure of the asset" is false is described by $p(\neg H)$, which can be obtained by $p(\neg H) = 100\,\% - 1\,\% = 99\,\%$.
- The total probability of seeing the evidence is represented by $p(E)$. The blue filled squares in Fig. 1 represented this probability. Since p(E) is difficult to determine, it is often calculated by $p(E) = p(H) \cdot p(E|H) + p(\neg H) \cdot \mathrm{p}(E|\neg H)$.
- The probability that the evidence supports the hypothesis when the hypothesis is true, is described by $p(E|H) = 80\,\%$ as the chance of detecting the failure when there is an actual failure.
- The probability that the evidence supports the hypothesis even so the hypothesis is false is expressed by $p(E|\neg H) = 3\,\%$ as the probability that the measurement indicating a failure when there is no failure.

Then the Bayes' Theorem can be used to calculated the probability that the hypothesis is true after seeing the evidence $p(H|E)$ to 21.2 %.

$$p(H|E) = p(H) \cdot \frac{p(E|H)}{p(E)} = p(H) \cdot \frac{p(E|H)}{p(H) \cdot p(E|H) + p(\neg H) \cdot p(E|\neg H)}$$

$$= 1\,\% \cdot \frac{80\,\%}{1\,\% \cdot 80\,\% + 99\,\% \cdot 3\,\%} = 21.2\,\%$$

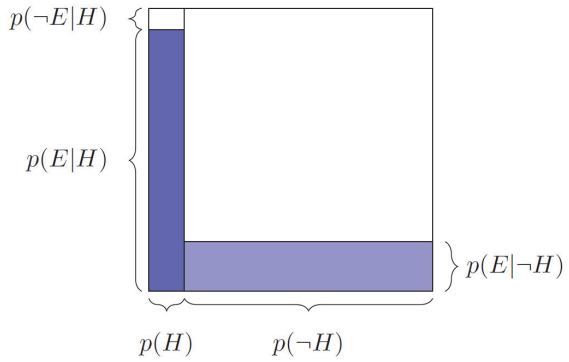

Figure 1: The probability of the two random variables H and E

In this case the measurement *A* updates the probability about a possible failure of the asset.

Generalised, after obtaining new evidence about a circumstance the knowledge of this circumstance is be adjusted. The a posteriori probability $p(H|E)$ as the mathematically expression to update the prior probability $p(H)$ allows to quantify the degree of belief and therefore supports an objective decision.

A risk assessment for a circuit breaker illustrates the practical use. The annual failure rate for live tanks rated 300 kV ≤ U ≤ 500 kV, while considering only major failures (MaF), is λ = 1.13 %. Together with the replacement costs, which are about $c = 200{,}000\,€$, the risk r is calculated

$$r = c \cdot \lambda = 200{,}000\,€ \cdot 1.13\,\% = 2{,}226\,€$$

A comparison of the manufacturers shows that the failure rate of manufacturer *Z* is about 40 % higher. Considering a total population of 885 live tanks, 10 failures are expected. If there are 10 different manufacturers with equally distributed shares of installed circuit breakers, 0.86 failures are expected for each manufacturer, respectively 1.4 failures for manufacturer *Z*. Then 87.1 circuit breaker of manufacturer *Z* and 875 in total stay without failure. This leads to the probability of about 10 % that assuming a circuit breaker failure of manufacturer *Z* is wrong and there is no failure $\mathrm{p}(\mathrm{E_A}|\neg H)$.

$$p(E_\mathrm{A}|\neg H) = \frac{87.1}{875} = 9.95\%$$

Now Bayes' theorem can be used to update the a priori probability $p(H)$ to the a posterior probability $p(H|E)$ after seeing the evidence. In this case, the higher failure rate of manufacturer *Z*.

$$p(H|E) = p(H) \cdot \frac{p(E|H)}{p(E)} = p(H) \cdot \frac{p(E|H)}{p(H) \cdot p(E|H) + p(\neg H) \cdot p(E|\neg H)}$$

$$= 1.13\,\% \cdot \frac{40\,\%}{1.13\,\% \cdot 40\,\% + 98.87\,\% \cdot 9.95\,\%} = 4.4\,\%$$

Therefore, a new risk r_{new} can be calculated for circuit breakers of manufacturer *Z*.

$$r_{new} = c \cdot p(H|E) = 200{,}000\,€ \cdot 4.4\% = 8{,}786\,€$$

The update of the probability through the Bayes' theorem shifts the general perspective of the whole population to an individual point of view.

Classification of Measurements on Power Transformer

M.Sc. Henning Schnittker, M.Sc. Mahmoud Moh'd

The application of asset management in the course of the energy transition and digitalisation, as well as the development of new condition diagnosis procedures, generates large amounts of data that need to be analysed. Machine learning has established itself in recent years as a suitable tool for processing large amounts of data. The machine learning algorithms require a data set with appropriate data quality (completeness, relevance of the data, number of data points, etc.) to achieve a desired performance. In the practical environment of energy supply, the directly usable amount of data is relatively small. Data is often available or could be made available, but it is sometimes unclear that this data exists or is useful, sometimes the data is available for the algorithm in a format that cannot be used, such as scanned pdf format, or sometimes technical solutions for generating the data must first be installed. Therefore, the effort and benefit of providing data must always be considered. This creates a fundamental problem: on the one hand, it is unclear in terms of the application of the algorithm which data is needed and in what quality, and on the other hand, it is unclear for data management which data is available or must be made available.

Here, the necessary data volume of the classification algorithms linear discriminant analysis (LDA), probabilistic generative models (PGM), probabilistic discriminative models (PDM), Laplace approximation (LA), support vector machines (SVM) and neural networks (NN) was investigated with regard to accuracy using the example of measurements on power transformers. These classification algorithms assign data to discrete classes and are therefore particularly suitable for categorical evaluations. In this case, the measurements of the winding resistance (R), the bushing (C) as well as the standard oil test (SOT) and the dissolved gas analysis (DGA) were evaluated with the categorical classification good, medium and poor.

First, randomised artificial data sets with a number of 100, 500, 1000 and 10000 data points are generated for each measurement method based on gamma, Gaussian and beta distributions. These data were then labelled. The label represents an evaluation of the measurements. For example, one of the categories good, medium or bad was assigned to the individual data of the resistance measurement using the evaluation scale shown in Table 1. Absolute resistance values R_{abs} and changes in the values ΔR are considered.

Table 1: Assumed evaluation standard for measurement parameters of the winding resistance

Value	good	fair	poor
R_{abs} in Ω	< 1		≥ 1
ΔR in %	< 5	5 – 10	> 10

Changes in resistance values of more than 5 % compared to a reference measurement, e.g. in the Factory Acceptance Test, may indicate a fault. Higher deviations increase the probability of an error. Furthermore, an abnormally high absolute value is also to be regarded as critical. This evaluation is only carried out in the categories good and bad, since the winding resistance depends on the transformer

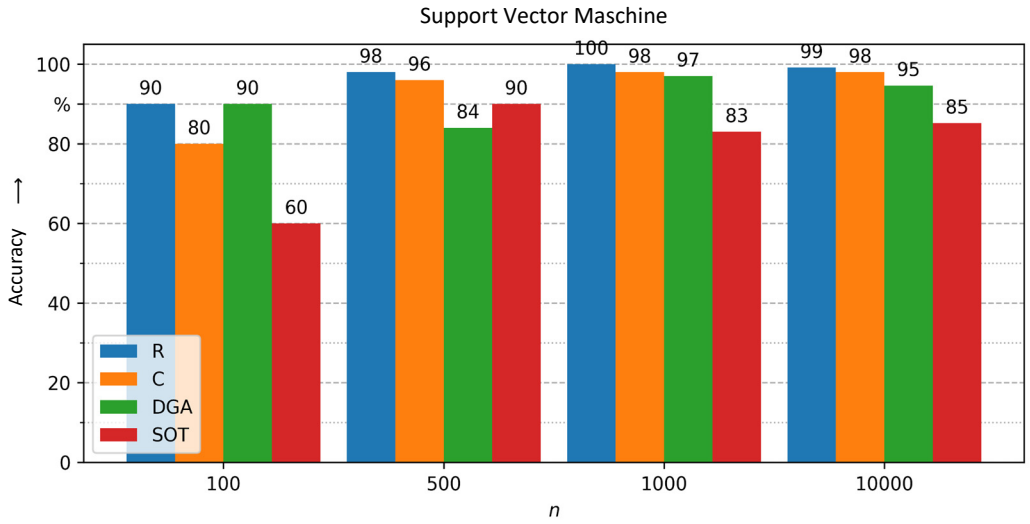

Fig. 1: Accuracy of the SVM for different measurement methods and numbers of data *n*

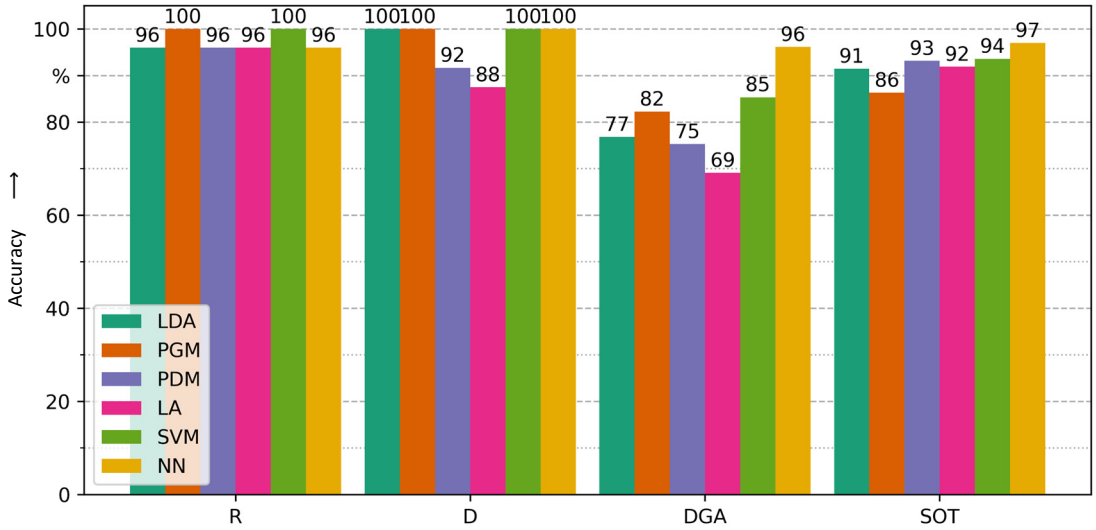

Fig. 2: Accuracy of the algorithms when trained with real measurement data for different measurement methods

design and thus varies too much to define the classification medium. Thus, a total of 16 classified data sets are available, which are used for the training of the algorithms (the four measurement procedures with the four different numbers of data points). It should be noted that when creating the data sets, care was taken to ensure that each class (good, medium, poor) has approximately the same number of data points. The individual data sets are now divided so that 90% of the data is available for training the algorithms and 10% of the data for a subsequent test.

The SVM shows the accuracy shown in Figure 1 for the different measurement methods and the different sized training data sets. Overall, it can be stated that in the comparison of the algorithms in this use case, the SVM achieves the highest accuracy in the evaluation of the measurements for all considered measurement methods.

Finally, the accuracy of the algorithms was checked using real measurement data of different numbers. Besides the SVM, the NN, the LDA and the PGM achieve high accuracies (cf. Figure 2).

Here, an attempt was made to simulate limit values. Since the limit values were known beforehand, the algorithms do not exhibit any intelligence in this sense. However, limit values are to be regarded individually, which ultimately makes the condition assessment more precise. At this point, machine learning classification algorithms can be used for a categorical evaluation, whereby real training data with a number of 500 data points can achieve sufficient accuracy. Figure 3 illustrates that evaluation becomes more difficult as the complexity of the data increases, although relatively simple algorithms such as SVM can generally be used cheaply, so that special AI methods such as NN are not always necessary.

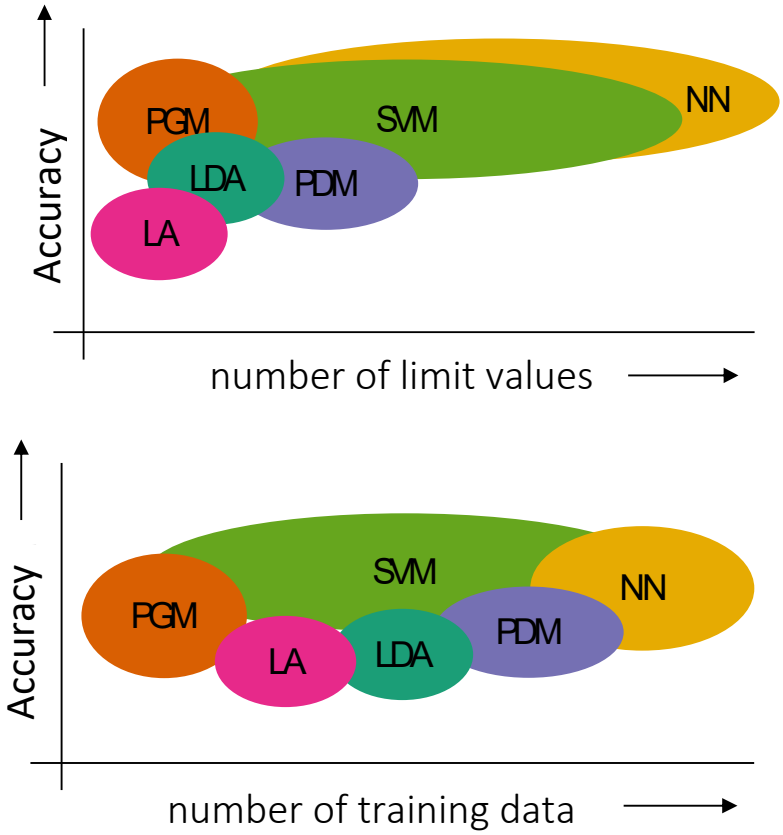

Fig. 3: Suitability of the algorithms as a function of the number of training data and as a function of the number of limit values

Possibilities and limits of diagnostic methods for operational aged power transformers

M.Sc. Sebastian Schreiter

Power Transformers are elementary elements in electrical power grids. Therefore, an unplanned outage of a transformer can lead to enormous financial consequences. For this reason, it is of fundamental interest to operators of such equipment to detect the condition and possible faults of transformers at an early stage. A number of different diagnostic methods are available for this purpose. From the wide range of diagnostic methods operators have to select the suitable procedures to ensure a reliable operation of power transformers. Already in the Schering Newsletter 2017 a new collaboration between the Schering Institute, the HTWK Leipzig and the current Hitachi Energy was introduced. Within this cooperation the possibilities and limits of diagnostic measures were investigated. For this, several hundred findings on active parts of transformers aged in operation and the results of the corresponding diagnostic methods were compared and analysed to answer the question which methods or combination of methods are necessary to indicate which type of faults. For this purpose, a fleet of operational aged transformers of different manufacturers, years of manufacture, applications and voltage and power classes were available. In this contribution, the results for the detection of hot spots are presented in an overview.

In order to investigate with which diagnostic methods or combination of methods hot spot can be indicated a comparison between all cases with showing traces of carbonization, burn-off or thermal discoloration on the active part were compared with the results of diagnostic measurements. In addition to the results of DGA, the results of electrical measurements such as winding and insulation resistances, transformer ratios and short-circuit voltage, as well as the results of the high voltage tests were taken into account. If there were any abnormality, such as exceedances of the reference value or deviations in the comparison of the phases, these were evaluated as anomalies. The results of this comparison are shown in Fig. 1. It can be seen that with the help of a single diagnostic methods not all cases were indicated. The results of DGA showed in 96 % of the cases abnormalities, the results of the winding resistances were increased in 62 % of all cases. However, the combination of the winding resistance measurement and the check whether abnormalities were present in the DGA led to a correct indication in each of the cases considered.

In addition to the active hot spots, a number of cases were observed with increased winding resistances, which had not (yet) developed into a hot spot. In these cases, it was investigated where these resistance increases were located and whether they would have been detectable later with the help of the DGA. As shown in Fig. 2, 90 % of all cases of resistance increases were located in the main oil chamber and were locally limited, such as a single contact of the diverter or tap changer (green). If

contacts with increased resistances are not loaded heavily the additional resistance may not lead to a hot spot. In case the load is increased a hot spot can develop which can be detected with the DGA. However, a total of 10 % of the cases were located in a separate oil chamber or occurred as global resistance increases (yellow or red). Thus, these would have remained hidden from regular oil-diagnostic monitoring, although a potential hazard to the equipment would be associated. This underlines the necessity of combining these two measuring methods.

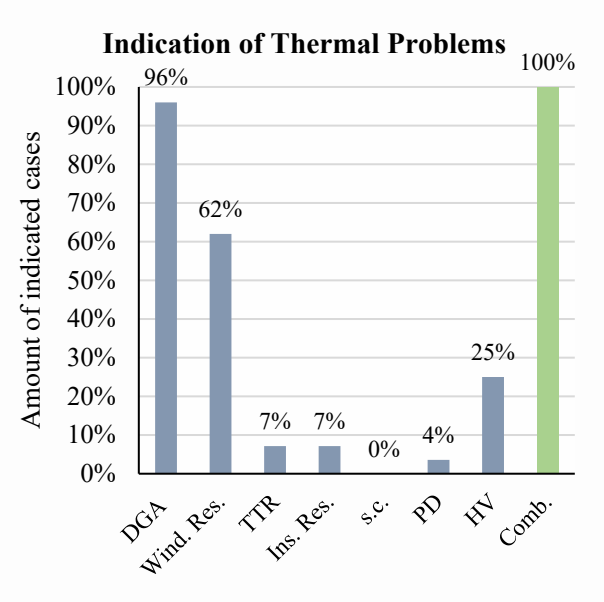

Fig. 1: Indication of thermal problems with the help of different diagnostic methods (blue) and combination of methods (green)

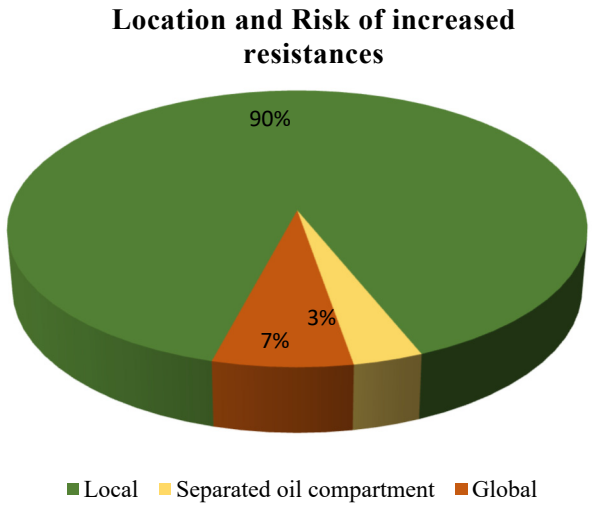

Fig. 2: Type an location of increased resistances

In summary, it can be stated that hot spots can usually only be reliably detected by combining DGA and winding resistance measurement. Together with the results on other typical fault such as PD or arcing as well as an investigation on the possibilities of fault identification with different DGA interpretation methods, transformer operators are thus provided with a basis for a targeted selection of diagnostic methods.

In addition to these results, a further cooperation between the Schering Institute and the HTWK Leipzig arose from this research work, in which the diagnostics of power transformers is to be improved with the aid of machine learning. In a first step, a new approach to estimate the condition of the paper insulation of power transformers was investigated. To do so, the DP values of operational aged power transformers were related to the insulation oil properties of these units. With the help of methods of machine learning a new method to predict the DP value based on the oil properties was developed.

Reduction of moisture content in insulating oils

M.Sc. Junaid Shaikh

Power transformers are an important part of our power system. In order to ensure their efficient and secured operation, it is necessary that the existing system be appropriately operated and serviced. Due to the increasing renewable sources of energy, the transformer is often stressed electrically, as well as, thermally. Considering their physical structure, transformers must be permanently cooled, for which a dielectric liquid is used to cool and insulate the windings.

Mineral-based oils have been commonly used as the insulation fluid of transformers. However, in the last decades some alternative synthetic and natural products have emerged e.g. synthetic/natural ester and silicone oils.

Due to pyrolysis, hydrolysis and oxidation of the organic insulation material in the transformer, various substances are produced, which are absorbed in insulating oil. This can promote ageing and lead to failure of the transformer. Therefore, the transformer oil must be processed externally to reduce ageing accelerators like water, solid particles and acid content.

For the reduction of moisture in transformer oil, zeolite filters are commonly used. However, other materials e.g. cellulose filter, silica gel and bentonite can also be used.

In this study, tests were performed to achieve moisture reduction in transformer oil using various filter materials. The oil type used was Shell Diala S4. The oil was filled in Erlenmeyer flasks of 300 ml volume. In each Erlenmeyer flask, the weight of oil was 250 g and the weight of the filter material was 2.5 g. The moisture content at the start was measured using Karl Fischer titration.

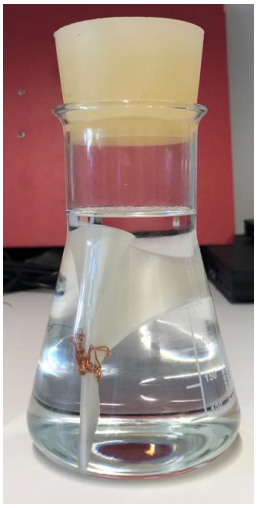

Figure 1: Test sample

The filter materials used were zeolite, bentonite, silica gel, cellulose paper, combination of zeolite with bentonite and combination of zeolite with silica gel. Before the tests, the filter materials were heated in the oven to regenerate them. Zeolite was heated at 250 °C for 1 day, bentonite was heated at 150 °C for 4 hours, silica gel was heated at 130 °C for 4 hours and cellulose paper was heated at 120 °C for 12 hours. The filter materials were filled in a filter paper and wrapped with a copper wire before putting them in the Erlenmeyer flask filled with oil. The Erlenmeyer flasks were closed and left at room temperature. A picture of one of the test samples can be seen in Figure 1. One set of samples was left for 3 days and the other set was left for 7 days. At the end of the test, the moisture content was again measured using Karl Fischer titration and compared with the original measurements.

Figure 2 shows the results with the change in moisture content of the test samples after 3 days and 7 days The moisture content measured initially was 34.5 ppm. The results indicate that there is a reduction in moisture content of the oil with the filter materials used. The reduction of moisture after 3 days is much rapid as compared to that after 7 days.

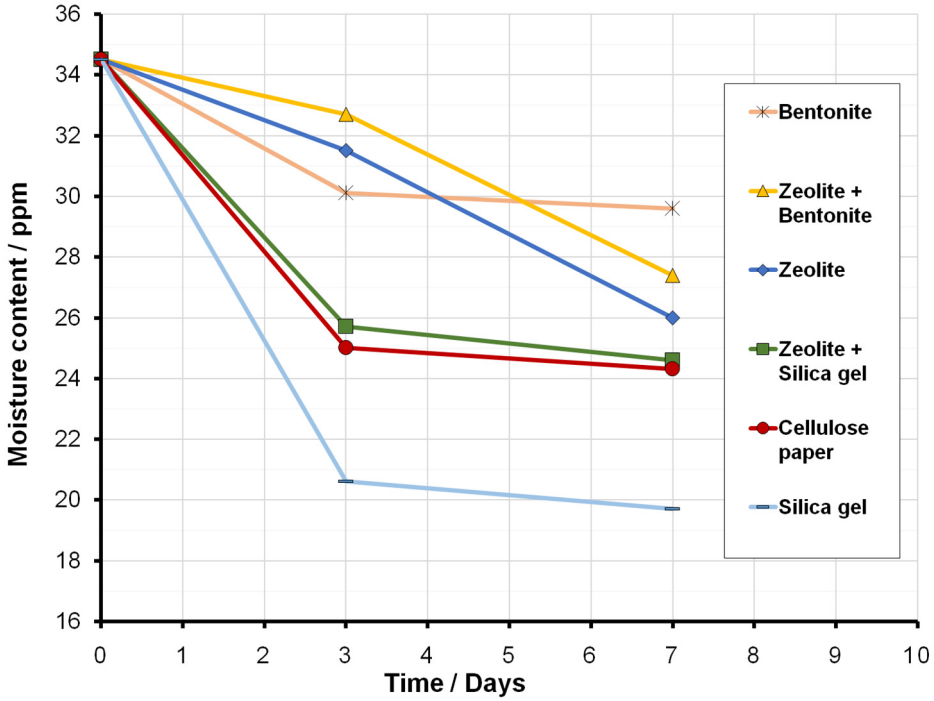

Figure 2: Moisture content of test samples after 3 days and 7 days

The results in Table 1 indicate the percentage change in moisture content of the oil after 3 days and 7 days. The reduction of moisture content is best with silica gel. Cellulose paper and the combination of zeolite with silica gel are the next good options.

Table 1: Change in moisture content after 3 days and 7 days

Material	Change in moisture content / %	
	after 3 days	after 7 days
Bentonite	-12.8	-14.2
Zeolite + Bentonite	-5.2	-20.6
Zeolite	-8.7	-24.6
Zeolite + Silica gel	-25.5	-28.7
Cellulose Paper	-27.5	-29.6
Silica gel	-40.3	-42.9

In this investigation, the effect of different filter materials on the moisture content was investigated. However, the impact of other parameters such as temperature and rate of flow of oil through the oil processing system is yet to be investigated. Furthermore, the influence of the filter material on the gas content in the oil has to be thoroughly inspected. These issues will be addressed in future investigations.

Photoconductive elements for the detection of electric arcs in transformers

M.Sc. Aref Sharifi

As a matter of fact, the explosion of a transformer tank due to an electric arc can have several serious consequences. A fast and reliable detection method is required to reduce extra financial costs and prevent accidents, which could endanger the life of personnel. One special idea could be using photosensitive elements as an electric arc detection system in power transformers. However, such an application entails choosing of an appropriate element concerning the requirements of transformer service conditions. The most common photosensitive light elements are photodiodes and photo resistors.

Figure 1 depicts the equivalent circuit of conventional photodiodes.

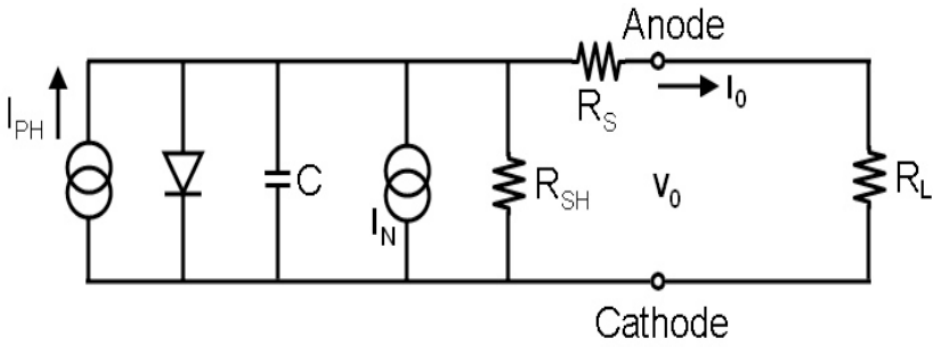

Figure 1: An electrical model for photodiodes

In Figure 1

- I_{ph} represents the current generated by the incident light,
- C is the diode capacitance,
- R_{SH} is the shunt resistance,
- R_s is the series resistance,
- I_N is the noise current, and
- R_L is the load resistance.

Photodiodes can be implemented in photoconductive or photovoltaic modes. In the photoconductive mode, the photodiode is reverse biased by a DC voltage, while in the second mode it is used as a light dependent current source. Although an external DC bias increases the detection speed, it increases both dark and noise current. This behaviour is problematic in the case of low light intensity, where the dark and noise current can saturate the current due to the light. Due to EM (Electromagnetic) in presence

of an electric arc, a very fast response is not achievable. Hence, for this application, a transimpedance circuit in zero bias voltage (photovoltaic mode) is preferred.

There are three different types of noise currents in photodiodes including Johnson, shot and flicker noise. Johnson noise is attributed to the shunts, series as well as load resistance, which is physically expressed by (1).

$$I_j = \sqrt{\frac{4\,KTB}{R}} \tag{1}$$

Where

- I_j is the Johnson noise
- K is Boltzmann constant
- T is the temperature in Kelvin
- R is equivalent resistance lead to noise

Shot noise presents in reversed bias photodiodes and increases with increment of a DC bias, in particular at high temperatures. Typically, the dark current I_{dark} of photodiodes doubles for each 10 °C as the flowing relation.

$$I_{dark}(T_2) = I_{dark}(T_1) \cdot 2^{\frac{T_2 - T_1}{10}} \tag{2}$$

Also, a higher temperature reduces the absorption coefficient of photodetectors. Thus, it may not be advisable to use photo sensors beyond their recommended working temperature.

Figure 2 illustrates internal structure of a typical photoresistor manufactured by cadmium sulfide (CdS) technology, where an indium tin oxide (ITO) acts as transparent surface for CdS materials. The substrate of photo resistors is usually manufactured by ceramic as well. Clearly, the electrical model of a photo resistor is comprised of resistive and capacitive elements; hence, an RC parallel circuit is an appropriate model for LDRs. Photo resistors (LDRs) have working temperature limitation generally up to 75 °C and photodiodes up to around 100 °C.

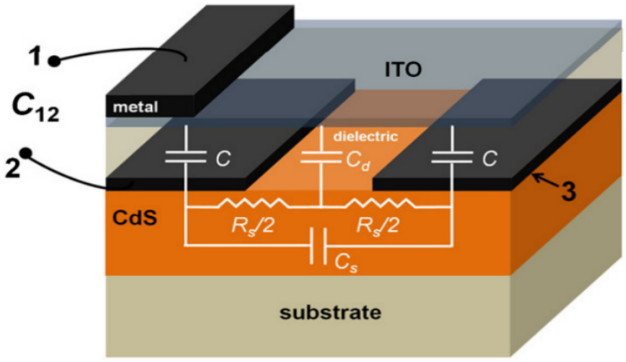

Figure 2: Internal structure of a Light dependant resistor

This temperature restriction might be a problem, when using this kind of semiconductor inside transformers.

Arc detection using semiconductive light sensing elements inside the transformer tank

M.Sc. Aref Sharifi

Transformer explosions and fires are the most dangerous consequences of transformer faults. Besides the financial loss, consequences are often environmental pollution, fires, personal injury, or even death. Especially for substations in densely populated areas, this is a very high risk. As protection each transformer is equipped with a Buchholz relay (BHR), which identifies such failures, thus a circuit breaker (CB) can trip the transformer. The time between the internal breakdown and the disconnection of the transformer is approximately 5 cycles. However, in some cases, the tripping of the transformer is not fast enough in order to prevent a tank rupture and the catastrophic collateral damages described above. Therefore, faster arc detection systems are under investigation like the use of photo sensitive semiconductors inside the transformer tank to detect the light emission from an arc and to trigger the circuit breaker. Currently, there are many unanswered questions about the reliability, sensitivity, operating temperatures, and lifespan of these new optic systems, which will be partly discussed in the following.

Figure 1 shows the implemented setup. In this circuit, the current is first converted to the voltage using resistance R_1, and then the voltage signal will be amplified with a feedback resistance. Based on the current signal, the resistance values are selected carefully to intensify the signal sufficiently. Also, an EMI (Electromagnetic Interference) filter is embedded before the oscilloscope to improve the signal-to-noise ratio. The electrodes (needle-plate) are placed inside the oil and the distance between the electrodes is 1 cm.

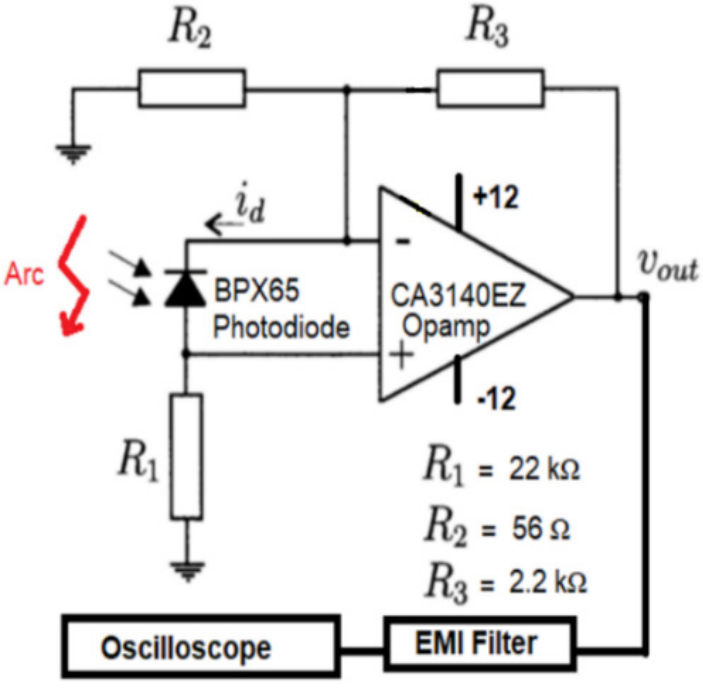

Figure 1: Transimpedance amplifier circuit

Figure 2 demonstrates the signal from the arc at different distances. The arc happened inside new oil at room temperature. As it can be seen, when the distance between the arc and photodiode sensor is increased, the signal intensity is decreased, but also EMI effects are considerable at longer distances.

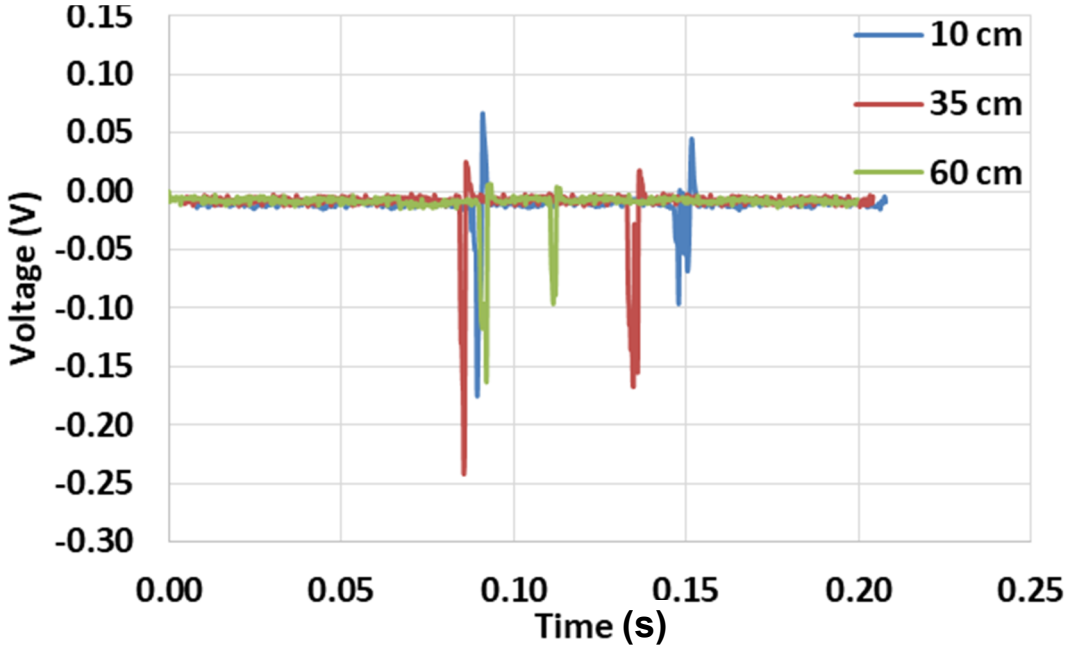

Figure 2: Signal profile in the oil (25 °C) at different distances

The photoresistor is like a variable resistance against light intensity. When the light increases, the resistance decreases. Therefore, based on the specifications of the photoresistor, the measurement circuit is shown in Figure 3.

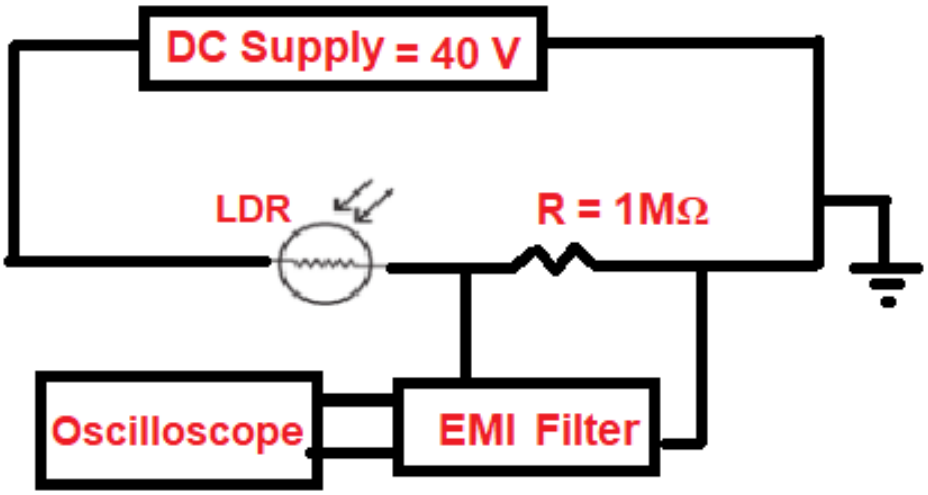

Figure 3: LDR measurement setup

The signal profile is indicated in the oil (25 °C) at different distances in Figure 4. As it can be seen, it is well observed that as the light intensity is reduced over longer distances, thus the signal becomes weaker. Also, other results showed that the photoresistor is sensitive to temperature variations.

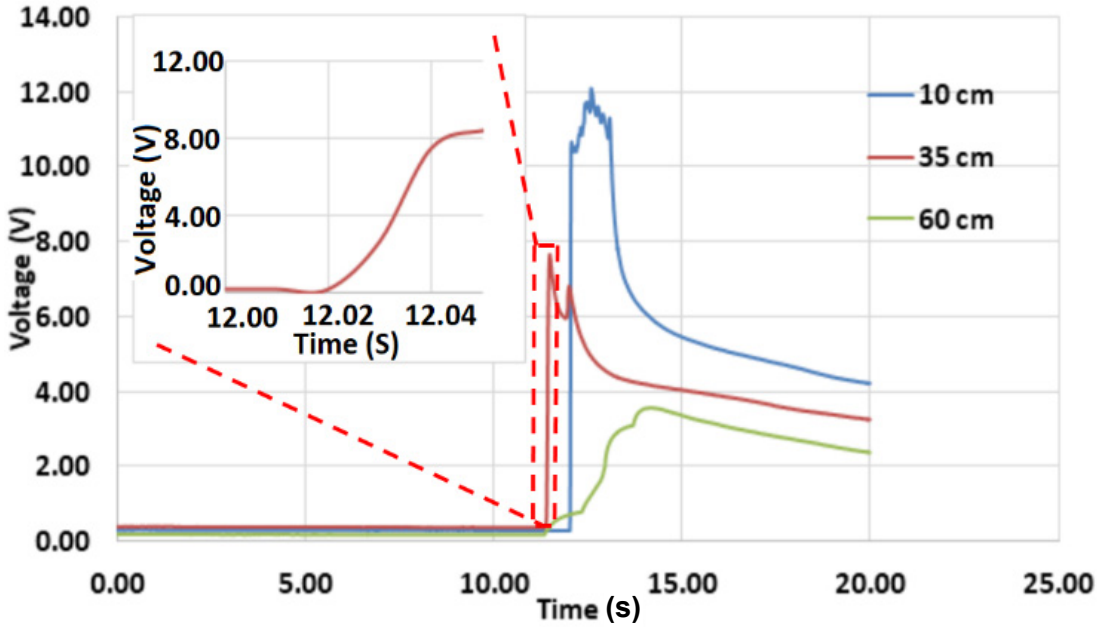

Figure 4: Signal profile in the oil (25 °C) at different distances without barrier

Based on these and additional investigations it is concluded that photoresistors or photodiodes seems not to be a reliable solution for an arc detection, thus they can not replace this function of a BHR.

Investigation on type of faults on stators isolated with paper

M.Sc. Laureen Stahl

The implementation of climate policy goals is accompanied by measures to reduce greenhouse gas emissions in all sectors. Accordingly, energy efficiency measures and energy savings also affect the energy and electricity sector. There is currently a focus on the use of electric motors in research and development, because the demand will increase steadily in connection with the transition to electrification and mobility. Due to higher demands on electric motors and the expected increase in demand, further development and the realization of manufacturing and quality testing processes are required. The aim is to improve quality and service life, and at the same time to reduce the cost of materials and production.

A wound stator consists of a stator core, a slot insulation and a winding with impregnation or casting. A common reason for failures on rotating electrical machines are damages on the stator insulation. The production losses associated with the failures are costly and not economical, which is why a meaningful and efficient diagnosis of the stator insulation is indispensable.

In consideration of that context, possible faults that can occur in the insulation of a stator or the bundle of laminations are first defined.

Faults in a stator are distinguished between those that occur in the insulation layer of a slot, during the production of the bundle of laminations and further faults that can only occur when the winding is already placed. Defects in the insulation layer include, for example, internal voids and leaking particles, which occur directly in the insulation material or, in the case of composites, are caused by decomposition into the individual components. As a result of temperature changes and cooling processes, there may be embrittlement and subsequent formation of cracks and cavities, direct formation of cracks and cavities, warpage of the insulation and incomplete syringing. Due to temperature changes and cooling processes a delamination of the main insulation is also possible, as well as incomplete curing.

In addition to the temperature as an influencing variable, non-uniform casting contributes to insulation displacement, incomplete syringing or variation in layer thickness. Furthermore, slot discharges can be counted among the defects of the insulation layer. Some faults can only occur when the winding is already inserted. These types of faults include cracks at the leading edge due to the shaping of the winding, delamination between the conductor and the insulation, surface discharges at the winding head and

winding head vibrations, which occur because the conductor bars are not firmly clamped, but are merely stiffened by support elements.

Moreover, faults are also possible in the manufacture of the bundle of laminations. These include sharp edges, which lead to cracks and abrasion of the main insulation, and punching defects, which affect the layer thickness and capacitance. The displacement of the punched sheets and an uneven slot base can also influence the layer thickness and capacitance and lead to abrasion of the main insulation. After insertion of the winding, further influencing factors are a loose fastening and insulation shrinkage, which lead to friction on the bundle of laminations and ultimately to abrasion of the main insulation. In addition to these defects of the bundle of laminations, which influence the insulation, defects between the laminations are possible. These lead to changes in the magnetic circuit and can be detected by flux leakage measurement.

Taking into account the defined defects, dielectric and electrical measurements were performed in the laboratory on stators with paper insulation. The aim was to investigate the influence of modelled fault replicas. Based on the defects defined above, the slot without defects, the defect types of void, crack, delamination, double layer thickness and conductive particles were modelled and investigated. In order to investigate only the influence of the defects on the slot insulation, a metal tube wrapped with a conductive elastomer, which was pressed against the inside of the slot, was used as a counter-electrode to the bundle of laminations (Fig. 1).

Figure 1: Stator with metal tube as counter electrode

Due to different modelled faults, the PD measurement under AC showed differences in the insertion voltages (Fig. 2). For the tests, 5 pC (50 Hz) was defined as the PD inception threshold.

Accordingly, as expected, the PDIV decreases as a result of voids and a crack in contrast to the slot without defects. In the case of delamination the PDIV takes a value between the levels measured for crack and the voids, which is attributed to air entrapment as a result of delamination. The delamination was simulated by means of a piece of heat-shrink tubing placed between the slot insulation and the bundle of laminations.

As a result, air inclusions may form at the edges, which are larger than the replicated voids, so that the PDIV decreases.

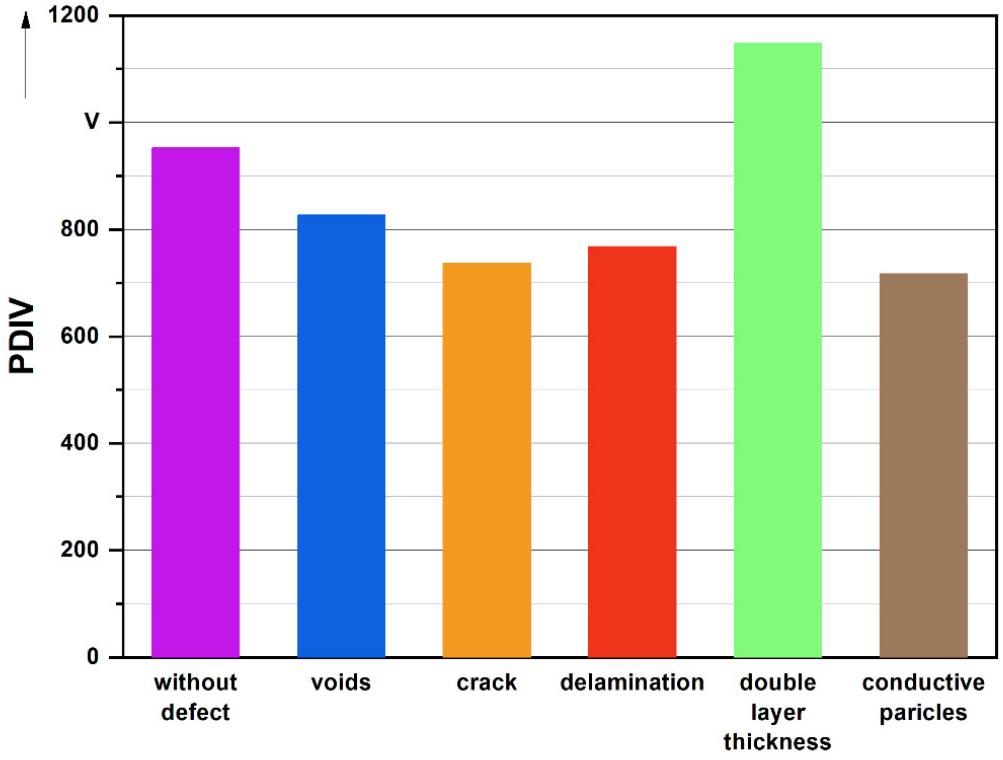

Figure 2: PDIV of the paper-insulated stators for different types of faults

Compared to the insulating paper without defects, partial discharges occur for a double layer thickness in the entire slot at a higher voltage. It is also clear that conductive particles have an influence on the inception of partial discharges. To simulate this type of fault, copper particles were rubbed onto the insulating paper.

Based on these initial investigations, it is evident that the types of faults can be detected and characterised at an early stage by means of PD measurements with the used set-up. For this purpose, further investigations are needed with regard to other types of faults and the variation of these, as well as the investigation on the types of faults for other dielectric and electrical parameters.

Investigations on isolated round wires using water as a test medium

M.Sc. Laureen Stahl

The change towards electrification and mobility is accompanied by the use of electric and hybrid vehicles. With the increasing demand for electric motors, reliability and a certain service life are required. Accordingly, knowledge about the ageing of the electrical insulation system is essential.

Polymeric dielectrics are used in rotating machines for insulating live parts. In the case of low-voltage motors, for example, a flat insulating material is inserted into the slot and enamelled wires are placed on top. The stator is then either sprinkled with lacquer, dipped in lacquer or impregnated under vacuum with epoxy resin. During operation, the insulation system is subject to various stress factors. These stress factors, which can lead to deterioration or even electrical breakdown of the insulating samples, include thermal, electrical and mechanical stress. In addition, the ageing process can be accelerated by ambient conditions such as humidity, temperature and the surrounding material. Accordingly, the impregnation, which is an additional insulation, has further tasks. This additional insulation protects the enamelled wires from moisture and stabilises the enamelled wires in the slot. It also helps to prevent the insulation from being worn through by vibrations and dissipates the heat that is generated during operation. The winding insulation is usually the weakest point of the insulation system, which is the reason why it is to be examined more closely. Within the scope of this investigation, the suitability of water as a test medium for enamelled stator windings is to be researched. For this purpose, twisted magnet wires (Fig. 1) are produced by means of a winding machine, according to *DIN EN 60851-5*. This standard describes a method for measuring the breakdown voltage of insulated wires. In an initial investigation into the suitability of tap water as a test medium, wires insulated with polyurethane (PUR) with a diameter of 0.63 mm are used.

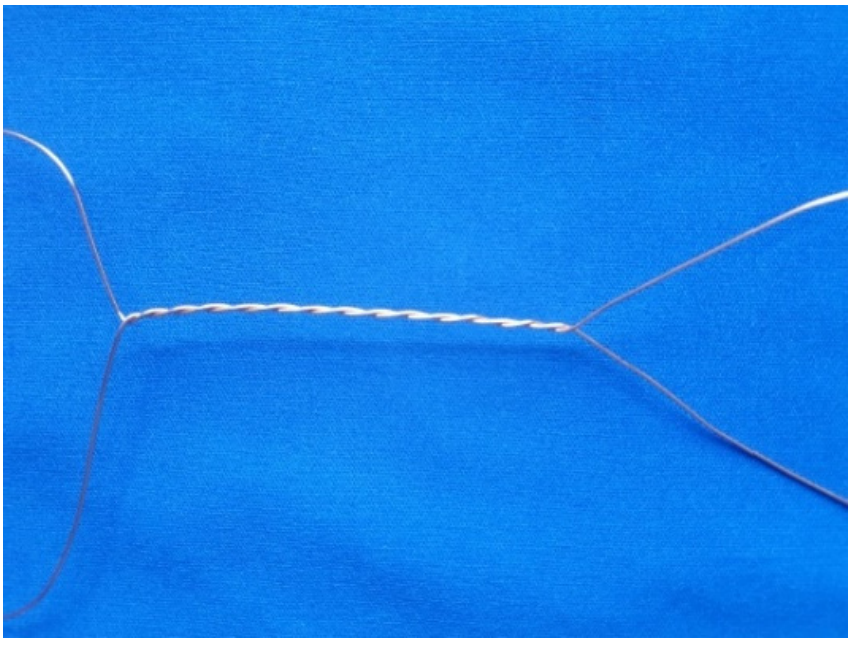

Figure 1: Twisted magnet wire

The winding wire originally consists of a continuous wire which has been cut through, which is why there is contact between the water and the copper wire at the cut edge when water is used as a counter-electrode. This cut edge is not relevant when measuring the breakdown voltage according to the standard, for example in insulating oil. Due to the high conductivity, however, there is contact between the voltage side and earth in the setup with water used for these investigations. To avoid this, the copper contact is insulated with epoxy resin. At the triple point between the insulating material, epoxy resin and water, there is an increase in the electric field strength, which is why an attempt is made to control the electric field geometrically at the end of the winding wire. The test object with conical field control is shown in Fig. 2 (left).

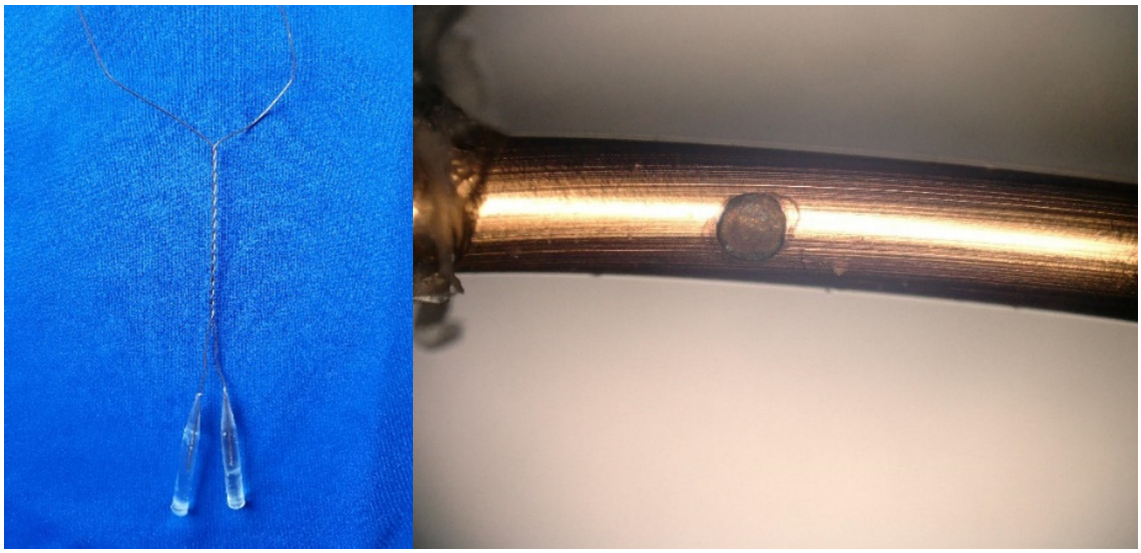

Figure 2: Test object with conical field control (left) and microscopic view of the breakdown (right)

The test object made in this way was then loaded with an increasing voltage of 500 V/s applied to one wire while the second wire was connected to earth. Despite the implemented geometric field control, the breakdown did not occur at the contact point of the two wires to each other as desired, but at or near the triple point (Fig. 2 right). Based on this result, the set-up for investigating the breakdown voltage is further adapted to the method with water. By using water as a counter-electrode, it is possible to examine the entire insulating material of the wire and not just the contact of the two wires. Against this background, the wire is still twisted with the help of the winding machine to simulate a winding, but both wires are connected to the voltage (Fig. 3).

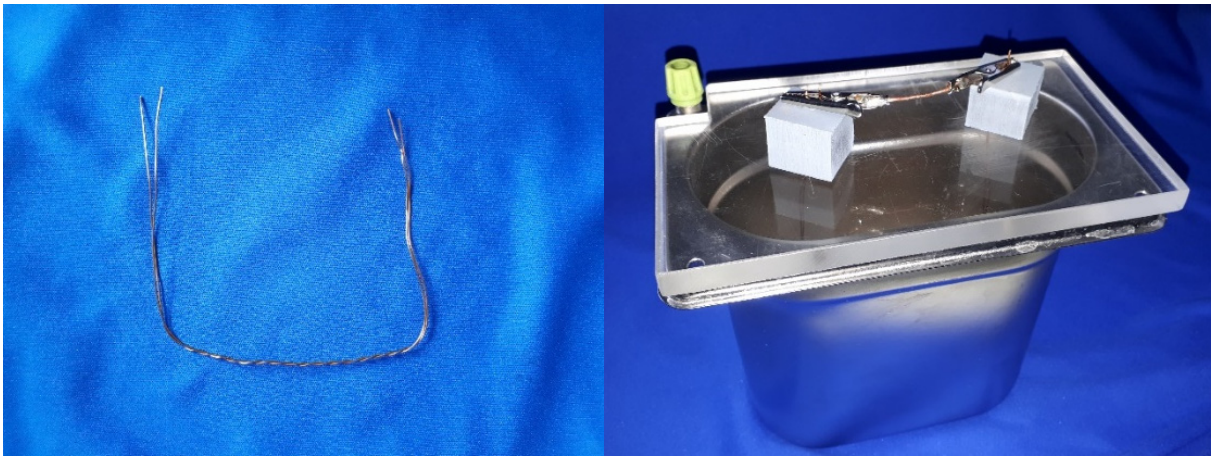

Figure 3: Adapted test-setup for measurement of breakdown voltage in water

In this test set-up, the breakdown point is mainly caused due to the twisted area, which is why this set-up can be used for further investigations with water as the electrode in order to investigate the influence of the water. However, this test method will also be used to investigate various enamelled wires and their PD and breakdown voltage behaviour.

Development of a circuit for the generation of voltage pulses with high slope for the aging of solid insulating materials

M.Sc. Javier Torres

Equipment, especially transformers, are exposed to additional electrical loads due to the changed grid operating conditions caused by the energy transition, such as the increased use of power electronic converters. Semiconductors made of silicon carbide (SiC) are increasingly being used in modern converters. When SiC semiconductors are switched, pulsed voltages that can reach slope values of up to 100 kV/µs and repetition rates of up to 20 kHz occur. This pulsed loading can affect the insulation's life of high-voltage equipment and lead to earlier failure. In this context, research on the effect of impulsive stresses on the life of insulation materials emerges as a major factor in the safe operation of medium-voltage transformers.

The *IEC 62068* standard specifies the criteria for evaluating the influence of repetitive impulse voltages. Test systems that meet the test specifications of the *IEC 62068* standard are hardly to be found on the market due to the specific application and usually exist as self-built installations in research facilities. With, a prototype generator for the generation of voltage pulses with slope values of about 20 kV/µs and amplitudes up to 3 kV was constructed at the *Schering-Institute*. This design represents a compromise between the desired slope values and the power necessary to generate them.

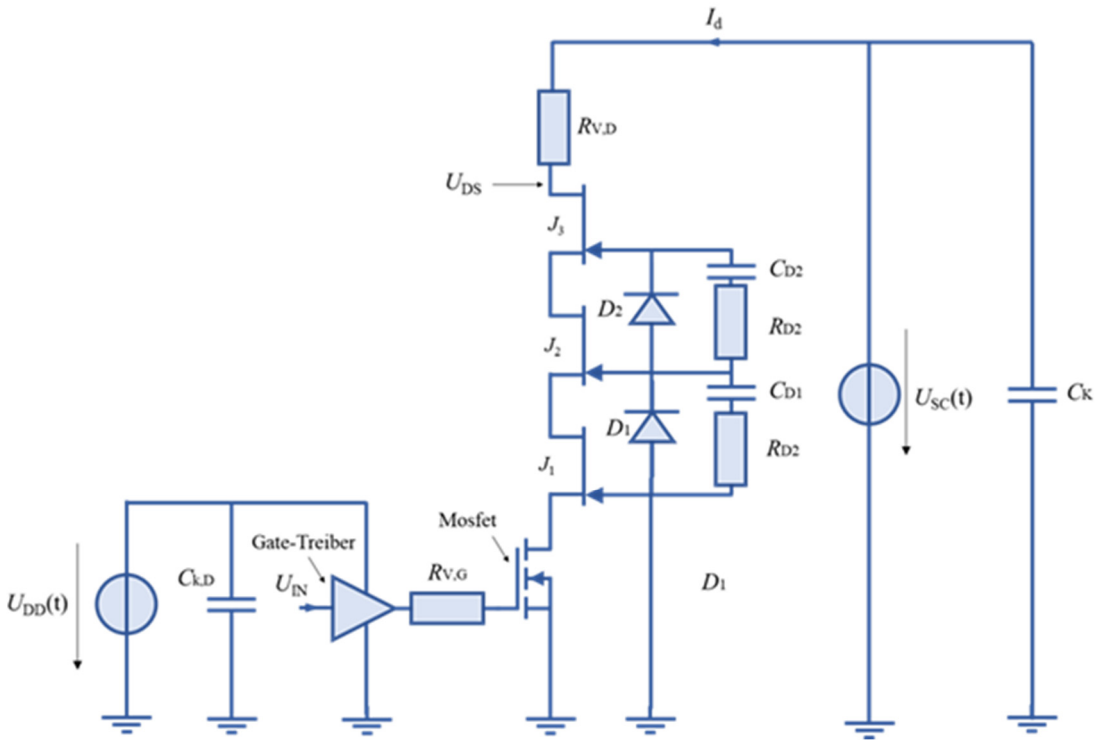

Figure 1: Equivalent circuit diagram of a three-stage supercascode circuit with compensation network

The topology of the generator is based on the supercascode circuit. This structure consists of several JFET transistors, which have an individual reverse voltage of 1.2 kV, are connected in series across the drain and source terminals and controlled by a MOSFET. Figure 1 shows the equivalent circuit diagram of the arrangement.

In this case, each JFET forms a stage of the circuit. The mostly undesirable "normally on" behavior, which JFET transistors typically exhibit and can limit their use in industrial applications for safety reasons, is avoided by the MOSFET. Thus, the advantages of JFETs, such as low input capacitance and low on-resistance, which allows the transistors to be used as amplifiers at higher frequencies, can be used.

Nevertheless, with an increasing number of stages in the circuit, difficulties arise in synchronizing the switching moments of the transistors, because these must be switched as simultaneously as possible in order to generate pulses with the desired voltage slope. For this reason, a compensation network with a precise design is necessary. A simulation model was created to dimension the compensation network. Accurate models of the transistors, developed by their fabricants were used for the simulation. This approach allowed the design of the compensation network, the series resistor of the circuit and the DC link capacitor. The series resistor of the arrangement has a relatively low value (a few kΩ) and was constructed from resistors with a high pulse power on a circuit board designed for this purpose.

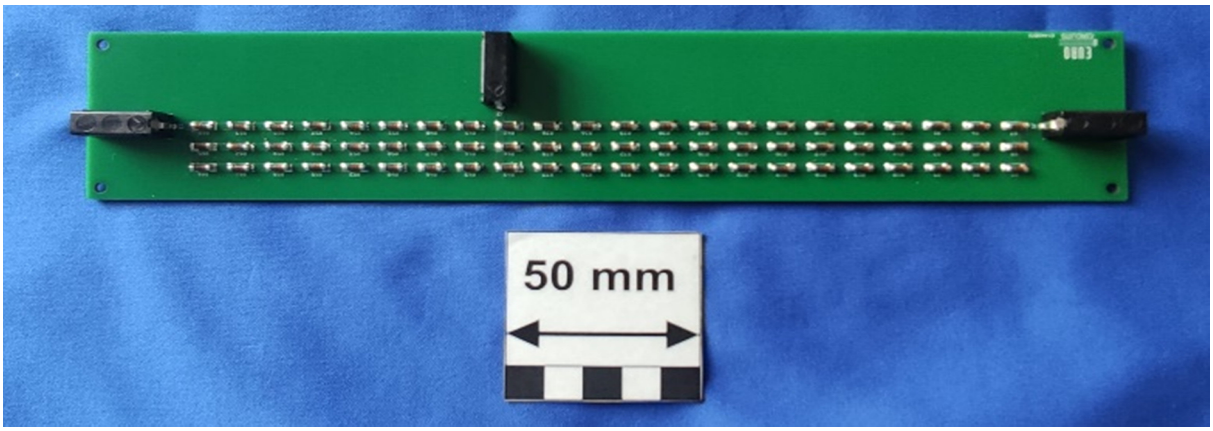

Figure 2: Developed series resistor for the supercascode circuit

The circuit was tested accordingly. A 6 kV-1.2 kW source was used as the DC voltage source. Rectangular voltage pulses with slope values of 21.4 kV/ µs and an amplitude of 3.5 kV could be generated. The results are shown in Figure 3. U_{sig} shows the trigger signal of the circuit. U_{ein} and U_{DS} represent the input voltage and the drain-source voltage of the supercascode in kV, respectively.

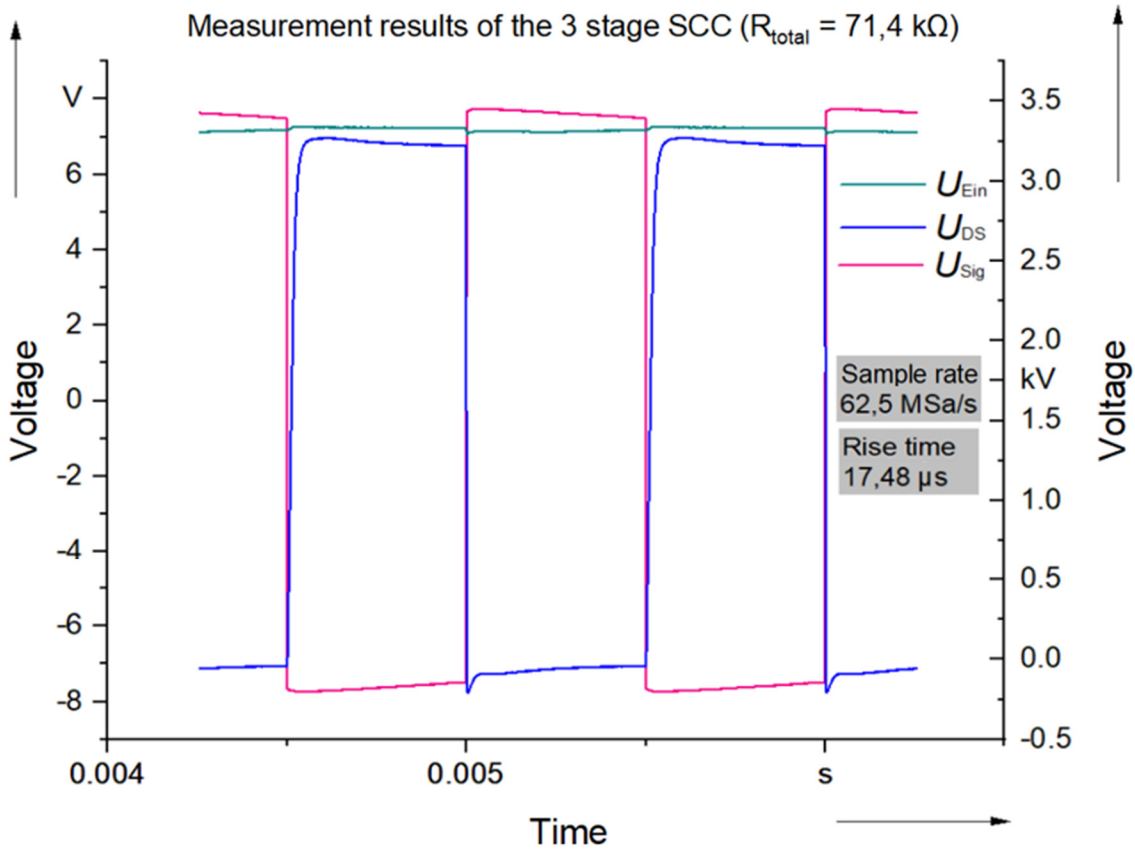

Figure 3: Test results of the supercascode circuit

Investigation on the characterization of partial discharge processes on polymeric solids under DC stress

M.Sc. Javier Torres

In the context of the energy transition and the optimization of resource consumption, the grid conditions as well as the topology of electrical power systems are constantly changing. Therefore, the transmission of electrical energy with high voltage DC systems (HVDC) is becoming increasingly important. By using HVDC systems, better transmission capacity over long distances and lower losses over long transmission distances can be achieved. The stresses to which the insulating materials in HVDC systems are subjected differ from those that occur in AC systems.

Since the field distribution in the insulating material can be locally distorted, the formation of space charges under the action of high DC voltages over long periods of time is a potential hazard. The apparition of partial discharges (PD) can be favorized by these field distortions and accelerate the aging of the HVDC system insulation. Therefore, the detection of PD and the correct identification of the fault type are extremely important for the operational safety of HDVC components. In AC systems, PD types can be identified with relatively high accuracy, but in HVDC, such identification is still limited. For this reason, an approach for fault type identification of PD under DC stress was investigated in this work.

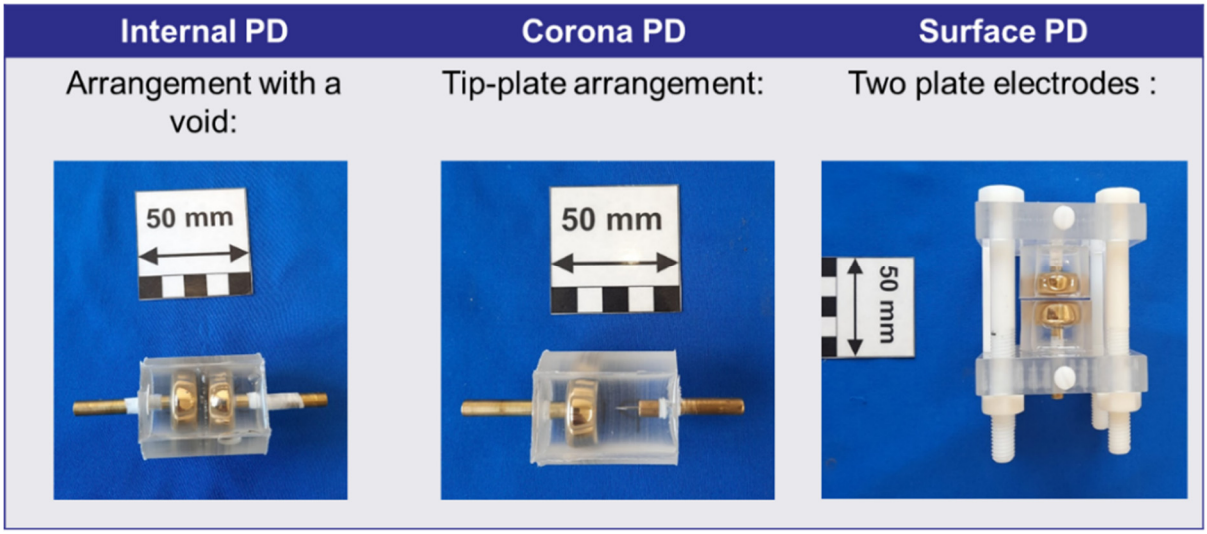

Figure 1: Test specimens for the simulation of faults in insulation systems

For the investigation of PD events, different configurations were first created, which reproduce three typical faults (internal discharges, corona discharges and surface discharges) in insulating systems. To ensure the statistical reliability of the tests, several test specimens of each fault type were manufactured. To account for the influence of

the material on the behavior of the discharges, test specimens were made of two polymers. The test specimens were then subjected to DC voltage and, for comparison, also to AC voltage so that partial discharges occur.

The approach for identifying the defect is based on the detection of differences between the measured stress pulses, which is shown in Figure 2. In the upper part of the image, a histogram of the fast Fourier transforms (FFT) can be seen. In the area with reddish color are the FFT of the pulses, which occur with high occurrence and thus are representative of a certain type of fault. In the lower part of the image, the time courses as well as the FFT of representative pulses for each type of defect are shown. Broad and narrowband measurements were performed, with 1024 pulses per stress type recorded for each test specimen.

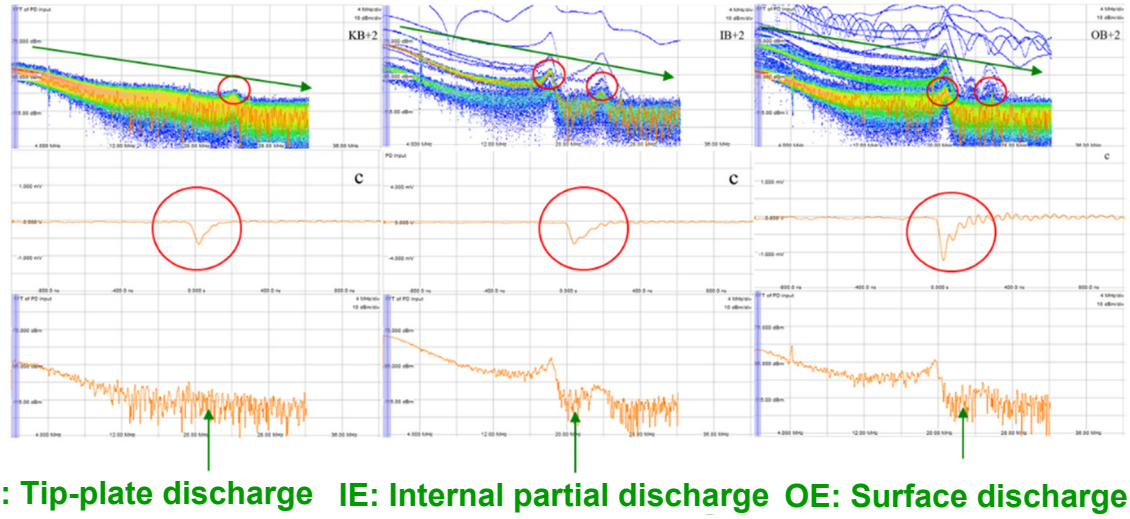

Figure 2: Differences in the discharge pulses for three different types of discharge

To investigate the characteristics of the PD pulse signal, both in the frequency and time domains, a three-stage wavelet packet transform was performed on each pulse. The energy component of each subband and the wavelet energy entropy were extracted as feature vectors and processed as learning data using a support vector machine algorithm. After training the algorithm with the input data, it was tested, using further PD measurements on the test samples. The measured pulses were then classified by the algorithm.

The results of the algorithm showed an approximately 80% correct identification rate for the investigated PD types, with better identification rates generally obtained for the broadband measurements, which can be explained through the bigger amount of information contained in the recorded impulse. When the analysis was repeated on the silicone test specimens, similar results were obtained and thus the suitability of the method for different materials could be evaluated.

Comparison of air and liquid cooling for hybrid-electric propulsion systems from an insulation point of view

M.Sc. Yunfei Wang

With the ongoing development of hybrid- and all-electric aircraft, propulsion systems are reaching megawatt power levels. For efficient systems with high power densities, high power dissipation densities in the electric motor, inverter, and battery storage are also expected. The electrical components of the propulsion system generate large amounts of heat that must be dissipated to ensure the system safety and reliability. There are several cooling methods, each with a different Technology Readiness Level (TRL [1...9]). According to the literature, the methods can be divided into passive and active mechanisms. Table 1 lists the main cooling methods and their associated media as well as the TRL for aviation.

Table 1: Essential cooling methods for hybrid-electric aircraft

Cooling method	Cooling media	TRL
Air cooling	Forced air, Ram air	9
Liquid cooling	Oil, Fuel, Water, Glycol-water mixtures, Synthetic fluids, Refrigerants, etc.	>7
Phase change materials	Graphite carbon, Sodium acetate, etc.	4-6
Heat pipes	Water, Refrigerant, etc.	4-6
Cryogenic cooling	Liquid hydrogen, Liquid Nitrogen, etc.	1-3

According to the state of the art, there are other cooling methods besides air and liquid cooling with high TRL that could be used in aerospace. These include, for example, cooling techniques based on phase change materials, heat pipes, thermoelectric effects, cryogenic cooling, etc. These cooling methods are still at the feasibility study stage and are not yet sufficiently mature for practical application.

The voltages of the motors and generators in hybrid electric drive systems can reach thousands of volts, resulting in large heat losses in the windings. Two options for cooling the motor windings are currently being pursued in parallel. One is air cooling of the windings, the other is liquid cooling. Both variants have advantages and disadvantages. Air cooling is divided into active and passive cooling, depending on the energy consumption of the cooling system. When comparing passive air cooling (natural convection) and active air cooling (forced convection), the heat transfer coefficient is usually much higher for active cooling. Passive air cooling is therefore less suitable for applications with high heat losses and compact arrangements. In liquid cooling, two types of heat absorption can be distinguished, namely direct and indirect cooling. In indirect liquid cooling, heat is transferred to the coolant through a liquid channel located at the heat source. In contrast, direct liquid cooling is based on direct contact between the coolant and the component surface. In general, direct liquid cooling results in better cooling and thus higher performance of the propulsion system.

In addition to cooling performance, there are also differences in electrical insulation between air cooling and direct liquid cooling. In general, dry air at room temperature and normal atmospheric pressure has good insulating properties. The dielectric strength of air can reach up to 30 kV/cm. After a breakdown, the insulating properties of air can be immediately and automatically restored. However, the breakdown voltage of the air gap and the external insulation of the electrical components is affected by environmental factors such as air pressure, temperature, and humidity, in addition to field homogeneity. For example, at high humidity, water molecules are deposited on the insulating material surface, resulting in increased surface conductivity and decreased surface resistance, respectively. Conductivity promotes electron mobility and charges are distributed over the entire insulating material surface. This leads to many small discharge pulses and eventually to electrical breakdown or insulation failure. In addition, the sand and dust contained in the cooling air can erode the insulating material surface at high speed, causing wear to the insulating material. Finally, the salt spray in the sea air can form electrolytes on the surfaces of insulating materials and metals, accelerating the corrosive effect and affecting the insulation properties.

For direct liquid cooling of electrical components, the requirements for electrical insulation must be taken into account. Transformer oils, turbine oils as well as fluorinated dielectric fluids are suitable for direct liquid cooling. Transformer oils, due to their excellent insulation properties, can meet the insulation requirements of the high-power direct liquid-cooled motor and generator. The dielectric strength of the treated insulating oil can be about 30 kV/mm, which is much higher than that of air. In addition, insulating oils are particularly suitable for the operating temperature range of 0 to 150 °C. If the insulating oils are used beyond the temperature range described, they experience accelerated aging. There are three main aging processes for organic insulating fluids according to the aging mechanism, namely pyrolysis, oxidation and hydrolysis. Pyrolysis is the term used for the thermal cracking of chemical synthetics. In this process, the effects of temperature force bond breaking within the macromolecules. Oxidative aging is the reaction of an insulating liquid with oxygen to produce oxides. Hydrolysis is the cleavage of a compound by reaction with water. In this process, a hydrogen atom is released onto a molecular residue and the remaining hydroxyl residue is bonded to the remaining molecular residue. The aging products formed as a result of aging can have a negative effect on the insulating properties. For example, an increased amount of dissolved water or dissolved gases due to high pressure and temperature changes could lead to bubble formation, which reduces electrical strength.

Selection of cooling and insulating media for hybrid-electric applications

M.Sc. Yunfei Wang

Against the backdrop of reducing greenhouse emissions, there is an increasing demand for innovative technologies in aviation. Through the use of hybrid-electric as well as fully-electric propulsion technologies, there is the possibility of partially or completely displacing fossil fuels from aviation, especially on short to medium distances.

One of the technical challenges of hybrid-electric propulsion systems is how to deal with the heat generated during operation. The thermal management system is responsible for heat dissipation and is used to control the heat transfer between the heat source and the heat sink to keep the temperature of the aircraft subsystems and components within the required temperature range. Therefore, the selection of an appropriate cooling medium is critical for an efficient and stable propulsion system.

Currently, liquid cooling is widely used in the aerospace industry. The aerospace industry has requirements for cooling and insulating fluids that they should be cooling, insulating, lubricating and embedding. In addition, the main focus is on a medium with a significantly high thermal conductivity to ensure efficient cooling, as well as a low fire hazard combined with sufficient electrical strength. The cooling and insulating fluids for aerospace applications should have good thermal stability and oxidation resistance to prevent aging and ensure long service life. Accordingly, the cooling and insulating fluids are subject to stringent safety requirements. If possible, the fluids should be non-flammable, non-toxic and non-climatic. A further requirement of the cooling and insulating liquid for use in aviation is that, in addition to large temperature fluctuations, the liquid must also be able to withstand strong pressure changes, which can promote the bubbling out of gas bubbles.

To select a suitable cooling and insulating fluid, three work steps were undertaken by the cooperation partner Rolls-Royce. First, the cooling methods available for each subsystem were investigated and the technical data of the cooling fluids that could be used were collected. In the second step, the fluids were filtered according to the thermal requirements of the propulsion system (e.g. operating temperature limits of the components, lowest ambient temperature -40 °C). Finally, the thermal and electrical properties of the fluids were compared. After weighing the advantages and disadvantages of each fluid, the cooling and insulating fluids were selected for further investigation and testing. Table 1 lists the detailed inclusion and exclusion criteria.

Various fluids can be selected and tested for use as cooling and insulating media in aviation. In the field of high-voltage technology, alternative insulating fluids have been increasingly used in recent years. These are Gas-to-Liquid oils (GTL oil), synthetic and natural ester fluids, silicone oils, etc. One advantage of these insulating fluids over

Table 1: Inclusion and exclusion criteria of the cooling and insulating fluids

	Inclusion and exclusion criteria
1.	The flash point of the coolant must be higher than the operating temperature of the system components.
2.	The pour point of the coolant must be below the lowest ambient temperature.
3.	Coolants with lower viscosity are preferred for better cooling.
4.	For direct liquid cooling, the cooling liquid must be dielectrically insulated.
5.	For selection, the resistance of the coolant under continuous load under team factors (e.g. in other applications) should be known.
6.	The coolant must be compatible with the materials of the cooling system and the materials of the system components.

conventional mineral oil is an increased flash and fire point and a special resistance to aging. Ester insulating fluids have high thermal conductivity and are particularly suitable for higher operating temperatures. Furthermore, ester oils are divided into synthetic and natural esters. However, the hydrophilic group of the natural ester is such that it tends to dissolve more water, which decreases the electrical strength. In addition, natural esters oxidize in contact with atmospheric oxygen, which leads to an increase in viscosity.

In the aviation industry, turbine oils are already used to lubricate and cool the mechanical components of aircraft engines such as bearings and gears. Typically, turbine oils have a flash point of up to 220 °C, so they have excellent oxidation and thermal stability for long-term performance. At the same time, low viscosity turbine oils are ideal for use in low temperature environments. In addition, turbine oils also have some insulating properties and can be used to cool and insulate electrical components in generators and electric motors. However, turbine oils contain several additives to improve corrosion and wear resistance, which could lead to a reduction in the electrical strength of turbine oils. Therefore, turbine oils would have to be investigated primarily with regard to sufficiently high electrical strength.

In addition to hydrocarbon-based fluids used as coolants in various fields, fluorocarbon fluids should also be investigated and tested because they are inert, non-flammable and non-conductive. This increases the safety of the cooling system. In addition, these fluids have a low boiling point. When the liquid evaporates, a large amount of waste heat will be removed from the electrical components. Therefore, these fluids are suitable for single- and two-phase immersion cooling of temperature sensitive power electronics and batteries. In the two-phase immersion liquid cooling, the coolant continuously undergoes a phase change process from liquid to gas and back to liquid in the process of heat dissipation. The power electronics are completely submerged in a closed container with a low boiling point cooling fluid. The heat generated by the equipment is absorbed by the coolant and the temperature of the coolant starts to rise, when the temperature reaches the boiling point the coolant starts to boil from the liquid phase to the gaseous phase.

7 Conferences and Excursions

Conference participation

Due to the mitigation of the Corona pandemic, national and international conferences took place this year. In previous years, these conferences could only take place in online-offline format or had to be cancelled completely.

So after a long time, the staff of the Schering-Institute was able to participate in various conferences and present their own research results as well as to get in touch with other researchers from all over the world.

This year, the Schering Institute's contributions were presented at 3 conferences, namely *International Conference on Dielectric Liquids (ICDL)* in Spain, *Condition Monitoring and Diagnosis (CMD)* in Japan, as well as this year's last national conference *VDE Fachtagung Hochspannungstechnik 2022* in Berlin, which took place from 08/11 to 10/11/22.

Visit to the IEEE International Conference on Dielectric Liquids (ICDL)

After taking a year off due to the Corona pandemic, the ICDL was held this year from 29/05/2022 - 02/06/2022 in Spain at the University of Seville. About 200 visitors took part, arriving in good weather conditions of 34 degrees and enjoying the time, which is illustrated in Figure 1.

Figure 1: Conference participants in front of the Escuela Superior de Ingenieria in Sevilla

The ICDL is a research-oriented conference and offers a platform for discussions and exchange of ideas, research results and practical experiences on the properties and applications of insulating fluids. Special attention is given to fluid dynamics, electrical discharges and breakdowns as well as new findings in basic research.

In addition to the scientific presentations, the conference programme included a Cigré tutorial dealing with the requirements and test standards for dielectric fluids. In addition, the behaviour of dielectric fluids under different electrical voltages was discussed. Besides this, the social programme was rounded off by joint events, which provided a relaxed setting for a lively exchange of ideas and networking (Fig. 2). These included the opening excursion to the Metrosol Setas de Sevilla and the excursion to the Alcázar, the medieval royal palace of Seville. The social programme was rounded off with a closing dinner at the Guadalquivir.

Figure 2: The Gala Dinner (left) and Metrosol - Setas de Sevilla (right)

During the conference, the Schering-Institute was represented by Ms Homeier and Ms Özdemir, each with a conference contribution. Ms Homeier presented her latest results on "Modified Dissolved Gas Analysis with Additional Detection of Higher Hydrocarbons for Transformer Fault Diagnosis". Ms Özdemir also gave a presentation on her research topic "Investigation of the Diffusion Behaviour of Different Acid Configurations in Insulating Paper in a Closed Transformer System".

VDE Hochspannungstechnik 2022

After an online event in 2020, this year the "VDE Hochspannungstechnik" conference was held in Berlin from 08.11.2022 to 10.11.2022 for the first time since 2018 in presence again. On the first day of the conference, tutorials provided an insight into the work status of various Cigré working groups. Among other things, the special features of on-site commissioning of power transformers in Japan and China or new testing possibilities for solid-insulated power cables were discussed. On the second and third day of the conference, new findings from the areas of testing and measuring, materials and insulation systems, diagnosis of transformers and other topics of high-voltage technology were presented and discussed in parallel sessions. The focus this year, was on new technologies with regard to digitalization and energy transition. The staff of the Schering Institute presented a total of six publications this year on the topics of asset management, the ageing of polymer insulating materials and the diagnosis and examination of transformers (see Figure 1).

Figure 1: Presentation by Kristin Homeier on higher-value hydrocarbons

Almost all PhD students of the Schering Institute were able to attend the event and enjoyed the evening event in addition to the interesting discussions (see picture 2).

Figure 2: The Schering-Team at the evening event

Visit of the International Conference on Condition Monitoring and Diagnosis (CMD)

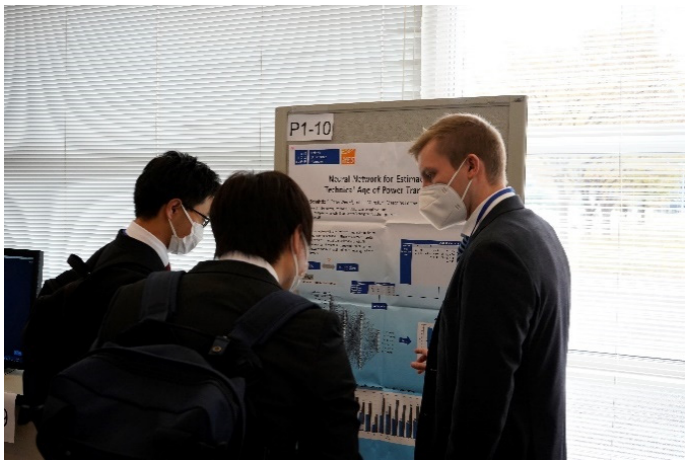

Fig. 1: Mr Schnittker in a scientific discussion

The ninth international conference on Condition Monitoring and Diagnosis (CMD) was held in Kitakyushu, Japan, from 13-18 November 2022. Due to the extreme entry restrictions imposed by Japan because of the corona pandemic, it was unclear for a long time whether the conference would take place online only. After the entry restrictions were eased on 11 October, travel preparations could begin. The conference focuses on monitoring, fault diagnosis and ageing assessment of electrical power systems, in particular partial discharge and space charge measurement, methods of effective maintenance, use of AI technologies and sensor technologies. The hybrid conference attracted 272 participants (212 on-site and 60 online) with 178 papers presented. Mr. Schnittker presented the paper "Neural Network for Estimating the Technical Age of Power Transformers".

In addition to the presentations, there were also interesting workshops, e.g. on the use of Weibull distribution for decision-making in asset management or on the construction of measuring equipment for measuring space charges in real high-voltage cables. An excursion to the Buzen battery storage power plant (50MW, 300MWh) completed the supporting programme. An interesting innovation was also the "Demo Event" in the accompanying technical exhibition. For this purpose, the hosts had set up a high-voltage test field in the exhibition hall and the exhibited partial discharge measuring and locating devices of different manufacturers could be directly compared with each other.

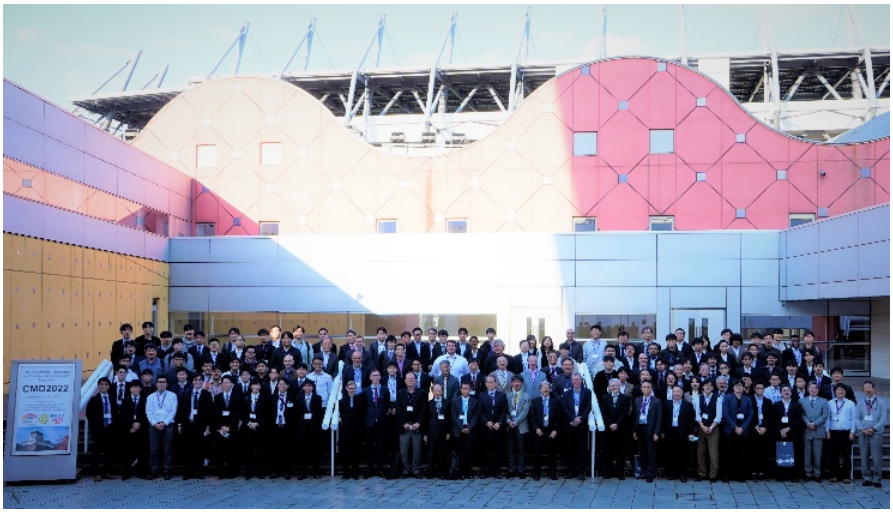

Fig. 2: Participants of the CMD 2022 in Kitakyushu, Japan

Transformer Life Management Conference

This year's Transformer Life Management Conference, which is held annually at different locations in Germany, took place on September 19th and 20th in Bad Gögging, Bavaria. The conference, organized in cooperation between the company Energy Support GmbH, Hitachi Energy Germany AG and the Schering Institute, which is responsible for the scientific chair, counted this year more than 200 participants and 29 exhibitors. In addition to the technical presentations, which were divided into five thematic blocks, four workshops were held on the topics of asset management, transformer databases, monitoring and "Transformers Go Green", as well as, for the first time, a poster session with contributions on current topics from university research.

Figure 1: TLM 2022 in Bad Gögging

Due to climate policy goals and constant technological progress, new challenges are arising in the field of energy supply, especially in the area of security. In the electrical power supply network, transformers represent an important operating resource for the transmission and distribution of electrical energy and connect the various voltage levels of the power grid with each other. Accordingly, the operational safety of transformers is directly related to a safe and efficient power supply. The new age in electrical power engineering was on the agenda this year as well as new technologies, for example the electrification of maritime shipping, future DC voltage systems and traction and special transformers. In addition, the conference focused on other topics such as

condition diagnosis and monitoring, insulating fluids for transformers and lifetime management, with the aim of ensuring reliable transformer operation, optimum maintenance, high operational safety and a long service life.
Therefore, as in previous events, the TLM addresses experts, operators, manufacturers, suppliers, exhibitors and scientists, and provides an excellent platform for discussing problems and challenges, exchanging the developments in transformer technology and maintaining and expanding one's network.

Preparations for the next symposium have already begun. The TLM 2023 will take place on September 18th and 19th at the Mercure Hotel Maininsel in Schweinfurt. In addition to the interesting contributions, there will be again an evening program.

Participation in the CIGRE Working Group JWG D1/A2.77

Kristin Homeier, Moritz Kuhnke

The CIGRE Working Group JWG D1/A2.77 mainly focuses on the topic of insulation liquid tests for electrical equipment, especially the dissolved gas analysis (DGA), but also the measurements of furans, acids, alcohols and other chemical and physical measurements as diagnostic opportunities for the condition monitoring of the solid insulation material in oil-filled electrical equipment.

Thus, this working group was divided into three major task forces (TF): TF 1 with the general measurement aspects, TF 2 with the data management and TF 3 with the modeling and case studies. The participants from the Schering Institute Prof. Peter Werle, Mr. Moritz Kuhnke and Ms. Kristin Homeier are primarily involved in TF 1 and TF 3. Prof. Werle chairs the Task Force 1, which specializes especially in the Ostwald coefficient (OC) and the partition coefficient (PC) of the headspace technique and also analyzes and verifies the possibilities of new DGA sensors such as helium, NDIR or photoacoustic detectors. The Schering Institute offers a great experience especially for the measurement of gas solubilities and has already developed and tested several promising possibilities for the determination of gas solubility. With this knowledge, the Schering Institute has developed a simplified, cost-effective measuring method for the determination of OC, which can also be performed in other laboratories, based on DGA measurement with a full vacuum degassing unit and which still has sufficient accuracy. In addition, a simple measurement method, which allows the determination of PC in the headspace technique, was developed by Ms. Senja Leivo and Mr. Jarkko Larkio from Vaisalla, who are also participants of the CIGRE working group.

The two measurement possibilities were tested in a Round Robin Test (RRT) regarding reproducibility and repeatability with selected liquids and gases. First promising measurement results were obtained. However, only a few laboratories participated in the first RRT on OC, which made static evaluation difficult. In recent months, a second RRT has been performed and the results are currently being evaluated. This time a larger number of laboratories participated in the RRT, so that a statistical evaluation will be more accurate. After this second RRT, the next steps in the next year will be decided.

Excursion to Maschinenfabrik Reinhausen

On Wednesday, 21.09.2022, the Schering-Team has visited the Maschinenfabrik Reinhausen (MR) in Regensburg. After a short welcome, Dr. Viereck, Mr. Kirchner and Mr. Gruber introduced the company MR, which was founded in 1868. Afterwards,
the functional principle of an on-load tap-changer was discussed and a switching operation of an on-load tap-changer was demonstrated. Furthermore, Mr. Gruber presented the ETOS system for recording and evaluating all relevant operating data of a transformer.
Finally, Dr. Viereck presented the newest vibro-acoustic tap-changer monitoring system. A sensor records the vibration profile of a switching operation and with the help of a machine learning algorithm the condition of the switching system is assessed and in critical conditions interrupted.
After a guided tour through the on-load tap-changer assembly, a joint lunch was taken. At the end of an interesting visit we took a tour through MR's test field.

Figure 1: Schering-Team and Dr. Viereck from MR (left) at MR

8 Publications

Transformers Magazine, Volume 9, Issue 1, Januar 2022
Possibility of electric arc detection in power transformers by directly embedded photoconductive elements in the transformer tank
A. Akbari, R. Sargazi, P. Werle, M. Kuhnke

IEEE Transactions on Dielectrics and Electrical Insulation, Volume: 29, Issue: 1, pp. 119 – 126, Februar 2022
Study of Oil/Pressboard Creeping Discharges under Divergent AC Voltage Part 3: Effects of Temperature and Stress Type
X. Zhou, P. Werle, E. Gockenbach, M. Imani

Water and Energy International, Volume 65r, Issue 1, April 2022
Possibility of Electric Arc Detection in Power Transformers by Directly Embedded Photoconductive Elements in the Transformer Tank (Limitations and Obstacles-An experimental investigation)
R. Sargazi, A. Akbari, M. Kuhnke, P. Werle

IEEE Transactions on Plasma Science, Volume: 50, Issue: 9, pp. 3169 – 3177, September 2022
Simulation of Negative and Positive Corona Discharges in Air for Investigation of Electromagnetic Waves Propagation
V. Javandel, A. Akbari, M. Ardebili, P. Werle

International Conference on Hydropower and Dams Development for Water and Energy Security – Under Changing Climate, 07. – 09.04.2022, Rishikesh, India
Possibility of Electric Arc Detection in Power Transformers by Directly Embedded Photoconductive Elements in the Transformer Tank (Limitations and Obstacles - An experimental investigation)
R. Sargazi, A. Akbari, M. Kuhnke, P. Werle

IEEE International Conference on Dielectric Liquids (ICDL), 29.05. – 02.06.2022, Seville, Spain
Investigation of the Diffusion Behaviour of Different Acid Configurations in Insulating Paper in a Closed Transformer System
B. Özdemir, Y. Wang, P. Werle

Modified Dissolved Gas Analysis with Additional Detection of higher Hydrocarbons for Transformer Fault Diagnosis
K. Homeier, P. Werle, M. Hahn, D. Wilke

Determination of Partition Coefficients of Gases for Insulation Liquids - Results of a CIGRE WG Round Robin Test
S. Leivo, J. Larkio, P. Werle, F. Scatiggio

IEEE International Conference on Dielectrics (ICD), 03. – 07.07.2022, Palermo, Italy
Set-Up for Space Charge Measurement with LIPP-Method During Aging of Polymeric Insulating Materials Under High DC Voltage
H. Hirte, S. Braun, S. Kornhuber, P. Werle

CIGRE 2022, 28.08. – 02.09.2022, Paris, France
Novel Fiber Optic Sensor Technology for Determining the DP Value of Insulation Paper for Transformers
T. Münster, P. Werle, K. Hämel, J. Preusel

IEEE International Conference on Diagnostics in Electrical Engineering (Diagnostika), 06. – 08.09.2022, Pilsen, Czech Republic
Review on Space Charge Induced Aging and Voltage Endurance Tests of Polymeric Insulating Materials Under High DC Voltage
H. Hirte, S. Kornhuber, S. Braun, P. Werle

Transformer Life Management (TLM), 19. – 20.09.2022, Bad Gögging, Deutschland
Bildung von C4- und C5-Kohlenwasserstoffen als Fehlergase in Isolierflüssigkeiten unter verschiedenen Fehlerszenarien in Leistungstransformatoren
K. Homeier, L. Stahl, P. Werle, D. Wilke, M. Hahn

Untersuchung des Diffusionsverhaltens von verschiedenen Säurekonfigurationen in Papier-Öl-Isolierungen
B. Özdemir, Y. Wang, P. Werle

Abschätzung des technischen Alters von Leistungstransformatoren mit einem neuronalen Netz
H. Schnittker, P. Werle, T. Münster, M. Lottner

Prediction of DP-Value of Power Transformers based on Machine Learning
S. Schreiter, H. Lohmeyer, P. Werle, F. Derbel

Möglichkeiten und Grenzen etablierter diagnostischer Verfahren
S. Schreiter, H. Lohmeyer, F. Derbel, P. Werle

Fachtagung VDE Hochspannungstechnik, 08. – 10.11.2022, Berlin Deutschland
Concept for Long-Term Space Charge Measurement of Polymeric Insulating Materials Under High DC Voltage Stress
S. Braun, H. Hirte, P. Werle, S. Kornhuber

Entstehung von höherwertigen Kohlenwasserstoffen neben konventionellen Fehlergasen in der Isolierflüssigkeit von Leistungstransformatoren
K. Homeier, P. Werle, M. Hahn, D. Wilke

A new method for health index determination for power transformers
M. Moh'd, H. Schnittker, P. Werle

Klassifikation von Messungen an Leistungstransformatoren
H. Schnittker, M. Moh'd, P. Werle, M. Westbomke, T. Münster, M. Lottner

Möglichkeiten und Grenzen diagnostischer Verfahren bei betriebsgealterten Transformatoren
S. Schreiter, H. Lohmeyer, P. Werle

On-Site Assembly, On-Site Rebuild, and On-Site High Voltage Testing of Power Transformers
P. Werle

IEEE International Conference on Condition Monitoring and Diagnosis (CMD), 12. - 18.11.2022, Kitakyushu, Japan
Neural Network for Estimating the Technical Age of Power Transformers
H. Schnittker, P. Werle, T. Münster, M. Lottner

9 Site Plan and Equipment

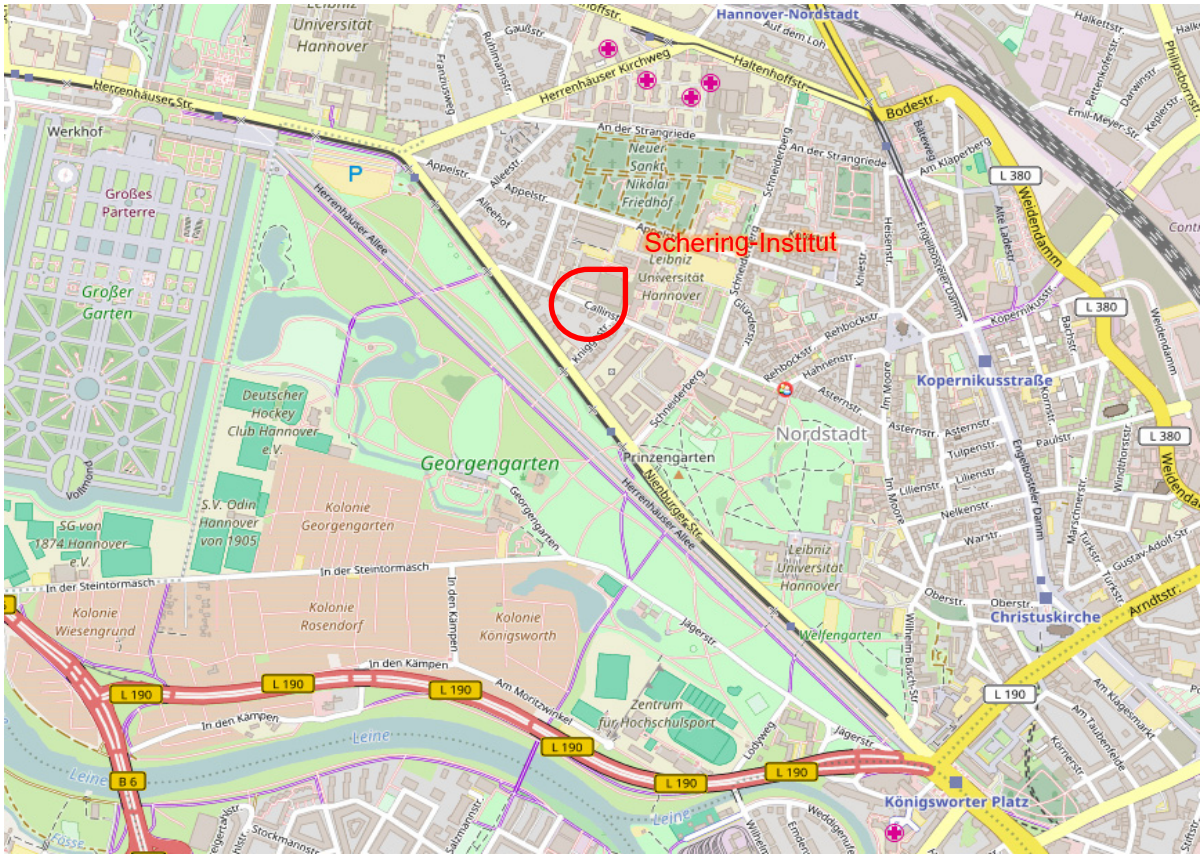

Equipment

- Sources: - Impulse voltage 3 MV, 300 kJ
  - AC voltage 800 kV, 1 A, 50 Hz
  - DC voltage 800 kV, 100 mA
  - Impulse current 200 kA, 300 kWs
- Shielded rooms and systems for partial dischargemeasurement and localization
- Clomate chamber for investigation of solid and liquid dielectrics
- Loss factor bridge for high voltage (50 Hz) and low voltage (10 Hz - 100 kHz)
- Nachbildung direkter und indirekter Effekte von Blitzentladungen
- Continuous test rigs for material testing with high batch sizes
- Facilities for the production of test specimens with plastic presses, extruders and resin casting equipment
- Extensive laboratory for analysis of insulating liquids
- Systems for high-quality preparation of insulating fluids
- Extensively equipped workshop for the production of various electrode configurations and special test equipment